Hybrid Materials Consisting of Silver(I) Purine Complexes, Protonated Purines and Polyoxometalates

Inaugural-Dissertation

zur

Erlangung des Doktorgrades

der Mathematisch-Naturwissenschaftlichen Fakultät

der Universität zu Köln

vorgelegt von

Vladislav Kulikov

aus Taschkent

Köln 2013

Vorsitz:	Prof. Dr. Hans-Günther Schmalz
Berichterstatter:	Prof. Dr. Gerd Meyer
	Prof. Dr. Lee Cronin
	Prof. Dr. Bernhard Lippert

Tag der mündlichen Prüfung: 28.10.2013

Die vorliegende Arbeit wurde im Zeitraum von November 2011 bis August 2013 am Institut für Anorganische Chemie der Universität zu Köln unter der Anleitung von Prof. Dr. Gerd Meyer angefertigt. Die experimentellen Arbeiten, die als Grundlage für das Kapitel 5 der vorliegenden Arbeit dienten, wurden im Zeitraum von Januar bis April 2013 an der School of Chemistry der University of Glasgow unter Anleitung von Prof. Dr. Lee Cronin durchgeführt.

Границ научному познанию и предсказанию предвидеть невозможно.

Boundaries of scientific knowledge and prediction cannot be foreseen.

D. I. Mendeleev

Abstract

The present work is the first thorough exploration of the chemistry of the systems comprising purine bases[1] and polyoxometalates (POMs).[2] Different modes of interplay of these chemical species were employed in order to design and synthesize new compounds.

The first type consisted majorly of materials in which polyoxoanions are interconnected by ditheobromine silver(I) complexes. The convenient aspect of the synthetic procedures is the possibility of obtaining the desired POM from basic materials by adjustment of the pH value of the reaction mixture. A ubiquitous structural trait of the target materials were one-dimensional coordination polymers consisting of polyoxoanions interconnected by $[Ag(thb)_2]^+$-complexes. Compounds based on iso- and heteropolyoxometalates of vanadium, chromium and molybdenum were obtained by this reaction procedure.

Several similar compounds were obtained from benzonitrile as solvent. An intriguing unusual chemoselectivity regulated by guanine was observed under these reaction conditions. The solvent partly replaced the purine bases in the coordination sphere of silver(I) due to its strong σ-donor character.

The protonated purine bases could also be employed for crystal engineering of organic-inorganic materials containing polyoxotungstates. The aromatic cations are arranged parallel to the faces of the POMs in all of the resulting crystal structures. The arrangement was named “nanoboxes” reflecting the size of the units.

A compound containing a purine base covalently bound to a polyoxometalate $Na_2[(HGMP)_2(Mo_5O_{15})]\bullet 7H_2O$ (GMP = guanosine monophosphate), crystallizes in space group $P6_522$, which implies a helical structure in the solid state. The crystal structure consists of guanosine Strandberg anions interconnected by a network of coordinative, H-bonding and stacking interactions.

---

[1] These biomolecules are detrimental to constitution and regulation of nucleic acids as well as intra- and intercellular signalling and energy conversion.

[2] Polyoxometalates (POMs) are oligomeric transition metal oxyanions linked by shared oxygen atoms which may form large, closed three-dimensional frameworks; the metals are usually from groups 5 and 6 of the periodic table.

Zusammenfassung

Die vorliegende Arbeit stellt die erste eingehende Untersuchung der Hybridmaterialien, die aus Purinbasen[1] und Polyoxometallaten[2] bestehen, dar. Die Stabilität der Zielverbindungen sowie die Synthesewege werden durch vielfältige Arten der koordinativen und nichtkovalenten Wechselwirkungen rationalisiert.

Die erste Klasse der synthetisierten Verbindungen besteht aus Polyoxoanionen, die vorwiegend durch Ditheobrominsilber(I)-Komplexe zu Koordinationspolymeren miteinander verknüpft wurden. Der pragmatische Aspekt der ausgearbeiteten experimentellen Strategie ist die Möglichkeit der Synthese der Hybridmaterialien aus Grundchemikalien in Wasser durch die Einstellung des geeigneten pH-Werts. Verbindungen der Iso- und Hetero-Polyoxometallate der Elemente Vanadium, Chrom und Molybdän wurden auf diese Art gewonnen.

Einige ähnliche Verbindungen mit Polyoxomolybdaten und -wolframaten wurden aus Benzonitril isoliert. Eine bemerkenswerte Eigenschaft von Guanin wurde unter diesen Reaktionsbedingungen festgestellt: Obwohl stöchiometrisch eingesetzt, wurde es nicht im Reaktionsprodukt gefunden, sondern diente als Reaktionsmodulator. Das Lösungsmittel verdrängt teilweise die Purinbase aus der Koordinationssphäre der Silber(I)-Kationen.

Die protonierten Purinbasen wurden ebenfalls für die Synthese der Hybridmaterialien eingesetzt. Die aromatischen Kationen sind in den resultierenden Kristallstrukturen parallel zu den Flächen der Polyoxoanionen angeordnet. Diese Anordnung wird als „Nanobox“ bezeichnet.

Die Verbindung $Na_2[(HGMP)_2(Mo_5O_{15})]\bullet 7H_2O$ (GMP = Guanosin Monophosphat) kristallisiert in der Raumgruppe $P6_522$. Die Kristallstruktur wird durch ein Netzwerk aus von koordinativen, H-Brücken- und Stapel-Wechselwirkungen stabilisiert. Die Raumgruppe impliziert eine helicale Anordnung der Bausteine.

---

[1] Purinbasen sind von sehr großer Bedeutung für den Aufbau und Regulation von Nucleinsäuren sowie für die intra- und interzelluläre Signalübertragung und biologische Energieumwandlung.

[2] Polyoxometallate sind komplexe Oxoanionen der Übergangsmetalle, die über verbrückende Sauerstoffatome verbunden sind; die gerüstbildenden Übergangsmetalle gehören in der Regel zu der fünften und sechsten Gruppe des PSE.

Acknowledgements

I am indebted to Prof. Dr. Meyer as to my teacher, mentor and understanding and encouraging supervisor. His fostering of my development as scientist and as supervisor of students and co-workers was tailored to my personality. The unlimited freedom of research and the possibilities to follow my own ideas were unparalleled under Prof. Dr. Meyer's supervision. The responsibility for organization of practical courses for biology students was to me a proof of his trust and a splendid opportunity for my personal development.

I am highly thankful to Prof. Dr. Lee Cronin from the University of Glasgow for invitation for a research secondment and a very warm welcome, which I experienced in his work group. I am especially thankful to Dr. Marie Hutin and Dr. De-Liang Long from Cronin Group for the productive and pleasant common work.

I enjoyed a lot of support from my colleagues Edem Tamakloe and Dr. Ingo Pantenburg on personal and professional basis. I value their scientific and organisational advices as well as their help in conducting experiments and organizing practical courses very highly. I also thank the rest of the work group Meyer and all colleagues involved in practical courses for biology students for a friendly and productive atmosphere.

The accomplishment of my work on the thesis within the fairly short period of time would not be possible without my previous experiences. I am indebted to Prof. Dr. Filippou and his co-workers from the University of Bonn for teaching me the art of experimental inorganic chemistry. I appreciate the steady support in my personal and organisational development, which I enjoyed under the supervision of Richard Lange and Christian Fränkel during my time at work for Inhouse Consulting of the Deutsche Post DHL.

I am also indebted to my family and close friends which I could rely on in every situation. Among them I am especially thankful to my father Prof. Dr. Yuri Kulikov as well as my friends Roman Zahn, Alexander Zimmer, Dmitri Gebel and Edem Tamakloe.

Table of Contents

Chapter 1

1. Introduction 1

1.1. Polyoxometalates and the Classification of their Compounds in the Present Work 2

1.2. Materials Consisting of Organoamine-Silver(I) Complexes and Isopolyoxoanions 4

1.3. Synthetic Strategies for the Preparation of Hybrids of Organoamine-Silver(I) Complexes and POMs 13

1.4. The Scope and Objectives of the Present Thesis 15

1.5. References 17

Chapter 2

2. A Novel Strategy for the Synthetic Assembly of Inorganic-Organic Silver(I)-Polyoxometalate Hybrid Structures Employing Non-Covalent Interactions between Theobromine Ligands 20

2.1 Synthetic Strategy 20

2.2 Crystal Structures 23

2.3 Structural and Energetic Analysis 32

2.4 Conclusions 36

2.5 Experimental Section 38

2.5.1 Synthetic Procedures 38

2.5.2 Powder X-Ray Diffractograms 41

2.5.3 DTA/TG Measurements 44

2.5.4 X-Ray Crystallographic Studies 46

2.6 References 49

Chapter 3

3. New Organoamine Silver(I) Decatungstate Frameworks: Remarkable Chemoselectivity and Employment as Precursors for Potential Functional Materials. A Related β-Octamolybdate Compound 50

3.1 Synthesis and Crystal Structures of Materials Consisting of Organoamine Silver(I) Complexes and Decatungstate 50

3.2 Structural and Chemical Influence of the Replacement of Decatungstate by Octamolybdate 55

3.3 Conclusions 58

3.4 Experimental Section 60

3.4.1. Synthetic Procedures 60

3.4.2. Powder X-Ray Diffractograms 62

3.4.3. DTA/TG Measurements 64

3.4.4. Single Crystal X-Ray Crystallography 66

3.5. References 67

Chapter 4

4. Polyoxotungstates Packed in Molecular “Boxes” of Purine Bases 68

4.1 Introduction 68

4.2 Results and Discussion 69

4.3 Thermolysis Results 72

4.4 Conclusion 73

4.5 Experimental Section 74

4.5.1. Synthetic Procedures 74

4.5.2. X-Ray Diffractograms 75

4.5.3. DTA/TG Curves 76

4.5.4. X-Ray Powder Patterns of Thermolysis Residues 77

4.5.5. Single Crystal X-Ray Diffraction Studies 79
4.6 References 81

Chapter 5

5. Agglomeration of a Guanosine-Polyoxometalate Hybrid and its Helical Crystal Structure 82
5.1. Introduction 82
5.2. Results and Discussion 83
5.3. Experimental Section 88
5.4. References 92

Chapter 6

6. Summary and Conclusions 93
6.1 The types of obtained compounds 93
6.2 Key Conclusions 95
6.3 Notes and References 96

1. Introduction

1.1. Polyoxometalates and the Classification of their Compounds in the Present Work

Polyoxometalates (POMs) are oligomeric transition metal oxyanions linked by oxygen atoms which form two- or three-dimensional frameworks; the metals are usually from groups 5 and 6 of the periodic table.[1] These compounds were discovered already two centuries ago,[2] but they still fascinate the scientific community. Of special current interest is the impressive structural diversity and numerous applications in a multitude of areas ranging from catalysis to applications in medicine and energy generation, which have either already been found or begin to shape out from the basic research.[3]

There are two basic forms of polyoxometalate anions: iso- and heteropolyoxometalates (Figure 1.1). The first one comprises the class of polyoxoanions, in which only one metallic species is present, for instance decavanadate $[V_{10}O_{28}]^{6-}$. The second one comprises the class of polyoxoanions containing a central atom stabilizing the system. The most famous example of the second class is the Keggin-type phosphotungstate $[PW_{12}O_{40}]^{3-}$.[4] There is also a class of large reduced molybdenum polyoxoanions which were discovered only recently.[5] They include polyoxomolybdates with up to 368 molybdenum atoms per anion,[6] hence displaying a large potential in nanoscience.

The POM containing compounds can be classified as purely inorganic or inorganic-organic hybrids. The materials belonging to the first class are usually obtained from aqueous solutions and contain metal cations along with coordinating and co-crystallizing water molecules. The sheer number of cations and POMs imply a class of compounds of incredible diversity.

The second type of POM based materials – inorganic-organic hybrid compounds – is even more diverse. The increase in complexity is imposed by the possibility of variation of the organic component. A subdivision of this type of compounds according to the organic component into three classes is helpful for further discussion. Namely, the materials can contain the organic components as:

1. Discrete cations
2. Ligands of a transition metal complex (TMC)
3. Organic substituents covalently bound to the POM.

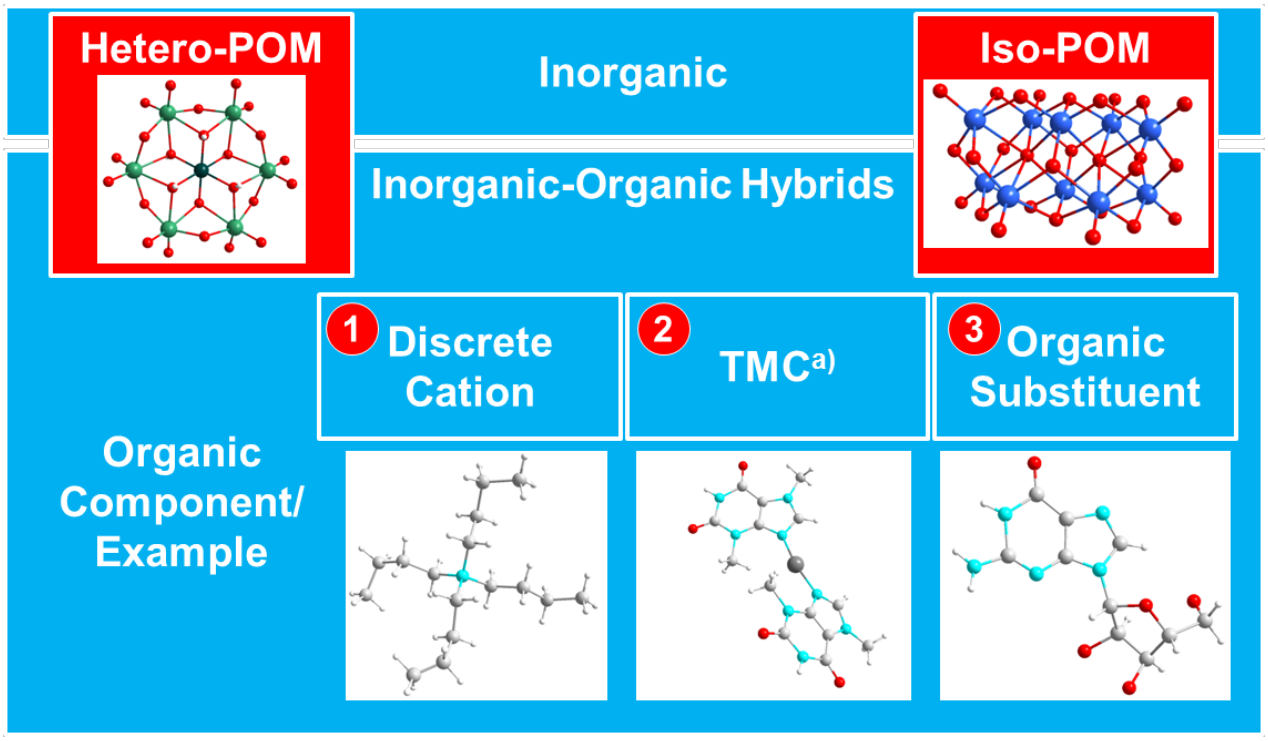

Figure 1.1: Classification of POMs exemplified by compounds synthesized in the present thesis (vide infra). C grey, H white, Ag silver, Cr dark green, Mo sea green, N turquoise, O red, V light blue. a) TMC = transition metal complex.

Compounds belonging to two or all three classes were characterized as well,[3b] but they are far rarer than the one belonging to only one class.

Compounds belonging to the first class and containing large organic cations were mainly synthesized and characterized by Cronin et al.[7] These materials are remarkable as they often contain large polyoxoanions not encountered before. These anions are usually highly symmetrical. $[H_{12}W_{36}O_{120}]^{12-}$ - the first inorganic crown ether[8] - displays C_{3v} symmetry, the reduced Dawson anion $[W_{18}O_{54}(SO_4)_2]^{8-}$ is highly symmetrical as well.[9] The appealing feature of these materials is the possibility to control the crystal architecture. Thus, there is a possibility of creation of 1 and 2D coordination polymers as well as ionic grids on the basis of silver(I)-polyoxomolybdate compounds, determining the structure by choice of the solvent and cation (these compounds simultaneously belong to the second class).[10]

As the synthetic procedures for this whole class of compounds were developed only recently, there are no direct applications for these materials as yet. Nonetheless, employment of the reduced POMs of the described class as singly molecular magnets could be anticipated.[7] Smaller organic cations or neutral N-donors were also employed for assembly of POM-based crystal structures, but they do not induce formation of large new polyoxoanions. The crystal structure

can be predicted only poorly. Accordingly, the design of the crystal lattice architecture cannot be accomplished with certainty.[11]

The second type of hybrid materials containing transition metal complexes was the most profoundly explored in two recent decades.[12] The reason for this surge of research interest is the easiness of preparation along with fascinating diversity of the crystal structures. This class can be considered also as the most complex one due to a multitude of choices for the ligand, the transition metal and the polyoxometalate. The forces determining the crystal structure are also diverse, ranging from strong coordination and Coulombic interactions to such weak non-covalent interactions as hydrophobic van-der-Waals forces. This class of materials exemplified by compounds containing silver(I) complexes is discussed thoroughly in Section 1.2.

The third class of compounds – covalent hybrids of POMs and organic molecules – is also relatively new, but already gained quite a lot of attention from the scientific community.[13] There are different possibilities for the preparation of these compounds, distinguishable into two types: *in situ* assembly of the POM component around the functional groups of the organic ligands and modification of already assembled covalent POM hybrids by organic chemical reactions.

There is a multitude of organic molecules which were employed in the synthesis of all mentioned classes of the inorganic-organic compounds. Most of the organic starting materials for the classes number 2 and 3 are aromatic nitrogen bases because they exhibit two crucial features making them suitable for the synthesis of such solids. Namely, they can build up an extensive framework of non-covalent interactions based on H-bonds, hydrophobic and stacking interactions. The second feature is the ability of these molecules to act as ligands to late transition metals, reinforcing the crystal structures of the materials from class number two.

Class one and class three materials were recently reviewed.[3b,13] No comprehensive review is available for materials belonging to the second class, i. e. materials consisting of POMs and transition metal complexes. The most likely reason for the absence of this comprehensive work is the diversity and vast quantity of compounds to review as well as the fact that most of them were synthesized and described only in the recent years. I will limit the scope of my review to the compounds containing silver(I) complexes, as all my experiments directed at the synthesis of this class of compounds were limited to this metal.

1.2. Materials Consisting of Organoamine-Silver(I) Complexes and Isopolyoxoanions

Silver(I) is one of the most frequently chosen cations for TMC-POM based materials.[3b,7] There are three main reasons for that preference:

- Silver(I) can adopt a multitude of geometries and coordination numbers in its complexes.[14] Accordingly, variation of coordinative connection modes can be accomplished in the crystal structures allowing a multitude of three dimensional design possibilities.[10]
- Silver(I) displays high affinity both to organic nitrogen bases and POMs.
- Coordination compounds of this transition metal are applied in luminescent, catalytic and anti-bacterial materials.[15] Hence the hope is to develop new functional materials with tailored properties.

Indeed, much of the work on silver(I)-POM compounds was focused on understanding mechanisms of assembly of complex inorganic-organic materials with the final aim of developing viable procedures for the synthesis of functional materials, where properties can be designed and controlled on the nanoscale.[3b]

As pointed out above, the amount of published data on the resulting compounds is very large; accordingly the discussion can be facilitated by introduction of a certain scheme. The literature overview of silver(I)-POM compounds is given subsequently according to the metal building the core of the polyoxoanion.

The literature describing the silver(I) hetero-POMs is similarly comprehensive as the one describing silver(I)-isopolyoxometalate based materials. I see the discussion of isopolyoxometalate based materials as sufficient in order to obtain a general overview of the area and more relevant for the discussion of my own results. Accordingly the subsequent overview is limited to silver(I)-isopolyoxoanions based materials.

Silver(I) isopolyoxovanadates display especially high structural diversity (Table 1.1). Silver(I)-complexes can be bound to distinct tetra-[16] and decavanadate[17] (Figure 1.3, Figure 1.4) anions as well as to di-[16a] and tetravanadate[18] chains and layers. The level of polyoxovanadate agglomeration is controlled by the reaction conditions. The synthesis from tetrabutylammonium decavanadate as precursor in strong coordinating solvents under ambient conditions yields structures, in which silver(I) complexes interlink distinct decavanadate units.[17b,17c] Under

hydrothermal conditions on the other hand, all agglomeration degrees mentioned above are possible depending on the solvent, concentration, pH, temperature and starting materials. Decreasing water content of the reaction mixture induces for instance agglomeration of the polyoxovanadates to infinite chains containing edge sharing polyhedra. Increasing water content on the other hand leads to a separation of these chains into individual polyoxometalate anions (compare entries 1-5 and 7-9 in Table 1.1).

Polyoxoniobates such as the Lindqvist hexaniobate $[Nb_6O_{19}]^{8-}$ are stable only in alkaline media.[19] Hence, to our best knowledge, there are no structurally characterized Ag(I)-polyoxoniobate compounds, probably due to the stability of Ag_2O under these conditions. The same is applicable to polyoxotantalate anions.

Table 1.1: Known complexes containing silver(I)-complexes with organonitrogen bases and isopolyoxovanadates.

Entry	Compound	Polyoxoanion/ Chain	d(Ag-O) [Å]	References
1	$[Ag(bpy)]_4[V_4O_{12}]\cdot 2H_2O$ (bpy = 4,4'-bipyridine)	Tetravanadate	2.67-2.85	16a
2	$[Ag(dpa)]_4[V_4O_{12}]\cdot 2H_2O$ (dpa = 1,2-bis-(4-pyridyl)-ethane)	Tetravanadate	2.62-2.70	16a
3	$[Ag(bbi)][Ag(bbi)_4][Ag_3(V_4O_{12})_2]\cdot 2H_2O$ (bbi = 1,1'-(1,4-butandiyl)bis(imidazole))	Tetravanadate	2.20 - 2.46	16b
4	$[Ag_2(bib)_2][V_4O_{12}]_{0.5}\cdot 3H_2O\cdot 2MeCN$ (bib = 1,3-bis(4,5-dihydro-1H-imidazol-2-yl)benzene)	Tetravanadate	–	16c
5	$[Ag(btx)]_4][H_2V_{10}O_{28}]\ 2H_2O$ (btx = 1,4-bis(triazol-1-ylmethyl)benzene)	Decavanadate	2.66-2.82	17a
6	$\{[Ag(CH_3CN)_3]_3[H_3V_{10}O_{28}]\cdot MeCN\}_2$	Decavanadate	2.48-2.65	17b
7	$[Ag_4(pzc)_2V_2O_6]$ (pzc = pyrazinecarboxylate)	VO_5-chains	2.33-2.35; 2.38-2.48 und 2.65-2.69	16a
8	$[Ag(biim)]_2V_4O_{11}]$ (biim = 1,1'-(1,4-butandiyl)bis(imidazole)	$[V_4O_{11}]^{2-}$-chains	–	17a
9	$[Ag(bpy)V_4O_{10}]$ (bpy = 4,4'-bipyridine)	$[V_4O_{10}]^-$-layers	2.74	18

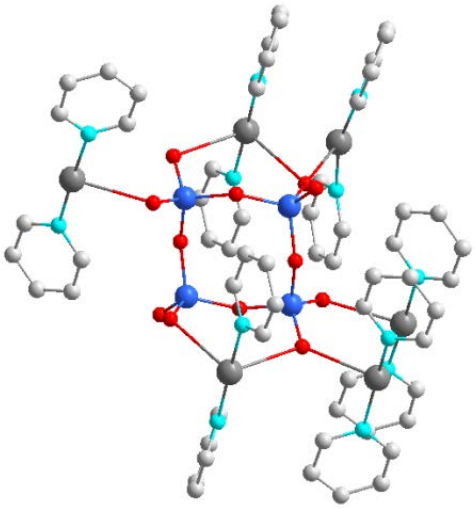

Figure 1.3: Coordination of Ag^+ by the tetravanadate anion in $[Ag(bpy)]_4[V_4O_{12}]\cdot 2H_2O$ (bpy = 4,4'-bipyridine).[16a] For clarity reasons only one bpy-ring is shown. H-atoms are omitted for clarity. C grey, Ag metallic grey, N turquoise, O red, V light blue. Same colour scheme applied to all subsequent illustrations.

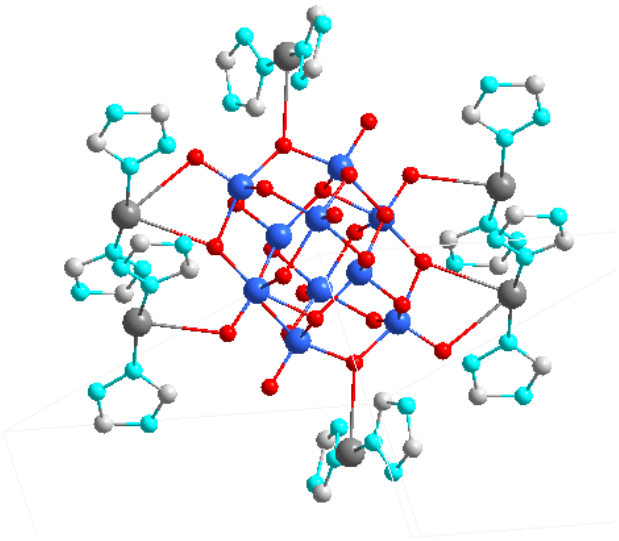

Figure 1.4: Interconnection of Ag^+ by a decavanadate anion in $[Ag(btx)]_4][H_2V_{10}O_{28}]\cdot 2H_2O$ (btx = 1,4-bis(triazol-1-ylmethyl)benzene).[17a] Only one triazole ring per btx is shown. H-atoms omitted for clarity.

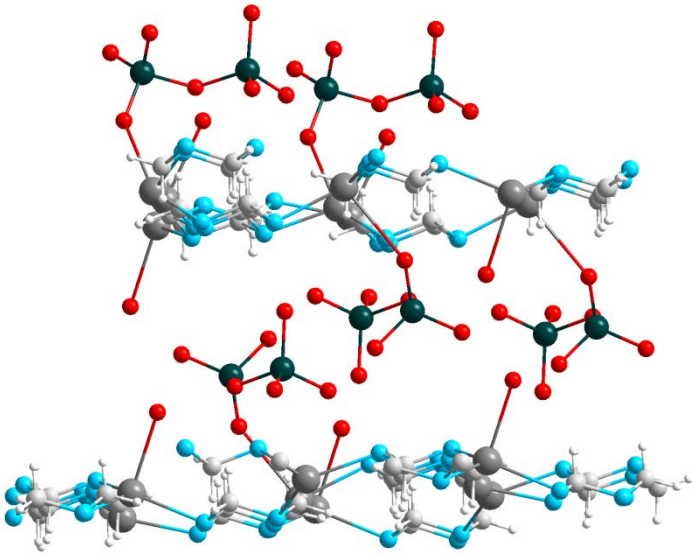

Figure 1.2: Layers of $[Ag(hmt)]^+$ complexes interconnected by dichromate anions in $[Ag(hmt)]_2[Cr_2O_7]\cdot H_2O$. Cr dark green, H white.[20]

The tendency of dichromate to condense to higher polyoxoanions is fairly limited. These can be accessed only via reactions with large excess of CrO_3 and in the presence of stoichiometric amounts of water. Accordingly it is a challenging task to conduct crystal engineering of organic-inorganic hybrid structures with polyoxochromates. On the other hand, the dichromate anion is readily built from monochromate anions under only slightly acidic conditions. Nevertheless no attempts to construct supramolecular architectures based on

silver(I)-dichromate frameworks has been conducted, to best of our knowledge. Only one structure, the $[Ag(hmt)]_2[Cr_2O_7]\cdot H_2O$ (hmt = urotropine), containing silver(I) dichromate and a nitrogen ligand has been published previous to present work (Figure 1.2).[20] In this compound Ag(I) ions are not connected by $Cr_2O_7^{2-}$. The structure consists of alternate layers of $[Ag(hmt)]^+$ complexes and dichromate units, where $Cr_2O_7^{2-}$ coordinates only to one Ag^+ ion. Hence this compound can be rather considered as a salt of Ag(I)-hmt complex and dichromate as opposed to supramolecular organic-inorganic hybrid structures, in which Ag(I)-ions are connected by polyoxometallate anions.

Ag(I) isopolyoxomolybdate solids were thoroughly investigated in the recent decade.[10,21] Contrary to the polyoxovanadate ions, which are encountered in different levels of agglomeration (Table 1.1), polyoxomolybdates in scope of this introduction crystallize almost exclusively in the octamolybdate form (Table 1.2). This fact is especially remarkble as a variety of starting materials is employed for the synthesis of hybrids of silver(I)-complexes and octamolybdates. MoO_3, Na_2MoO_4 and $(NH_4)_6[Mo_7O_{24}]$ are usually employed as starting materials under hydrothermal conditions, whereas bis(tetrabutylammonium) hexamolybdate is employed in reactions in organic solvents.

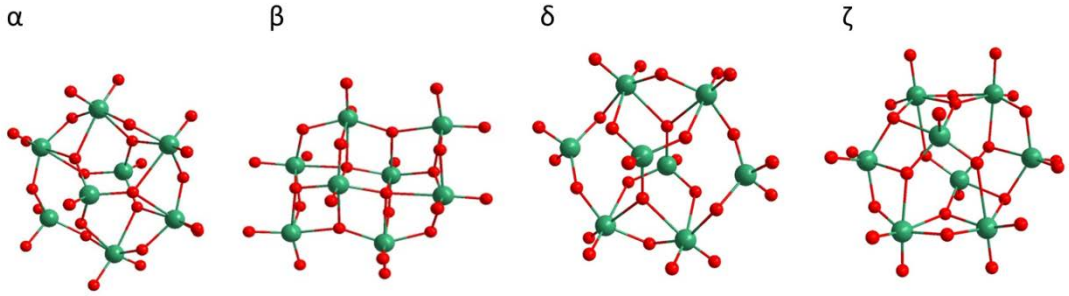

Figure 1.5: Most common isomers of octamolybdate. α: 6 octahedra, 2 tetrahedra; β: 8 octahedra; δ: 4 octahedra, 4 tetrahedra; ζ: 4 octahedra, 4 square pyramids.

Cronin et al. traced the mechanism of this rearrangement by cryospray mass spectrometry.[22] The results showed that the polyoxomolybdate anions exist in equilibrium of different agglomeration states of general formula $[AgMo_mO_{3m+1}]^-$ in solution. The stable $[Ag_2Mo_8O_{26}]^{2-}$ complexes are formed from these precursors in solution and precipitate as building blocks of the target compounds. This silver(I)-octamolybdate(VI) unit was used as a synthon for building up complex materials.[10,21b,22] The crystal structures of the obtained compounds exhibit different

characteristic traits on the nanoscale. One-dimensional silver(I)-octamolybdate chains, grids or even a two-dimensional network depending on the counterion and coordinating solvent molecules could be obtained.[10] These hybrid organic-inorganic solids containing organoamine-silver(I) complexes and β-octamolybdate anions are of special interest to the scientific community due to Ag(I)-Ag(I)-interactions[10,23] as well as conductivity[21e] and luminescence properties.[21e,21j,21k]

There are different isomers of octamolybdate encountered in the hybrid materials. The most often occuring ones are displayed in Figure 1.5. The β-isomer is encountered in vast majority of cases (Table 1.2). This fact is remarkble as theoretical calculations indicate lower stability of this isomere compared to the other ones.[24] The reason might lie in the mechanism of the reaction discussed above.

Table 1.2: Literature overview of complexes containing silver(I) complexes with organonitrogen bases and isopolyoxomolybdates.

Entry	Compound	Polyoxoanion/ Chain	d(Ag-O) [Å]	References
1	$\{Ag_8(L)_4[\alpha\text{-}Mo_8O_{26}][\beta\text{-}Mo_8O_{26}](H_2O)_3\}\cdot H_2O$ (L1 = 1,1'-(1,3-propanediyl)-bis[2-(4-pyridyl)benzimidazole])	α-octamolybdate / β-octamolybdate	2.18 – 2.93	21h
2	$(Bu_4N)_2Ag_2[Mo_8O_{26}]$	β-octamolybdate	2.28 – 2.42	25
3	$\{Ag_4(DMSO)_8[Mo_8O_{26}]\}_n$.	β-octamolybdate	2.30 – 2.58	21a
4	$(nBu_4N)_{2n}[Ag_2Mo_8O_{26}(CH_3CN)_2]_n$	β-octamolybdate	2.39 – 2.48	21b
5	$(nBu_4N)_{2n}[Ag_2Mo_8O_{26}]_n$	β-octamolybdate	2.27 – 2.41	21b
6	$(nBu_4N)_{2n}[Ag_2Mo_8O_{26}(DMSO)_2]_n$	β-octamolybdate	2.25 – 2.49	21b
7	$(HDMF)_n[Ag_3(Mo_8O_{26})(DMF)_4]_n$	β-octamolybdate	2.39 – 2.50	21b
8	$[(Ag(DMF))_2(Ag(DMF)_2)_2Mo_8O_{26}]_n$	β-octamolybdate	2.30 – 2.46	10
9	$(H_2NMe_2)_{2n}\{Ag_2(DMF)_2[Mo_8O_{26}]\}_n\cdot 2DMF$	β-octamolybdate	2.46 – 2.49	10
10	$(Ph_4P)_2[Ag_2Mo_8O_{26}(DMSO)_4]$	β-octamolybdate	2.36 – 2.48	21b
11	$(Ph_4P)_2\{Ag_2(CH_3CN)_2[Mo_8O_{26}]\}\cdot 2CH_3CN$	β-octamolybdate	2.32 – 2.79	10
12	$(Ph_4P)_{2n}\{Ag_2(DMF)_2[Mo_8O_{26}]\}_n\cdot 2DMF$	β-octamolybdate	2.40 – 2.49	10

13	$[Ag(C_7H_{12}O_2N)(CH_3CN)]_{2n}\{Ag_2(CH_3CN)_2\text{-}[Mo_8O_{26}]\}_n \cdot 2CH_3CN$ (($C_7H_{12}O_2N$) = 2,6-pyridine dimethanol)	β-octamolybdate	2.35 – 2.92	10
14	$Ag_4[Mo_8O_{26}](L)_{2.5}(H_2O)$ (L = 3,5-dimethyl-4-amino-4H-1,2,4-triazole)	β-octamolybdate	2.37 – 2.98	26
15	$(Hcpy)_3[AgMo_8O_{26}]$ (cpy = 4-(5-chloropyridin-2-yl)pyridine)	β-octamolybdate	2.37-2.38	21c
16	$\{Ag_4(ttb)_2[Mo_8O_{26}]\}$ (ttb = 1,3,5-tris(1,2,4-triazol-1-ylmethyl)-2,4,6-trimethyl benzene)	β-octamolybdate	2.67	21g
17	$(H_3O)[Ag_3(2,2'\text{-bpy})_2(phnz)_2Mo_8O_{26}]$ (bpy = bipyridine, phnz = phenazine)	β-octamolybdate	2.40 – 2.93	21j
18	$[Ag_4(dmtrz)_4][Mo_8O_{26}]$ (dmtrz = 3,5-dimethyl-1,2,4-triazole)	β-octamolybdate	2.62 – 2.74	21e
19	$[Ag_4(4atrz)_2Cl][AgMo_8O_{26}]$ (4atrz = 4-amino-1,2,4-triazole)	β-octamolybdate	2.36 – 3.00	21e
20	$\{Ag_4(fcz)_4[Mo_8O_{26}]\}$ (fcz = 2-(2,4-difluorophenyl)-1,3-di(1H-1,2,4-triazol-1-yl)propan-2-ol)	β-octamolybdate	2.59 – 2.81	21i
21	$[Ag_4L_2][Mo_8O_{26}]$ (L = 1,4-bis(1,2,4-triazol-1-ylmethyl)benzene)	β-octamolybdate	2.46 – 2.91	21k
22	$[Ag_5(trz)_4]_2[Ag_2Mo_8O_{26}]\cdot 4H_2O$	γ-octamolybdate	2.36 – 2.99	21e
23	$[Ag_2(trz)_2]_2[Mo_8O_{26}]$ (trz = 1,2,4-triazole)	γ-octamolybdate	2.63 – 2.97	21e
24	$[Ag_4L_4][Mo_8O_{26}]$ (L = 1,4-bis(imidazole-1-ylmethyl)benzene)	δ-octamolybdate	2.72 – 2.90	21k
25	$[[Ag_4(tpyprz)_2(H_2O)]Mo_8O_{26}]$ (tpyprz = tetra-2-pyridylpyrazine)	ζ-octamolybdate	2.39 – 2.47	27
26	$[Ag_4(3\text{-pttz})_2Mo_3O_{10}]$ (3-pttz = 5-(3-pyridyl) tetrazolate)	$[Mo_3O_{10}]^{2-}$ chains	2.34 – 2.60	21f
27	$[Ag_4(2\text{-pttz})_2Mo_4O_{13}]$ (2-pttz = 5-(2-pyridyl) tetrazolate)	$[Mo_4O_{13}]^{2-}$ chains	2.38 – 2.60	21f
28	$[Ag_4(pzttz)_2Mo_4O_{13}]$ ((pzttz = 5-(pyrazinyl) tetrazolate)	$[Mo_4O_{13}]^{2-}$ chains	2.43 – 2.68	21f
29	$[Ag_2(quinoxaline)_2Mo_4O_{13}]$	$[Mo_4O_{13}]^{2-}$ chains	2.43 – 2.57	21d
30	$[Ag_2(3atrz)_2]\{Ag_2(3atrz)_2[Mo_8O_{26}]\}$ (3atrz = 3-amino-1,2,4-triazole)	chains of condensed γ-octamolybdates	2.41 – 2.58	21e

Octamolybdates other than the β-isomer can be considered rather exotic. The interesting feature of the α-isomer is that it can coexist with the β-octamolybdate in the same compound

(Figure 1.6).[21h] Examples of hybrid materials of silver(I)-organoamine complexes with δ-[21k] and ζ-octamolybdates[27] are known as well.

Similarly to isopolyoxovanadates, different agglomeration patterns of Ag(I)-isopolyoxomolybdates under hydrothermal conditions are possible. If these reactions are performed with a low amount of water and with bulk solids such as MoO_3 as starting materials, highly condensed polyoxomolybdate chains are produced. These chains are interconnected by silver(I)-nitrogen ligand complexes (Figure 1.7).[21d-f] All Mo atoms in these one-dimensional inorganic polymers display characteristic octahedral ligand sphere consisting of oxygen atoms. Although the degree of condensation under hydrothermal conditions is determined by the quantity of water employed, the exact design of target materials is yet impossible.

The lengths of coordinative bonds between Ag(I) and oxygen atoms of the octamolybdates are largely extremely variable. They depend on a lot of factors such as strength of other ligands, general coordination environment, charge distribution of the octamolybdate etc. To conclude any general trend from the data is not possible (Table 1.2).

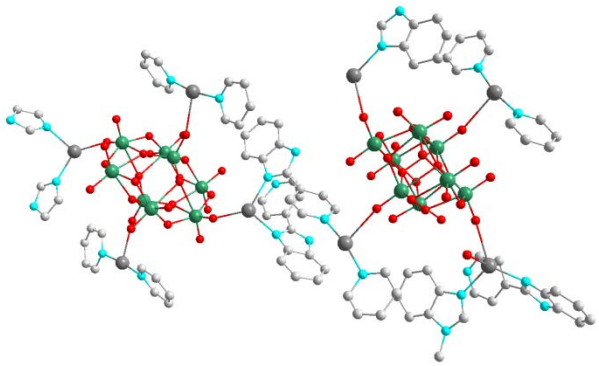

Figure 1.6: α-(left) and β-octamolybdates in $\{Ag_8(L)_4[\alpha\text{-}Mo_8O_{26}][\beta\text{-}Mo_8O_{26}](H_2O)_3]\cdot H_2O$ (L1 = 1,1'-(1,3-propanediyl)-bis[2-(4-pyridyl)benzimidazole]).[21h] For clarity reasons: H atoms are omitted, only selected parts of organic ligands shown.

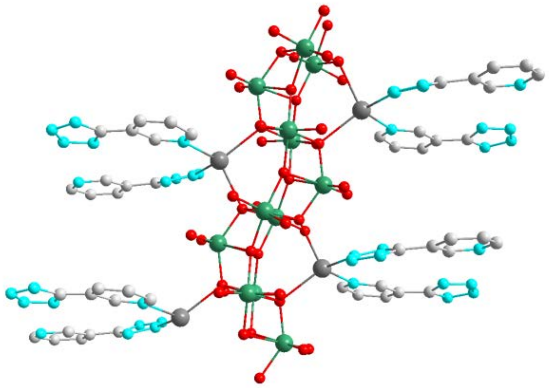

Figure 1.7: Condensed chain of $[Mo_3O_{10}]^{4-}$ supported by Ag^+-complexes in $[Ag_4(3\text{-pttz})_2Mo_3O_{10}]$ (3-pttz = 5-(3-pyridyl) tetrazolate).[21f] H atoms are omitted.

Silver(I)-isopolyoxotungstate chemistry is less thoroughly explored but much more diverse than the respective isopolyoxomolybdate chemistry. Organoamine silver(I) complexes of hexa-,[15] deca-,[28] dodeca-[29] and nonadecatungstate[30] have been characterized and described in the literature (Table 1.3). The synthesis is usually accomplished under ambient conditions in acetonitrile or via a hydrothermal pathway. A remarkable compound from this class is

$Ag_2(H_2biim)_4[W_6O_{19}]•2H_2O$ (H_2biim = 2,2‘-biimidazole), which was synthesized under hydrothermal conditions (Figure 1.8).[15] It is the only POM-organoamine-silver(I) complex containing a Lindqvist anion, which is contra-intuitive because Lindqvist geometry is encountered quite often in POM chemistry. Further intriguing materials are the silver(I)-dodeca- and nonadecatungstates only with acetonitrile as supporting ligand (Figure 1.9).[29a,30] These materials exhibit zeolite-like properties due to their nearly completely inorganic structures. They consist of three-dimensional networks of polyoxotungstates connected by silver(I) ions, whereby the charge is counterbalanced by additional Ag(I)-acetonitrile complexes in the cavities or channels within the silver(I)-polyoxoanion framework.

Table 1.3: Compounds containing silver(I) complexes with organonitrogen bases and isopolyoxotungstates.

Entry	Compound	Polyoxoanion/ Chain	d(Ag-O) [Å]	Reference
1	$Ag_2(H_2biim)_4[W_6O_{19}]·2H_2O$ (H_2biim = 2,2‘-biimidazole)	Hexatungstate	2.25	15
2	$(Ag(MeCN)_3)_2(Ag(MeCN)_2)_2[W_{10}O_{32}]$	Decatungstate	2.56 – 2.85	28
3	$[Ag(MeCN)_4]⊂[Ag(MeCN)_2]_4[H_3W_{12}O_{40}]$	α-meta-dodecatungstate	2.41	29a
4	$Na_4[Ag_6L_4][H_2W_{12}O_{40}]·12H_2O$	α-meta-dodecatungstate	2.21 – 2.95	29b
5	$[Na_2(H_2O)_8Ag_2(HINA)_3(INA)]\{Na(H_2O)_2Ag_2(HINA)_4[H_2W_{12}O_{40}]\}·2H_2O$ (HINA = isonicotinic acid)	α-meta-dodecatungstate	2.60 – 2.73	31
6	$\{[Ag(H_2O)_3(Bu^iNH_2)_4]_2Na_2H_2[H_2W_{12}O_{40}]\}·4H_2O$	α-meta-dodecatungstate	2.47 – 2.57	29c
7	$\{Na_2(H_2O)_4Ag_6(HNA)_2(NA)_2[H_2W_{12}O_{40}]\}$ ·8H2O	α-meta-dodecatungstate	2.21 – 2.95	31
8	$[(Ag(MeCN)_2)(MeCN)]⊂\{α–[H_4W_{19}O_{62}](TPA)_2(Ag(MeCN)_2)(Ag)_2\}·7MeCN$	α-nonadecatungstate	2.37 – 2.90	30
9	$[Ag(MeCN)_4]⊂[γ^*-[H_4W_{19}O_{62}](Ag(MeCN)_2)_4(Ag(MeCN)_2)·6(MeCN)$	$γ^*$-nonadecatungstate	2.48 -2.73	30

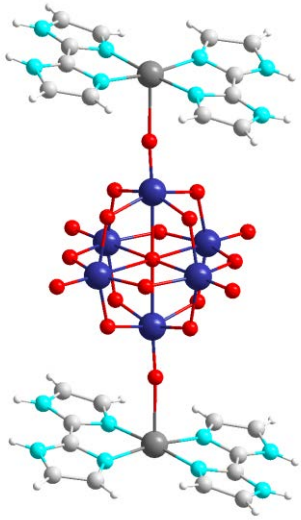

Figure 1.8: Lindqvist anion connecting two $[Ag(H_2biim)_2]$-complexes in $Ag_2(H_2biim)_4[W_6O_{19}]\cdot 2H_2O$ (H_2biim = 2,2'-biimidazole). W: indigo (same in subsequent illustrations).[16]

The review of the entire silver(I)-heteropolyoxoanion chemistry goes way beyond the scope of this intentionally short review. Nonetheless, one subclass of such materials has to be mentioned in order to be able to discuss the results in further sections. This is the subclass of the Anderson type B anion based compounds: $[X(OH)_6M_6O_{18}]^{m-}$;X = transition metal in the second or third oxidation state, M = Mo (VI) or W(VI).[32] Silver(I) compounds of Anderson type B anions are less thoroughly investigated than the isopolyoxomolybdate counterparts. The silver(I)-Anderson type B molybdate structures were characterized and described only for Cr^{3+} [33] and Ni^{2+} [34]. A similar type of silver(I) compounds with the polyoxoanion $[Mn(Mo_6O_{18})((OCH_2)_3CNH_2)_2]^{3-}$ was discovered recently.[21a] This polyoxometalate exhibits two triply covalently bound organic substituents $((OCH_2)_3CNH_2)^{3-}$ replacing the hydrogen atoms and hence supporting the central part.

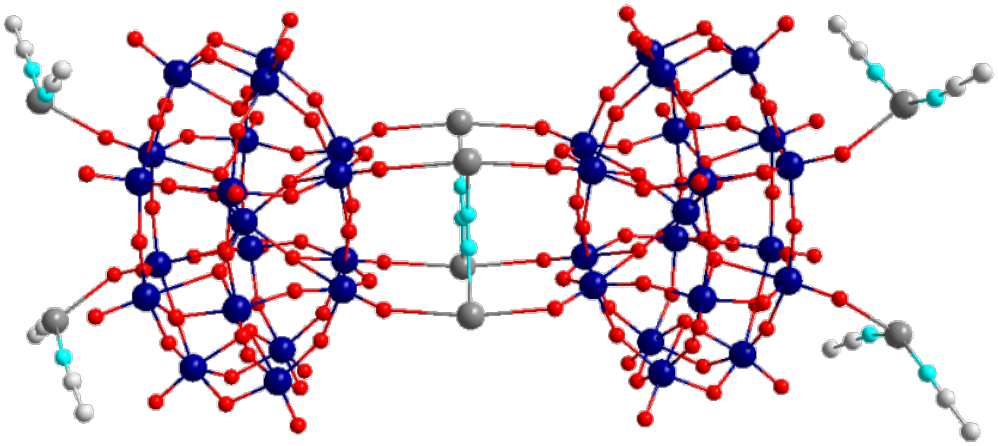

Figure 1.9: Two α-nonadecatungstates interconnected by four Ag^+-complexes in $[Ag(MeCN)_4]\subset[\gamma*-[H_4W_{19}O_{62}](Ag(MeCN)_2)_4(Ag(MeCN)_2)\bullet 6(MeCN)$.[31]

1.3. Synthetic Strategies for the Preparation of Hybrids of Organoamine-Silver(I) Complexes and POMs[35]

Four major synthetic strategies were developed for the preparation of organic-inorganic compounds containing silver(I) isopolyoxoanions.

The most widely used synthetic approach is the synthesis of the target compounds under hydrothermal conditions. Silver(I) salts (e. g. Ag_2SO_4) and an oxide or oxyanion of the group 5 or 6 metal (e. g. Na_2MoO_4) are used as starting materials and an aromatic N-base as organic component. Aromatic organonitrogen bases are preferably used in this chemistry, most likely due to the packing effects favouring the crystallization. The synthesis of most of the polyoxovanadate and octamolybdate based compounds (Tables 1.1 and 1.2) was accomplished via this route.

A less widely used but effective in the synthesis of new structures and fine-tuning of structural details is the so-called “Shrink-Wrapping Strategy” developed by Cronin et al.[21b] The content of the strategy is the reaction of POM salts of large organic cations with silver(I) salts in organic solvents. The resulting compounds are usually isolated via vapour diffusion of less polar solvents. They contain silver(I)-POM coordination polymers, which are surrounded by organic cations (“shrink-wrapping” the chains). Coulombic interactions between these units appear to be the detrimental stabilizing force for the crystal structures. The strategy was especially successfully applied to silver(I) octamolybdates which could be arranged into 1D-chains, grids and 2D-networks depending on the reaction conditions and the cation.[10]

A closely related approach was directed towards the isolation of silver(I)-POM compounds with solvent molecules (e. g. acetonitrile, DMSO) functioning as supporting ligands.[21a] The resulting materials are stabilized by hydrogen bonding frameworks, direct coordination of silver(I) by the POMs and Coulombic attraction between separate silver complexes and POMs. This strategy proved especially successful for the isolation of materials containing large polyoxotungstates[28-29,30] and decavanadate anions.[17b,17c]

The last major strategy for the synthesis of organic-inorganic silver(I)-isopolyoxometalates, in which the affinity of silver(I) to carboxylates is taken advantage of, was realized only for dodecatungstate containing compounds so far.[16c,29b,29c,31] The organic components applied in these reactions (e. g. nicotinic acid) bear additional carboxylate groups which coordinate to silver(I) ions. Due to the strength of this coordinative bond, these compounds are readily accessible under relatively mild reactions conditions (80 °C) from aqueous solutions.

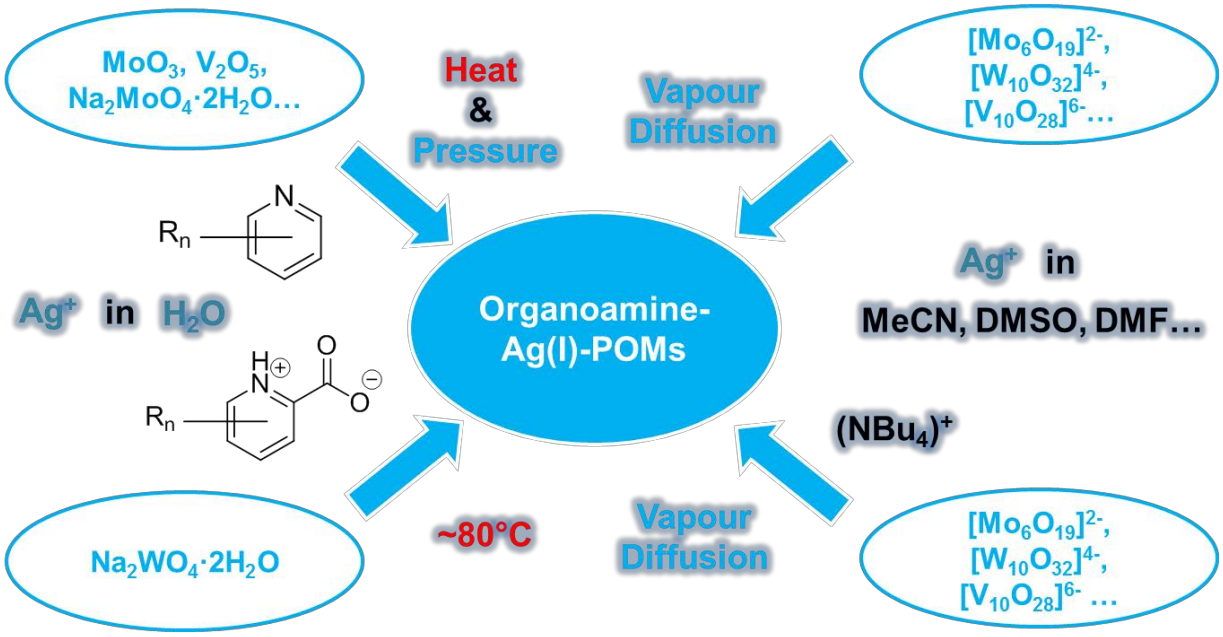

Scheme 1.1: General synthetic routes available for the synthesis of materials composed of the silver(I)-complexes and POMs.

A multitude of silver(I) heteropolyoxometalates was obtained and described in the literature following the same or similar procedures to the ones described above.[36] A slightly different synthetic strategy was applied for the isolation of organic-inorganic Anderson anion containing materials. These anions contain central Lewis-acidic metal cations such as Ni^{2+} or Cr^{3+}, which are surrounded by a condensed ring of six molybdates.[33-34] Thus, inorganic complex anions of the type $[M(OH_6)Mo_6O_{18}]^{n-}$ (M = Cr, Ni; n = 3 or 4) are readily assembled under mildly acidic conditions in aqueous solutions. Inorganic silver(I) POMs are crystallized upon the addition of a silver(I) salt. The isolation of the respective silver(I)-POMs containing organic ligands was accomplished by addition of pyridine carboxylic acid[33b] and histidine.[33c] As both ligands bear a carboxylate functionality, the strategy takes advantage of silver(I) affinity towards carboxylates, similarly to the synthetic procedures for silver(I) dodecatungstates as described above.

1.4. The Scope and Objectives of the Present Thesis[35]

There are three basic organizing forces for organic-inorganic hybrid materials: metal coordination, hydrogen bonds and stacking interactions.[37] Accordingly, the optimal ligand for the construction of a material assembled from silver(I) complexes and polyoxometalates, should show the chemical properties, allowing it to firmly coordinate to Ag(I) ions and establish a robust hydrogen bonding and π-π stacking interaction framework. Aromatic organoamine bases were extensively used for the assembly of these compounds (*vide supra*).

Although these organic molecules are fitting the profile of the ideal ligand, virtually all of the compounds described above have to be synthesized either under hydrothermal conditions or using large quantities of organic solvents. The major idea of the present thesis was to increase the strengths of these non-covalent interactions to such a degree, that it would be possible to assemble the target compounds in water at ambient conditions. To accomplish this task attention was turned to the probably most famous biomolecules, with a notoriously strong tendency towards non-covalent interactions: to purine bases.

Purine bases comprise a class of highly important biomolecules. It includes guanine and adenine – two of the four main constituents of DNA. DNA is the biopolymer known for the strength of its hydrogen bonds as well as stacking interactions.[38]

The methylated xanthine derivatives caffeine, theobromine and theophylline also belong to the class of purine bases. They are known as coffee and chocolate ingredients and found some pharmacological applications.[39] They also exhibit quite strong propensity for non-covalent interactions and were objects of several studies dedicated to the exploration of the nature of non-covalent forces.[40]

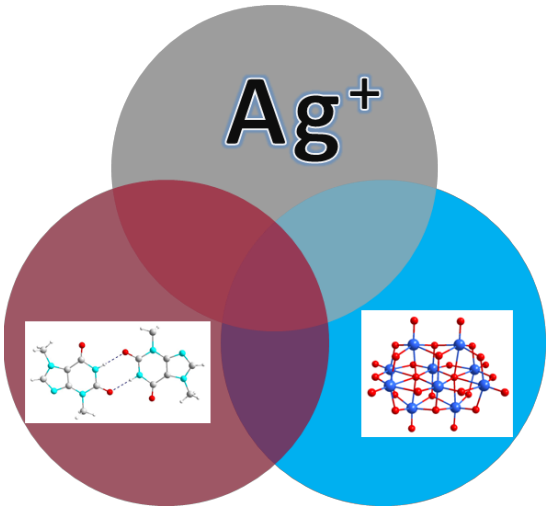

Figure 1.10: The scope of the present thesis.

Another interesting aspect of purine base chemistry, and an additional reason why these compounds attracted attention is the pharmacological effectiveness of some of the purine-silver(I) complexes. These compounds were proven to be active against respiratory pathogens, with an overall low toxicity.[41] Accordingly

promising is chemical and pharmacological research, but nevertheless there is only a limited amount of silver(I)-purine complexes that have been characterized crystallographically and were reported in the literature.[14] This is mostly due to the low solubility of purine derivatives and their silver(I) complexes, which makes their synthesis and the growth of single crystals as well as the acquisition of analytical data by spectroscopic measurements a challenging task.

Little is also known about purine-POM chemistry. So far only one compound containing a purine base and a POM was characterized crystallographically: $(NH_4)_2(caf)_4[H_4V_{10}O_{28}]\cdot 2H_2O$ (caf = caffeine).[42] Expectedly hydrogen bonding and stacking interactions play a decisive role in the definition of the crystal structure.

Due to these reasons, the choice of purines as the organic component was natural. Besides it was hoped to shed some light on the interactions between purine bases and POMs *in vivo*, as some POMs have been shown to exhibit quite profound physiological impact.[43] Accordingly, the scope was limited to the triangle displayed in Figure 1.10. Silver cations, purine bases and POMs build the vertices of the limiting triangle. The most intensely researched area in the scope of the present thesis is in the overlap of all three topics. There remains to be a lot to discover about the chemistry of the silver(I) complexes and POMs, silver(I)-purine complexes and compounds containing purine bases and POMs. Thus the overlaps on the sides of the triangle are considered as viable research topics within this thesis as well.

1.5. References

(1) Pope, M. T. In *Comp. Coord. Chem.*; Wilkinson, G., Ed.; Pergamon Press: Oxford, 1987; Vol. 3, p 1023.

(2) Berzellius, J. J. *Poggendorf's Ann. Phys. Chem.* **1826**, *6*, 369.

(3) a) Wang, X.-J.; Gui, L.-C.; Ni, Q.-L.; Liao, Y.-F.; Jiang, X.-F.; Tang, L.-H.; Zhang, Z.; Wu, Q. *CrystEngComm* **2008**, *10*, 1003; b) Long, D.-L.; Tsunashima, R.; Cronin, L. *Angew. Chem.* **2010**, *122*, 1780.

(4) Keggin, J. F. *Proc. R. Soc. Lond. A* **1934**, *144*, 75.

(5) Müller, A.; Krickemeyer, E.; Meyer, J.; Bögge, H.; Peters, F.; Plass, W.; Diemann, E.; Dillinger, S.; Nonnenbruch, F.; Randerath, M.; Menke, C. *Angew. Chem. Int. Ed.* **1995**, *34*, 2122.

(6) Müller, A.; Beckmann, E.; Bögge, H.; Schmidtmann, M.; Dress, A. *Angew. Chem. Int. Ed.* **2002**, *41*, 1162.

(7) Pradeep, C.; Long, D.-L.; Cronin, L. *Dalton Trans.* **2010**, *39*, 9443.

(8) Long, D.-L.; Abbas, H.; Kögerler, P.; Cronin, L. *J. Am. Chem. Soc.* **2004**, *126*, 13880.

(9) Long, D.-L.; Abbas, H.; Kögerler, P.; Cronin, L. *Angew. Chem. Int. Ed.* **2005**, *44*, 3415.

(10) Abbas, H.; Streb, C.; Pickering, A. L.; Neil, A. R.; Long, D.-L.; Cronin, L. *Cryst. Growth. & Des.* **2008**, *8*, 635.

(11) Upreti, S.; Ramanan, A. *Cryst. Growth. & Des.* **2006**, *6*, 2066.

(12) See section 1.2 for references.

(13) Dolbecq, A.; Dumas, E.; Mayer, C. R.; Mialane, P. *Chem. Rev.* **2010**, *110*, 6009.

(14) Meyer, G.; Pantenburg, I. In *Design and Construction of Coordination Polymers* Hong, M.-C., Chen, L., Eds.; John Wiley and Sons: 2009.

(15) Zhang, P.-p.; Peng, J.; Pang, H.-j.; Sha, J.-q.; Zhu, M.; Wang, D.-d.; Liu, M.-g. *CrystEngComm* **2011**, *13*, 3832.

(16) a) Lin, H.; Maggard, P. A. *Inorg. Chem.* **2008**, *47*, 8044; b) Hu, Y.; Luo, F.; Dong, F. *Chem. Comm.* **2011**, *47*, 761; c) Ren, C.-X.; Cheng, L.; Ye, B.-H.; Chen, X.-M. *Inorg. Chim. Acta* **2007**, *360*, 3741.

(17) a) Qi, Y.; Wang, E.; Li, J.; Li, Y. *J. Solid State Chem.* **2009**, *182*, 2640; b) McGlone, T.; Thiel, J.; Streb, C.; Long, D.-L.; Cronin, L. *Chem. Comm.* **2012**, *48*, 359; c) Streb, C.; Tsunashima, R.; MacLaren, D. A.; McGlone, T.; Akutagawa, T.; Nakamura, T.; Scandurra, A.; Pignataro, B.; Gadegaard, N.; Cronin, L. *Angew. Chem.* **2009**, *121*, 6612.

(18) Yan, B.; Maggard, P. A. *Inorg. Chem.* **2007**, *46*, 6640.

(19) Nyman, M.; Bonhomme, F. o.; M.Alam, T.; A.Rodriguez, M.; R.Cherry, B.; L.Krumhansl, J.; M.Nenoff, T.; M.Sattler, A. *Science* **2002**, *297*, 996.

(20) Lu, S.; Qin, S.; Ke, Y.; Li, J.; Pei, H.; Zhou, S.; Wu, X.; Du, W. *Cryst. Res. Technol.* **2004**, *39*, 89.

(21) a) Song, Y.-F.; Abbas, H.; Ritchie, C.; McMillian, N.; Long, D.-L.; Gadegaard, N.; Cronin, L. *J. Mater. Chem.* **2007**, *17*, 1903; b) Abbas, H.; Pickering, A. L.; Long, D.-L.; Kögerler, P.; Cronin, L. *Chem. Eur. J.* **2005**, *11*, 1071; c) Han, Z.; Gao, Y.; Hu, C. *Cryst.*

Growth. & Des. **2008**, *8*, 1261; d) Chen, L.-J.; He, X.; Xia, C.-K.; Zhang, Q.-Z.; Chen, J.-T.; Yang, W.-B.; Lu, C.-Z. *Cryst. Growth. & Des.* **2006**, *6*, 2076; e) Zhai, Q.-G.; Wu, X.-Y.; Chen, S.-M.; Zhao, Z.-G.; Lu, C.-Z. *Inorg. Chem.* **2007**, *46*, 5046; f) Yang, M.-X.; Chen, L.-J.; Lin, S.; Chen, X.-H.; Huang, H. *Dalton Trans.* **2011**, *40*, 1866; g) Liu, H.-Y.; Wu, H.; Ma, J.-F.; Liu, Y.-Y.; Yang, J.; Ma, J.-C. *Dalton Trans.* **2011**, *40*, 602; h) Liu, H.-Y.; Bo, L.; Yang, J.; Liu, Y.-Y.; Ma, J.-F.; Wu, H. *Dalton Trans.* **2011**, *40*, 9782; i) Li; Lan, Y.-Q.; Ma, J.-F.; Yang, J.; Wang, X.-H.; Su, Z.-M. *Inorg. Chem.* **2007**, *46*, 8283; j) Shi, Z.; Gu, X.; Peng, J.; Xin, Z. *Eur. J. Inorg. Chem.* **2005**, *2005*, 3811; k) Dong, B.-x.; Xu, Q. *Inorg. Chem.* **2009**, *48*, 5861.

(22) Wilson, E. F.; Abbas, H.; Duncombe, B. J.; Streb, C.; Long, D.-L.; Cronin, L. *J. Am. Chem. Soc.* **2008**, *130*, 13876.

(23) Abbas, H.; Pickering, A. L.; Long, D.-L.; Kögerler, P.; Cronin, L. *Chem. Eur. J.* **2005**, *11*, 1071.

(24) Allis, D. G.; Rarig, R. S.; Burkholder, E.; Zubieta, J. *J. Mol. Struct.* **2004**, *688*, 11.

(25) Chen, S.-M.; Lu, C.-Z.; Yu, Y.-Q.; Zhang, Q.-Z.; He, X. *Inorg. Chem. Commun.* **2004**, *7*, 1041.

(26) Gong, Y.; Wu, T.; Jiang, P. G.; Lin, J. H.; Yang, Y. X. *Inorg. Chem.* **2013**, *52*, 777.

(27) Burkholder, E.; Zubieta, J. *Solid State Sci.* **2004**, *6*, 1421.

(28) McGlone, T.; Streb, C.; Busquets-Fité, M.; Yan, J.; Gabb, D.; Long, D.-L.; Cronin, L. *Cryst. Growth. & Des.* **2011**, *11*, 2471.

(29) a) Streb, C.; Ritchie, C.; Long, D.-L.; Kögerler, P.; Cronin, L. *Angew. Chem.* **2007**, *119*, 7723; b) Zhang, C.-J.; Chen, Y.-G.; Pang, H.-J.; Shi, D.-M.; Hu, M.-X.; Li, J. *Inorg. Chem. Commun.* **2008**, *11*, 765; c) Yang, X.-D.; Chen, Y.-G.; Zhang, C.-J.; Kong, Q.-J.; Yao, F. *Solid State Sci.* **2011**, *13*, 476.

(30) McGlone, T.; Streb, C.; Long, D.-L.; Cronin, L. *Adv. Mater.* **2010**, *22*, 4275.

(31) Zhang, C.; Pang, H.; Hu, M.; Li, J.; Chen, Y. *J. Solid State Chem.* **2009**, *182*, 1772.

(32) The Anderson anions of type A have the general formula $[XO_6M_6O_{18}]^{m-}$ (X is usually a late main group element), the respective anions of type C – $[XO_{6-n}(OH)_nM_6O_{18}]^{(8-n)-}$ (X =Pt(IV), n = 0-5). For full discussion see: Wery, A. S. J.; Gutiérrez-Zorrilla, J. M.; Luque, A.; Ugalde, M.; Román, P.; Lezama, L.; Rojo, T. Acta Chem. Scand. 1998, 52, 1194-1201.

(33) a) An, H.; Li, Y.; Xiao, D.; Wang, E.; Sun, C. *Cryst. Growth. & Des.* **2006**, *6*, 1107; b) An, H.; Li, Y.; Wang, E.; Xiao, D.; Sun, C.; Xu, L. *Inorg. Chem.* **2005**, *44*, 6062; c) Zhang, P.-P.; Peng, J.; Tian, A.-X.; Pang, H.-J.; Chen, Y.; Zhu, M.; Wang, D.-D.; Liu, M.-G.; Wang, Y.-H. *J. Coord. Chem.* **2010**, *63*, 3610.

(34) Liu, F.-X.; Marchal-Roch, C.; Dambournet, D.; Acker, A.; Marrot, J.; Sécheresse, F. *Eur. J. Inorg. Chem.* **2008**, *2008*, 2191.

(35) Kulikov, V.; Meyer, G. *Cryst. Growth. & Des.* **2013**, *13*, 2916.

(36) a) Limei, D.; Wansheng, Y.; Enbo, W.; Shuixing, W.; Zhongmin, S.; Qinghua, D.; Yi, Z.; Yong, F. *Cryst. Growth. & Des.* **2009**, *9*, 2110; b) Xiu-li, W.; Hai-liang, H.; Ai-xiang, T. *Cryst. Growth. & Des.* **2010**, *10*, 4786; c) Nogueira, H.; Paz, F. A.; Teixeira, P.; Klinowski, J. *Chem. Comm.* **2006**, 2953.

(37) Roesky, H. W.; Andruh, M. *Coord. Chem. Rev.* **2003**, *236*, 91.

(38) Voet, D.; Voet, J. G. In *Biochemistry*; 4 ed.; Recta, P., Kalkut, J., Eds.; John Wiley & Sons, Inc.: United States of America, 2011, p 1145.

(39) Biradha, K.; Samai, S.; Maity, A. C.; Goswami, S. *Cryst. Growth. & Des.* **2010**, *10*, 937.

(40) a) Ford, K. A.; Ebisuzaki, Y.; Boyle, P. D. *Acta Cryst. C* **1998**, *54*, 1980; b) Carlucci, L.; Gavezzotti, A. *Chem. Eur. J.* **2005**, *11*, 271; c) Fucke, K.; McIntyre, G. J.; Wilkinson, C.; Henry, M.; Howard, J. A. K.; Steed, J. W. *Cryst. Growth. & Des.* **2012**, *12*, 1395.

(41) Kascatan-Nebioglu, A.; Melaiye, A.; Hindi, K.; Durmus, S.; Panzner, M. J.; Hogue, L. A.; Mallett, R. J.; Hovis, C. E.; Coughenour, M.; Crosby, S. D.; Milsted, A.; Ely, D. L.; Tessier, C. A.; Cannon, C. L.; Youngs, W. J. *J. Med. Chem.* **2006**, *49*, 6811.

(42) Zhai, H.; Liu, S.; Peng, J.; Hu, N.; Jia, H. *J. Chem. Crystallogr.* **2004**, *34*, 541.

(43) Rhule, J. T.; Hill, C. L.; Judd, D. A.; Schinazi, R. F. *Chem. Rev.* **1998**, *98*, 327.

2. A Novel Strategy for the Synthetic Assembly of Inorganic-Organic Silver(I)-Polyoxometalate Hybrid Structures Employing Non-Covalent Interactions between Theobromine Ligands[1]

2.1 Synthetic Strategy

Theobromine (thb) (**2.1**) was chosen among the purine bases for the present work as it combines an acceptable solubility with the ability to build amide-to-amide H-bonding interactions building symmetrical dimers[2] (via N1-H and O6, see Figure 2.1 for atom numbering) and affinity to silver(I) (by coordination via N9). The purine ring is capable of stacking interactions as well, stabilizing crystal structures containing theobromine in the third dimension.

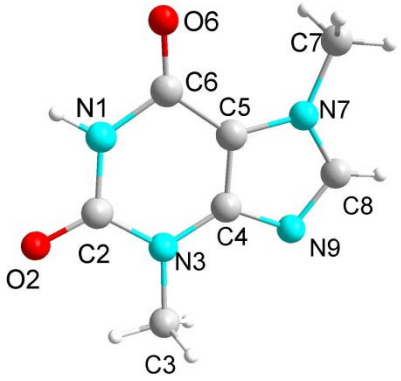

Figure 2.1. Atom numbering scheme for theobromine (**2.1**).

Despite these fortunate properties sufficient amounts of theobromine can be dissolved in most solvents only upon addition of a strong acid or base. Perchloric acid was chosen as a strong acid with a weakly coordinating conjugate base. The perchlorate anion does not disturb the crystallization by coordinating to silver(I) ions in the solution and does not coordinate to Ag^+ in silver(I)-theobromine complexes in the solid state (see section "Crystal Structures" for a detailed discussion).

$[Ag(thb)_2]ClO_4$ (**2.2**) and $[Ag(thb)_2(H_2O)]ClO_4$ (**2.3**) were obtained by crystallization from methanolic (**2.2**) and aqueous (**2.3**) solutions. The starting materials were thb and silver(I) perchlorate. They were dissolved in respective solvents acidified by perchloric acid. Addition of sodium dichromate(VI) to a strongly acidified solution of silver(I) nitrate and theobromine yielded $[Ag(thb)_2]_2[Cr_2O_7]\cdot 0.5H_2O$ (**2.5**). The formation of **2.5** even under strongly acidic conditions, under which the thb molecules are protonated,[3] hints at the high thermodynamic stability of the compound. The largest contribution to its stability should be expected from

silver(I) - dichromate interactions, as silver(I) dichromate(VI), $Ag_2Cr_2O_7$, is a notoriously stable solid itself.

As mentioned before, the above reactions need to be performed in acidic media in order to dissolve a sufficient amount of theobromine. Therefore the choice of polyoxometalate counterions to $[Ag(thb)_2]^+$ complexes was fairly limited as the POMs, except dichromate, are stable only in moderate pH ranges (Figure 2.2).

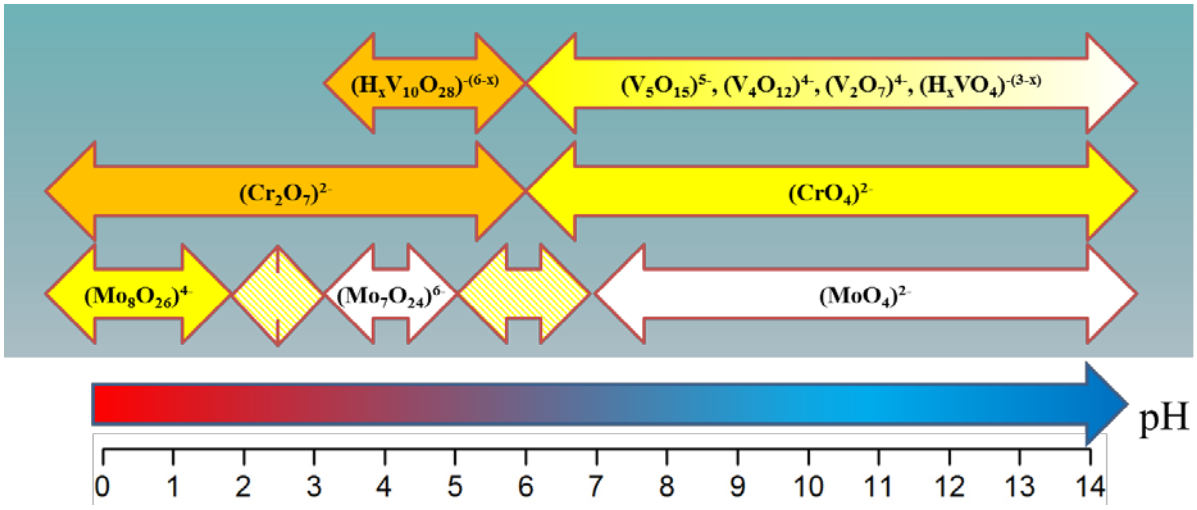

Figure 2.2. Stability ranges of selected POMs in aqueous solutions.[4]

Accidentally, it was discovered that after neutralizing acidic theobromine solutions with NaOH, the purine base does not precipitate right away, but remains in the solution for days or even weeks. It might very well be the case that the increased solvent polarity, due to $NaClO_4$, dissolved in the solution as a result of the neutralization, kinetically hinders the precipitation. The assumption is reinforced by the fact that after dissolving theobromine in distilled water by heating, it re-precipitates after cooling to room temperature quite fast.

After this discovery the pH values of the theobromine solutions could be adjusted at will. These were adjusted to the values within the scope of stability of the respective polyoxometalates as shown in Figure 2.2 and after addition of silver(I) perchlorate the respective target compound precipitated (Figure 2.3).

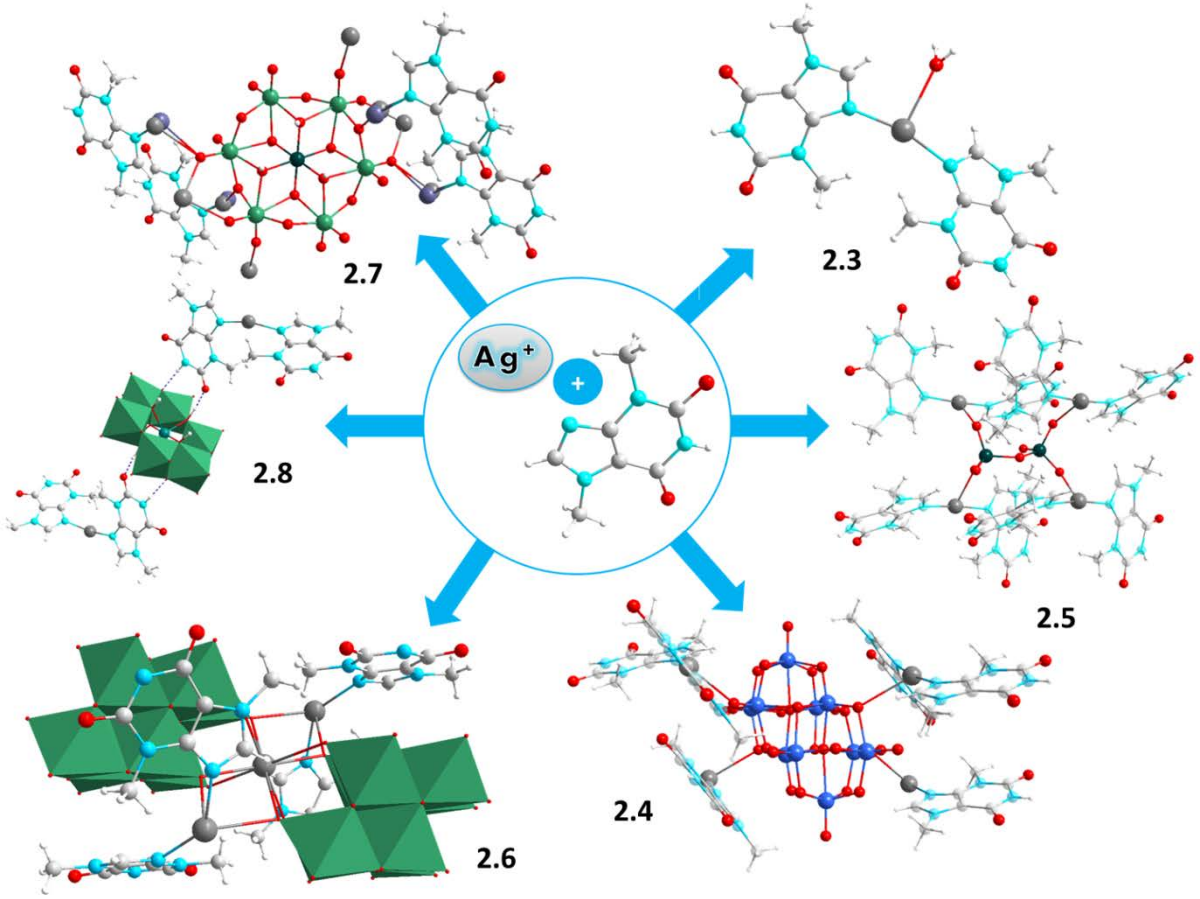

Figure 2.3. An overview of compounds accessible via the discussed strategy. Ag metallic grey, C grey, Cl green, Cr dark green, H white, Mo sea green, Ni turquoise, O red, V light blue. Same colour scheme applies to the subsequent illustrations.

Accordingly, $[Ag(thb)_2]_2[H_4V_{10}O_{28}]\cdot 3H_2O$ (**2.4**) was obtained by dissolving sodium metavanadate(V), $NaVO_3$, adding solutions of theobromine and silver(I) and adjusting the final pH to 2.5. Employing sodium molybdate(VI), Na_2MoO_4, instead of metavanadate(V), yielded $[Ag(thb)_2(H_2O)]_2(H_3O)\{Ag[\beta\text{-}Mo_8O_{26}]\}\cdot 4H_2O$ (**2.6**) under similar reaction conditions, with the pH value adjusted to 4.0.

Anderson type B anions are known to be stable at pH = 4.5.[5] Accordingly, the preparation of the same solution as was used for the synthesis of **2.6**, pH adjustment to 4.5 and addition of a Cr^{3+} yielded $[Ag(thb)]_2[Ag(Cr(OH)_6Mo_6O_{18})]\cdot 2H_2O$ (**2.7**). $[Ag(thb)_2]_2(H_3O)_4[Ni(OH)_6Mo_6O_{18}](CO_3)\cdot 13H_2O$ (**2.8**) was prepared accordingly.

2.2 Crystal Structures

Before attempting the synthesis of the organic-inorganic silver(I)-POM materials, structural properties of the simpler compounds containing perchlorate-ions instead of POMs were evaluated. Thus, the structural discussion starts with these materials in order to be able to explain the non-covalent interaction networks of the subsequent POM containing compounds.

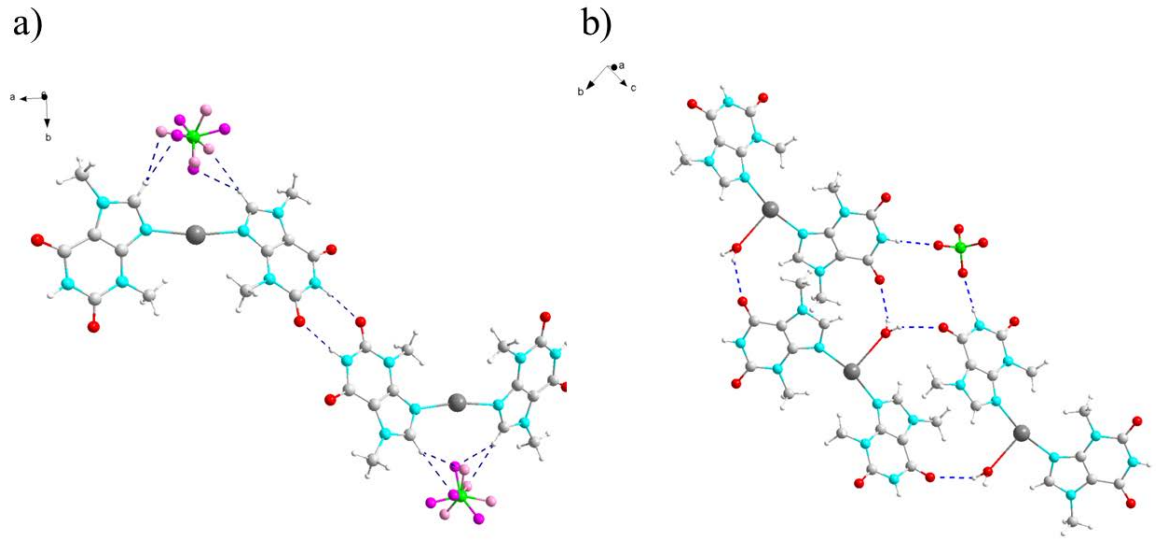

Figure 2.4. a) Amide-to-amide theobromine dimer joining two di-theobromine-silver(I) complexes in **2.2**. b) H-bonding framework of **2.3**. The positions of oxygen atoms of perchlorate are split in a 50:50 ratio. Split O magenta/rose.

$[Ag(thb)_2]ClO_4$ (2.2) and $[Ag(thb)_2(H_2O)]ClO_4$ (2.3). Despite obvious chemical similarities between **2.2** and **2.3**, the H-bonding frameworks, stabilizing their structures, are significantly different (Figure 2.4). **2.2** is stabilized by amide-to-amide H-bonds between theobromine ligands (N···O 2.8481(3) Å, N-H···O 173.50(1)°), geometrically similar to the adenine-thymine base pair in the DNA.[6] These dimers are readily built by theobromine molecules and are encountered in the subsequently described compounds **2.4-6** with approximately the same geometry.

The H atom bound to C8 is quite acidic, due to neighbouring N atoms of the imidazole rings, and accordingly conducts H bonding interactions with the perchlorate oxygen atoms (Figure 2.4a). These interactions are rather weak due to the low electronegativity difference between C

and H and accordingly are not suitable to attenuate the thermal motion of the accepting oxygen atoms. The structural stabilization in the third dimension is facilitated by stacking interactions between theobromine molecules (not shown, see below for a thorough discussion).

The H-bond framework of compound **2.3** is not built up by self-pairing theobromine ligands but shows a different pattern of H-bonding interactions (Figure 2.4b). The carbonyl oxygen atom O6 conducts an H-bond to the water molecule coordinating to silver(I), while the amide proton is donated to perchlorate oxygen atoms. This N1-H1···O-Cl non-covalent interaction is obviously stronger than the corresponding C8-H8···O-Cl bond in **2.2**, as now the perchlorate oxygen atoms are held firmly in place (compare Figures 2.4a and 2.4b). This framework extends in two dimensions and is stabilized by stacking interactions of theobromine molecules in the third one (not shown, see below).

The distances between Ag^+ and C3 of the theobromine ligand in **2.2** and **2.3** (3.39 and 3.43 Å, respectively) are both shorter than the sum of the van-der-Waals radii of Ag^+ and the methyl group (3.72 Å).[7] It is not clear if an agostic interaction exists between silver(I) and one of the protons of the methyl group,[8] or if this close distance is simply brought by the covalent theobromine framework. In any case a strong interaction is not expected, as it apparently does not significantly influence the complex geometry. Accordingly, Ag-H interactions in **2.2**, **2.3** and in all of the subsequent compounds are not indicated.

Isopolyoxometalate based materials. The basic principle of the frameworks of H-bonds in the POM-based compounds **2.4** to **2.6** is quite similar to **2.2** and **2.3**, despite the more complex large anions. All three compounds exhibit two crystallographically different theobromine ligands. The H-bonding interactions built by these molecules with surrounding entities can be considered a mixture of the networks of intermolecular interactions of **2.2** and **2.3**. One theobromine ligand stabilizes the structure by building amide-to-amide dimers and the other one conducts H-bonds either directly to POM anions or to water molecules. The stacking interactions perpendicular to the hydrogen bonds are also quite common. Theobromine molecules conduct additional stacking interactions with the POM anions, which are discussed below for each compound individually.

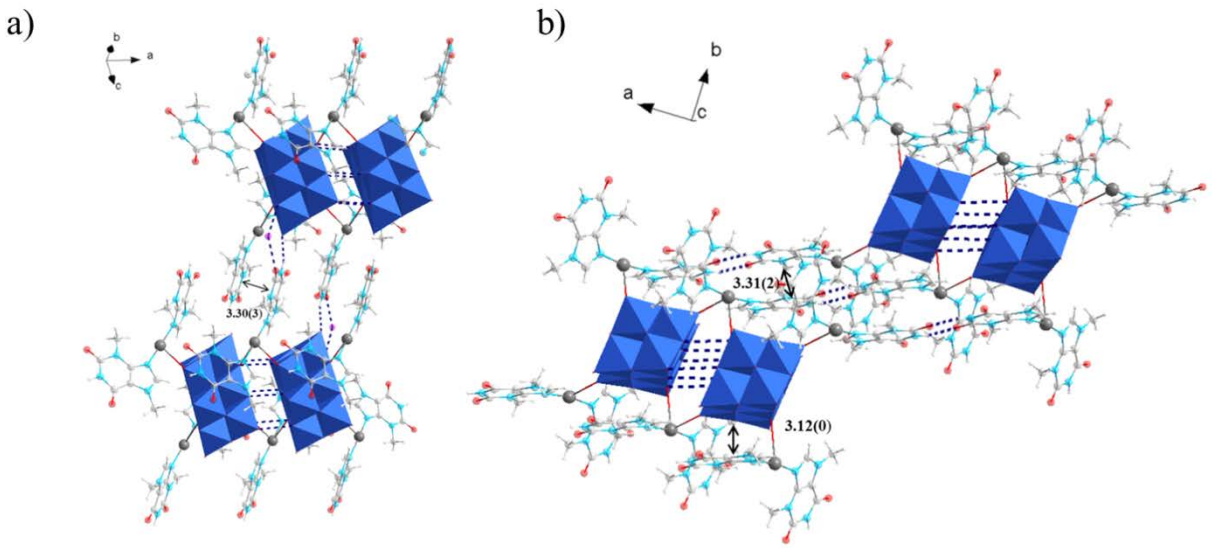

Figure 2.5. Parts of the crystal structure of **2.4**. a) Connection between the silver(I)-decavanadate(V) chains facilitated by H-bonds between amide proton of theobromine and POM as well as carbonyl oxygen, water molecule and POM. b) The same interconnection accomplished by theobromine self-pairing. Vanadate: blue polyhedra, distances are given in Å.

$[Ag(thb)_2]_2[H_4V_{10}O_{28}]\cdot 3H_2O$ (2.4). The decavanadate(V) ions, $[H_4V_{10}O_{28}]^{2-}$, in **2.4** are interconnected via silver(I) ions and H-bonds building coordination polymers running along the crystallographic a-axis (Figure 2.5). The H-bonds are built between the protonated and deprotonated oxygen atoms of the adjacent decavanadate(V) anions. The exact positions of the protons between the decavanadate(V) anions could not be detected, but the interatomic distances around 3.05 Å between the oxygen atoms of the adjacent POMs indicate hydrogen bonding of intermediate strength.[9] Charge balance considerations demand four protons shared between two decavanadate(V) anions, but there are altogether six pairs of oxygen atoms located within H-bonding distances from each other. The X-ray diffraction analysis does not allow determining whether the protons are shared between four of these pairs or delocalized over all six.

The theobromine ligands accomplish the interconnections between the chains via H-bonding and stacking interactions as shown in Figure 2.5. One of the crystallographically different theobromine molecules resides virtually parallel to one of the faces of decavanadate(V) ions (Figure 2.5a, interplanar angle: ca. 4.5°). Given a distance of 2.99-3.34Å between the decavanadate(V) face and aromatic atoms of the purine ring, anion-π interactions are suggested.[10] Energetic consequences of this geometry will be discussed below.

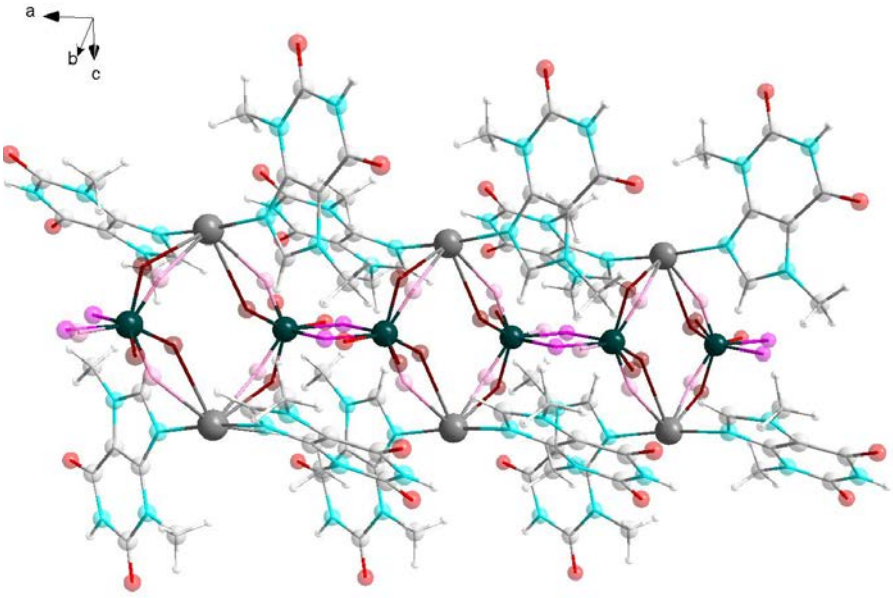

Figure 2.6. Ag(I)-Cr_2O_7 chains as part of the crystal structure of the room temperature modification of **2.5**. Cr: dark green; occupation of O-positions: dark red 64%, rose 36%, magenta 50%.

$[Ag(thb)_2]_2[Cr_2O_7]\cdot 0.5H_2O$ (2.5). The main structure defining motif of **2.5** are Ag(I)-Cr_2O_7 chains running along the crystallographic a-axis (Figure 2.6). Silver(I) cations connect dichromate(VI) units pairwise such that an 8-ring consisting of 2 Ag, 2 Cr and 4 O atoms is built. The terminal oxygen atoms are disordered in the ratio of 64% to 36%, due to thermal motions of the dichromate ions. Positions of the internal oxygen atoms of dichromate(VI) were split 50%/50%, due to overlapping thermal movements of the two parts of dichromate(VI) in opposite directions.

In order to attenuate the thermal motion of the dichromate(VI) anions, single crystal X-ray diffraction measurements were performed at low temperatures. During the data collection, a phase transition of **2.5** was detected. The temperature of the phase transition was determined by DSC analysis (Figure 2.7). Despite the very low heat exchange, indicating a second order phase transition, the transition temperature could be determined to be -83.2 °C.

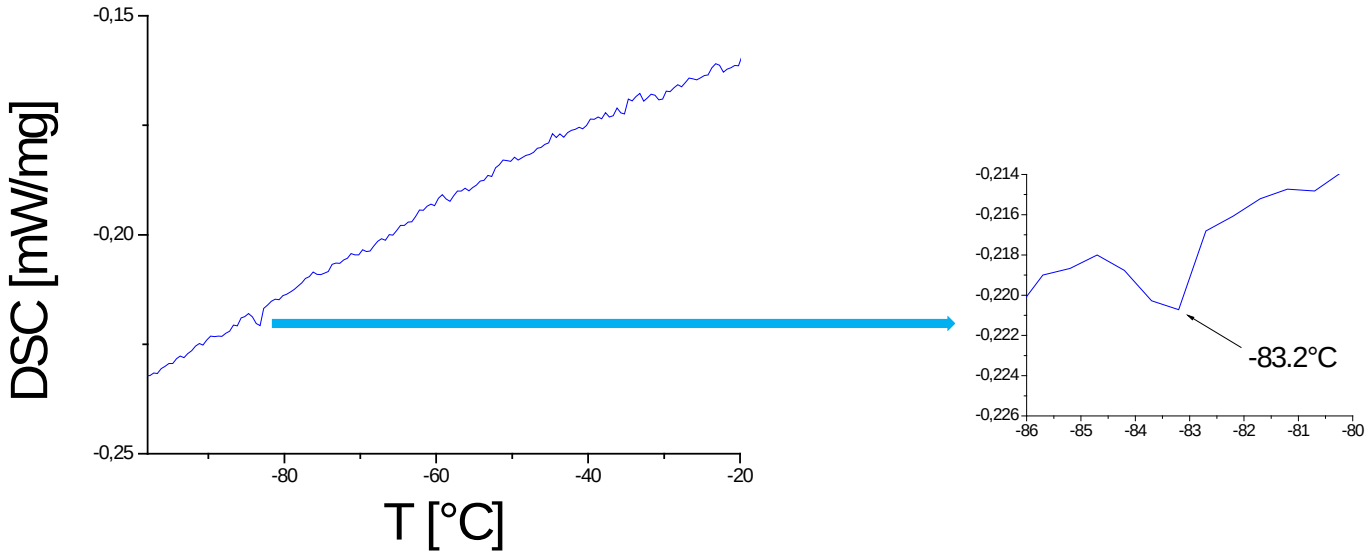

Figure 2.7: DSC-analysis of **2.5**.

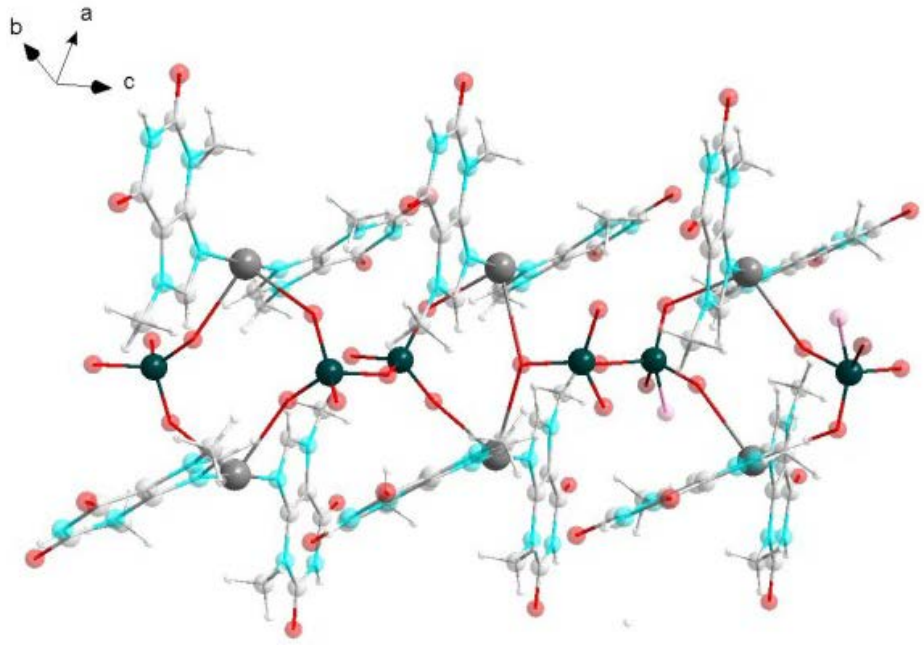

Figure 2.8. Silver(I)-dichromate chains in the low temperature modification of **2.5**. Occupation of oxygen positions: dark red 79%, rose 21%.

Structure determination at -173°C yielded a triclinic unit cell, but nearly four times as big as the one at room temperature (unit cell volume = 3980 $Å^3$ vs. 1027 $Å^3$ at room temperature). Accordingly, Z is increased from 1 to 4. Despite reduction in symmetry, which is quite common in phase transitions from higher to lower temperatures,[11] the silver(I)-dichromate(VI) chains, as described above, remain the main structure building motif (Figure 2.8). As expected for a second order phase transition, no fundamental change in the crystal structure occurred. The essential distinction of the low temperature modification is that the chains consist of alternating 7- and 8-membered rings of Ag, Cr and O atoms and run along the crystallographic c-axis. The Ag atoms occupy four different crystallographic positions. Two of these crystallographically inequivalent Ag atoms are interconnected by one O atom of dichromate in 7-membered rings, the other two build 8-membered rings.

The silver(I)-dichromate(VI) chains in both the high and low temperature phases are interconnected through H-bonding framework built by theobromine and water molecules quite similar to the one described for **2.4**. Stacking interactions between theobromine molecules are observed as well.

$[Ag(thb)_2(H_2O)]_2(H_3O)\{Ag[\beta\text{-}Mo_8O_{26}]\}\cdot 4H_2O$ (2.6). Similar to the previously described compounds, silver(I) octamolybdate(VI) chains connected by a framework consisting of H-bonds between self-pairing theobromine ligands, and H-bonds between theobromine ligands, water molecules and POMs, are the main

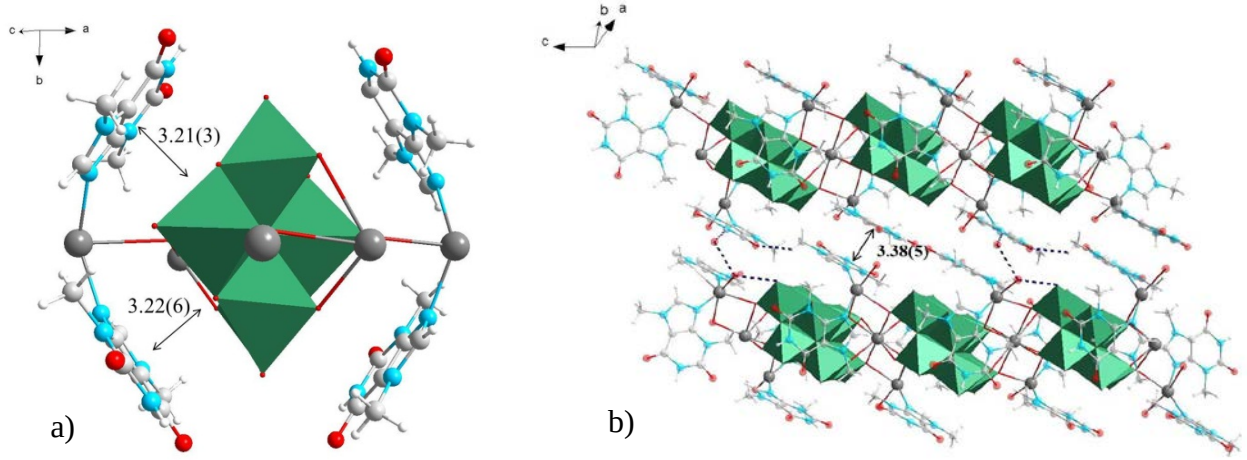

Figure 2.9. a) Coordinative surrounding of octamolybdate(VI) in **2.6**. B) Silver(I)-octamolybdate(VI) chains with indicated H-bonds and stacking interactions between theobromine ligands. Molybdate: sea-green polyhedra.

structural traits of **2.6**. Nonetheless there are some distinct characteristics of **2.6**.

The first remarkable feature of **2.6** is that every octamolybdate(VI) is surrounded by a frame of theobromine ligands (Figure 2.9a). Stacking interactions between theobromine and the polyoxomolybdate anion appear to be quite strong, not only due to the short interplanar distances between the ligand and the parallel POM surface (Figure 2.9a), but also due to an extremely bent geometry of the di-theobromine-silver(I) complexes (N-Ag-N: 137.166(1)°). The second remarkable aspect is the interconnection of octamolybdate(VI) anions via three silver(I) ions (Figure 2.9b), the usual case is one or two.[12] The central silver(I) ion displays a coordination number of 8 surrounded by four pairs of oxygen atoms from two different octamolybdate(VI) anions. The whole chain running along the crystallographic c-axis can be considered as one infinite POM, the central silver(I)-cations being part of the polyoxoanionic framework.

Anderson-anion based materials. In both $[Ag(thb)]_2[AgCr(OH)_6Mo_6O_{18}]\cdot 2H_2O$ (**2.7**) and $[Ag(thb)_2]_2(H_3O)_3[Ni(OH)_6Mo_6O_{18}](HCO_3)\cdot 14H_2O$ (**2.8**), there are no amide-to-amide dimers of theobromine. Ditheobromine silver(I) complexes are not encountered in **2.7**, substituted for mono-theobromine-silver(I) moieties H-bonded to the POM. On the other hand the ditheobromine-silver(I) complexes are encountered in **2.8**. Due to the large amount of water molecules in the crystal structure of this compound, the whole framework is distinctly different from the isopolyoxometalate based compounds **2.4-6**.

Both differences can be accounted for by the central cations of the Anderson anions. The strongly Lewis acidic Cr^{3+} in $[Cr(OH)_6Mo_6O_{18}]^{3-}$ renders the charge of the whole complex anion low and accordingly prone to build coordinative bonds to silver(I), which can be considered hard interactions compared to H-bonding. On the other hand, the less Lewis acidic Ni^{2+} with a lower positive charge renders the charge of the Anderson anion 4- in **2.8**. Accordingly the softer H-bonding interactions with water are more readily built by $[Ni(OH)_6Mo_6O_{18}]^{4-}$.

$[Ag(thb)]_2[AgCr(OH)_6Mo_6O_{18}]\cdot 2H_2O$ (2.7). The only familiar structural traits of **2.7** are chains of the Anderson anions running along the crystallographic b-axis. The anions are interconnected via hydrogen bonding between the protonated oxygen atoms of the central anionic moiety and the unprotonated oxygen atoms on the periphery of the anion (Figure 2.10).

Additionally the anions build coordinative bonds to silver(I) cations, which interconnect the chains. The plains of the so connected Anderson anions build an angle of 84° with each other. One crystallographically different silver(I) cation is coordinated to the theobromine molecule (right part of Figure 2.10). It is disordered due to the surrounding by eight oxygen ligands, one of which is an oscillating water molecule, and one a nitrogen donor ligand (Figure 2.11). The theobromine ligand builds a hydrogen bond with its amide proton to an Anderson anion, accomplishing an H-bond connection of two adjacent chains.

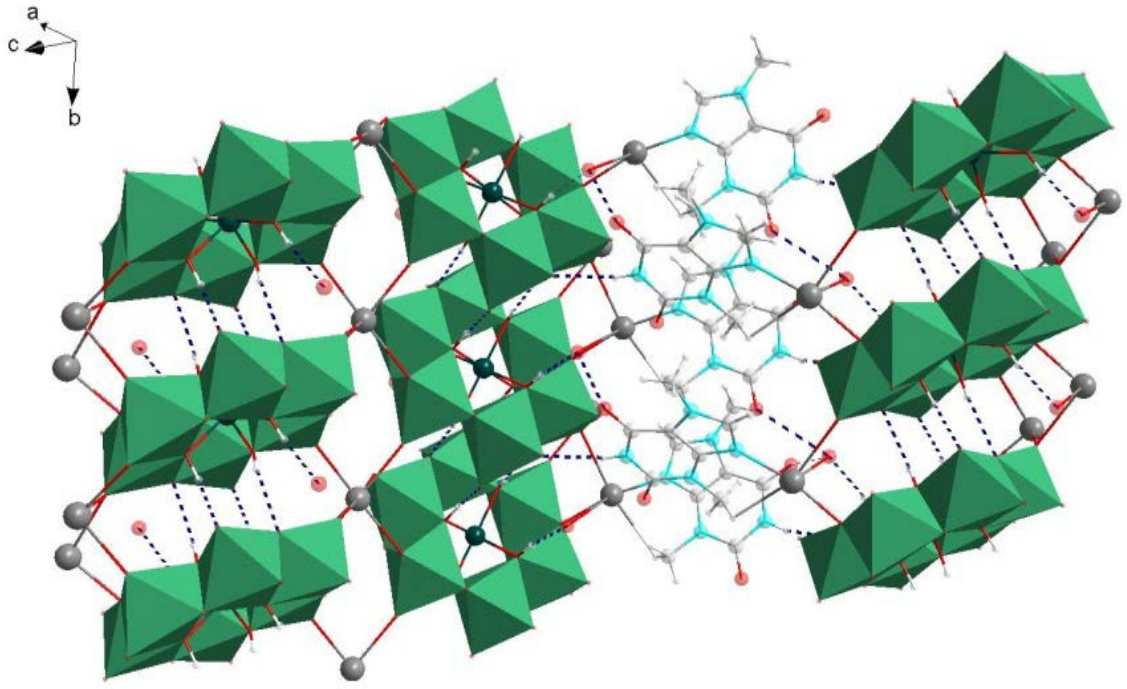

Figure 2.10: Connection of $[Cr(OH)_6Mo_6O_{18}]^{3-}$ chains by Ag^+ ions and $[Ag(thb)]^+$ fragments in **2.7**. Only the main part (70.7%) of the disordered Ag^+ ions is shown.

$[Ag(thb)_2]_2(H_3O)_3[Ni(OH)_6Mo_6O_{18}](HCO_3)\cdot 14H_2O$ (2.8): The crystal structure of **2.8** contains a lattice built by the Anderson anions interconnected by silver(I) in the c-axis direction and theobromine ligands connecting the silver(I)-POM chains in two orthogonal directions (Figure 2.12). This lattice serves as a frame for voids of a cuboid shape (Figure 2.12b, Figure 2.13). These "boxes" measure (14.5×12.1×6.2 = 1087.8) $Å^3$ and each one includes 13 water molecules, 4 hydronium ions and one carbonate ion.

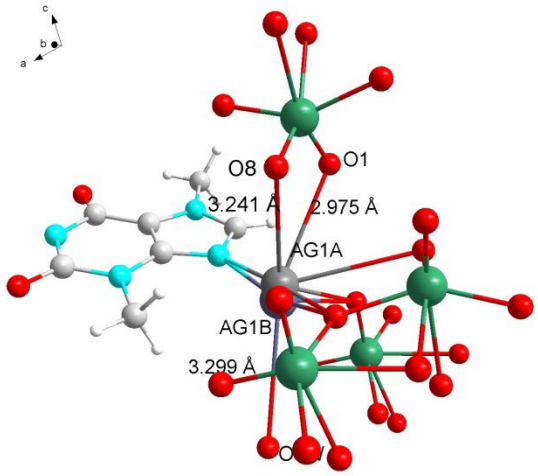

Figure 2.11: Coordinative surrounding of the disordered Ag(I)-Ion in compound **2.7**. The cation is disordered: AG1A/AG1B 70.1%/29.9%.

The H-bonding framework of **2.8** is significantly different from that of the compounds **2.2-6**. There are two crystallographically different theobromine ligands. The amide H-atom of one of these ligands conducts an H-bond to the carbonyl group of another one (Figure 2.12, top). The planes of the molecules are twisted by 63.7° with respect to one another. Accordingly, there is only one H-bond possible. The H-bond distance and angle indicate an H-bonding interaction of intermediate strength (N1···O16T 2.8184(3) Å, N1-H1···O16T 174.66(1)°).

a)

b)

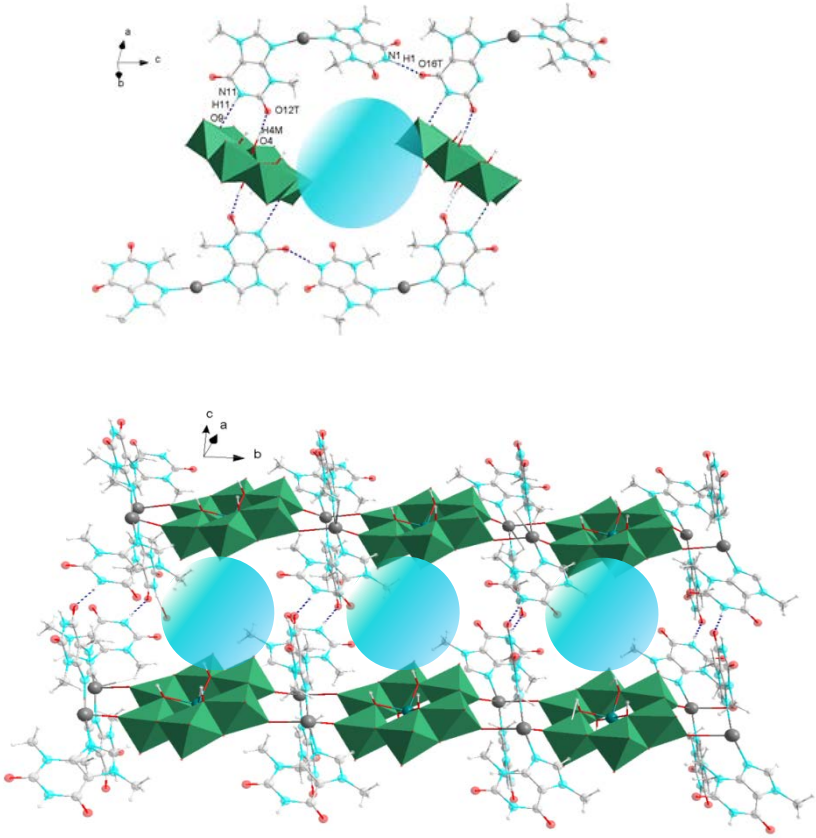

Figure 2.12. a) H-bonding framework in **2.8**. b) Molecular "boxes" built by Ag^{+} $[Ni(OH)_6Mo_6O_{18}]^{4-}$ chains and theobromine ligands. Ni: teal. The blue "bubbles" each include 14 water molecules, 4 hydronium ions and one bicarbonate ion.

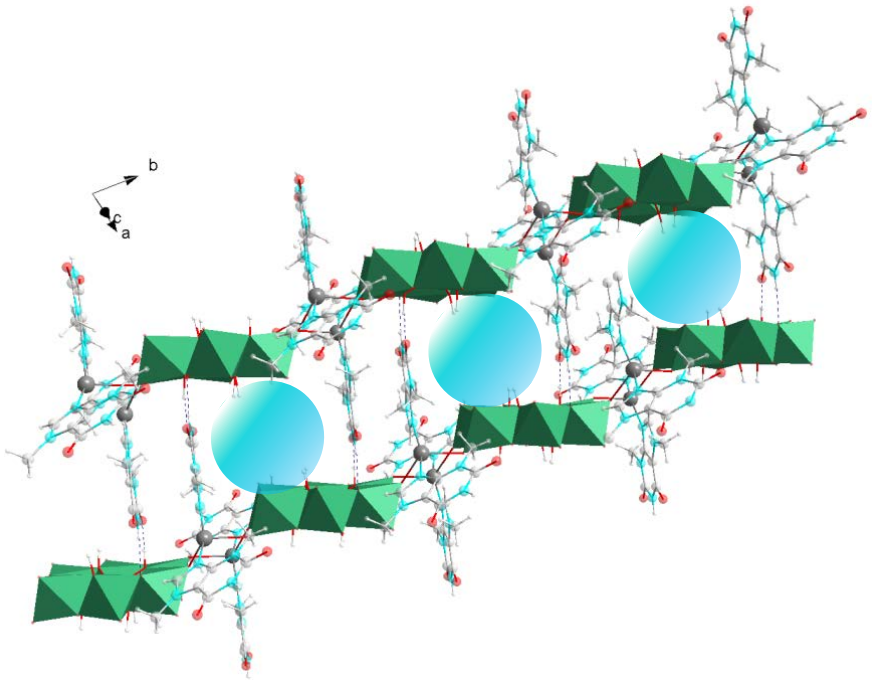

Figure 2.13. Hydrogen bonding framework in **2.8** perpendicular to silver(I)-nickel(II) hexamolybdate(VI) chains. Each blue bubble contains four H_3O^+-ions, 14 H_2O-molecules and one bicarbonate ion.

The theobromine acceptor ligand conducts H-bonding interactions with the Anderson anion, donating its amide proton and accepting a proton from the central moiety of the POM. The geometry indicates slightly stronger interactions, probably due to mutual synergistic effects of the both H-bonds (N11···O9 2.8190(3) Å, N11-H11···O9 173.25(2)°; O4···O12T 2.6275(3) Å, O4H4M···O12T 172.60(2)°).

2.3 Structural and Energetic Analysis

The reactions leading to the synthesis of the presented compounds can be considered as self-assembly of complex building blocks and simple chemical units: silver(I) ions, theobromine, water molecules and POMs. Energetic rationalization of the resulting crystal structures is considered an important task, as it allows for the design of further compounds on the basis of the obtained ones.

The self-assembly of all presented crystal structures can be traced back to four organizing forces: coordinative bonding, H-bonding as well stacking interactions between aromatic molecules and so-called anion-π stacking interactions.

Silver(I) ions and theobromine molecules build ditheobromine silver(I) complexes in almost all compounds discussed above (see Figures 5-9 and 11). Additionally, the metal ions are coordinated to POMs, connecting them into one-dimensional chains. The Ag-N and Ag-O coordination bond lengths are within the respective ranges of 2.14-2.28 Å and 2.57-2.80 Å for all compounds. These bond lengths are quite usual.[13] The minor differences in the bond lengths between the individual compounds are easily explainable by different ligand spheres or POM geometry.

The H-bond networks in **2.2-8** are quite robust and primarily formed by interactions of the amide group of theobromine either with an equivalent group or with an H-bond acceptor such as perchlorate or POM. The distances between the N1-amide H-bond donor and the O2-carbonyl acceptor in the amide-to-amide dimers are around 2.85 Å, the N1-H1···O2-angles are nearly 180°. These distances and angles are similar to those between hydrogen bonded atoms of the adenine-thymine base pair (2.85-2.92 Å) which also shows two H-bonds and a similar geometry.[6] The experimental value for the enthalpy of the adenine-thymine interactions was determined to amount to -12.1 kcal/mol (50.6 kJ/mol).[14]

To be more certain regarding the energetic value of amide-to-amide theobromine dimers PACHA (Partial atomic charges and hardness analysis) software for energetic evaluation was applied.[15,16] This is a facile theoretical approach based on spherical approximation of density functional equations.[17] The main advantages over other theoretical approaches evaluating solid-state structures are the usage of the atomic and crystal parameters from the CIF-files and the speed of calculations. The energetic evaluation of supramolecular interactions using PACHA is based on the quantity called “electrostatic balance”.

Table 2.1: Energetics of compound **2.2**.

Tecton	**Electrostatic Balance [kJ/mol]**	**Comment**
$2\times[Ag(thb)_2]^+$	-1721.1	Bound as amide-to-amide dimer
$2\times[Ag(thb)_2]^+$	-1678.0	Not interacting
Amide-to-amide H-bond interactions	**-43.1**	
$2\times[Ag(thb)_2]^+$	-1727.8	Bound as stacked dimer
$2\times[Ag(thb)_2]^+$	-1678.0	Not interacting
thb-thb stacking interactions	**-49.8**	

Table 2.2: Energetics of compound **2.6**.

Tecton (see Figure 2.14)	Electrostatic Balance (EB) [kJ/mol]	Comment
$2\times(Mo_8O_{26})^{4-}+Ag^{+}+3\times[Ag(thb)_2]^{+}+2\times thb$	-57503.3	Fragment **I**: Two molybdate units connected by 2 $Ag(thb)_2^{+}$-complexes and one Ag^{+}-ion, flanked by 2 $Ag(thb)_2^{+}$-complexes, one of which misses central Ag^{+}
$2\times(Mo_8O_{26})^{4-}+Ag^{+}+3\times[Ag(thb)_2]^{+}$	-56543.3	Fragment **II**: Same fragment without 2 thb molecules
$2\times thb$	-732.7	Fragment **III**
thb-$(Mo_8O_{26})^{4-}$-interactions	**-113.65**	Difference between the first EB and further two divided by 2

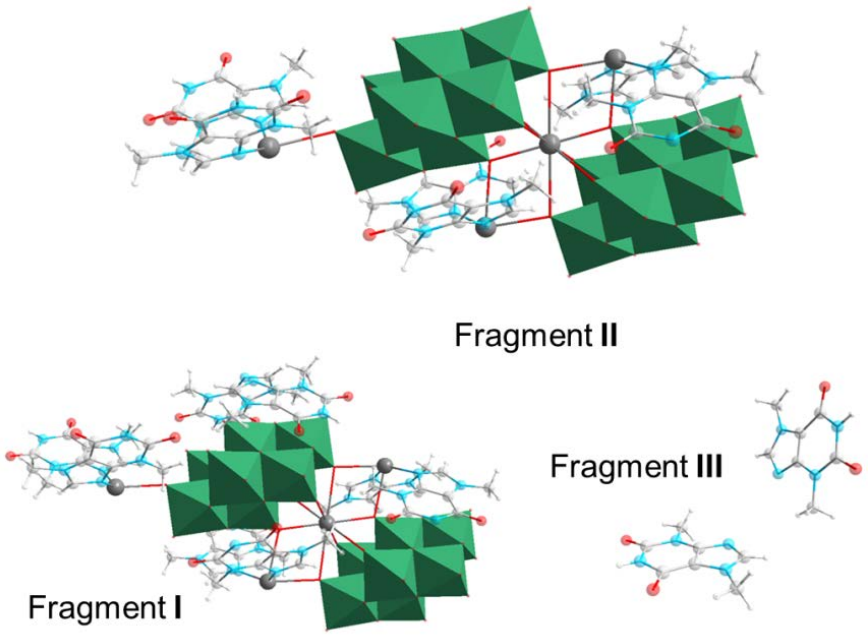

Figure 2.14: Fragments used for assessment of thb-$(Mo_8O_{26})^{4-}$ interactions in compound **2.6.**

In order to determine the energetic contribution of H-bonds the electrostatic balance of two amide-to-amide bound $[Ag(thb)_2]^{+}$ complexes was calculated and twice the electrostatic balance of the individual $[Ag(thb)_2]^{+}$ complexes in **2.2** subtracted (Table 2.1). The obtained value of -43.1 kJ/mol is in the same order of magnitude as the value obtained for adenine-thymine interactions stated above. As H-bond geometries between the amide group of theobromine and

other interaction partners are quite similar, their stabilization energies are considered to contribute similar amounts.

Stacking interactions of purine bases remained an area of continuous scientific interest throughout the last decade, due to its biological significance.[18] Quite profound theoretical and experimental investigations of theobromine dimers in the gas phase were accomplished by de Vries et al. regarding the formation of theobromine dimers in the gas phase.[19] The stacked theobromine dimer of similar geometry to that displayed in Figure 2.15 was assessed to be the most stable form of theobromine-theobromine interactions in the gas phase by density functional theory (DFT) calculations, which were verified by experimental results. The stacked dimer was estimated to be more stable than the amide-to-amide dimer by 4.3 kcal/mol. This rather surprising result is caused by the attractive dipole-dipole interactions between the carbonyl carbon atom of one theobromine ligand with the methylated nitrogen atom of the other (Figure 2.15). This attraction between electron poor carbon and electron rich nitrogen is much stronger than the repulsion between the methyl groups of the stacked theobromine molecules. Accordingly, the interplanar distance of the parallel theobromine molecules in compounds **2.2**-**6** is in general shorter than 3.3 Å, which is even less than the respective mean distance between DNA bases (3.4 Å).[20]

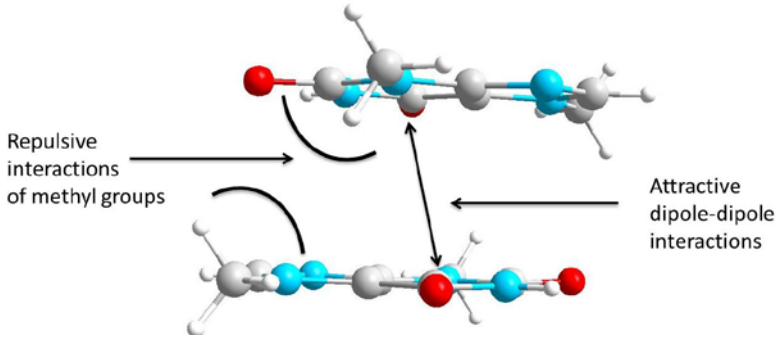

Figure 2.15. Attractive and repulsive interactions between stacked theobromine molecules.

The determination of the stabilization enthalpy of stacked theobromine dimers with the PACHA software based on the crystal structure of **2.2** yielded a value of -49.8 kJ/mol (Table 2.1). This value illustrates the same tendency that the stacking interactions in the synthesized compounds are even slightly more detrimental for the structural landscape than the amide-to-amide interactions discussed above.

Anion-π interactions gained a lot of attention in the last decade, due to the significant stabilizing effect.[10,21] Exploration of the interactions between anions and nucleic bases were in focus of this research due to their significance to the stabilization of RNA.[22] These forces are extremely sensitive towards the π-acidity of the aromatic rings with which they interact. For instance, the interactions between a phosphate residue and guanine were determined by *ab initio* calculations to destabilize the system by ≈ 20 kJ/mol, whereas the interactions of the same anion with a uracil ring are equally stabilizing.[22]

The theobromine ring system is π-acidic due to the electronegative nitrogen atoms and carbonyl groups comprising the purine ring. In compounds **2.2-8** this π-acidity is increased by coordination to silver(I) cations. It is therefore not surprising that the interaction energy between a theobromine ring and four oxygen atoms defining the parallel POM face in **2.6** was calculated to amount to -113.65 kJ/mol using the PACHA software (Table 2.2, Figure 2.14). This value is more than twice as high as the respective H-bonding and theobromine-theobromine stacking interactions and, hence, the strong distortion of the geometry of the $[Ag(thb)_2]^+$ complexes in **2.6** comes as no surprise.

In summary, H-bonds and stacking interactions contribute significant amounts of stabilization energy to the presented compounds and accordingly determine their three-dimensional crystal structures at room temperature.

These interactions obviously become less significant with increasing temperature. A large evolution of heat is observed in the DTA curves of compounds **2.4-7** in the temperature range 240 – 300 °C (Figures 2.22 – 2.25, see pages 44-46). This emission of heat is accompanied by a strong loss of mass in the TG-curve (30-50%). Both observations can be explained by an exothermic intramolecular redox reaction in course of which the ligand reduces Ag^+ and POMs and is oxidized to gaseous products (most likely carbon dioxide, nitrogen and water).

2.4 Conclusions

First silver(I)-purine POMs were synthesized setting an example of successful application of transition metal complexes of purines for the construction of POM-based supramolecular materials. In order to accomplish the synthesis, a novel strategy was developed and successfully applied. In general terms the experimental aspects of the strategy include dissolution of the

poorly soluble theobromine ligand in acidic media, pH adjustment to the desired value and addition of the POM-building salt. The subsequent addition of a silver(I) salt induces precipitation of the target compound.

According to the intentions of this thesis, the general advantage of the described synthetic approach is its simplicity. The POMs are assembled *in situ* from basic inorganic materials in aqueous solutions. The target materials are isolated by crystallization after addition of theobromine and silver(I) salt solutions to these reaction mixtures. The procedures do not require any precursors, organic solvents or high temperatures as are necessary for hydrothermal conditions.

The main organizing forces stabilizing the target materials are N-Ag^+ and O-Ag^+ coordinative bonds as well as non-covalent interactions between theobromine ligands and between theobromine ligands and polyoxoanions. The H-bonding framework of the structures is dominated by amide-to-amide theobromine dimers as well as amide-to-POM/water hydrogen bonds. π-π and anion-π stacking interactions are observed and considered to contribute to the overall structural stabilization quite appreciably. All isopolyoxometalate based structures contain silver(I)-POM coordination polymers interconnected by these non-covalent interactions. The Anderson anion based materials display two different structure landscapes depending on the Lewis acid in the center of the anion. In case of the hard Lewis acid Cr^{3+}, the POM content of the compound is increased and the stabilizing effect of the ligand is less pronounced than in the isopolyoxometalate containing materials. The softer Lewis acid Ni^{2+} induces building of a MOF stabilized by non-covalent interactions, which contains rectangular boxes filled with water molecules and carbonate.

The developed strategy is applicable to further molecules of the class of purine bases. Adenine, guanine and xanthine appear especially interesting ligands due to their ability to build robust networks based on H-bonding and stacking interactions as well as a multitude of potentially coordinating atoms. Thus, further research efforts will be directed towards the synthesis of their silver(I)-POM based compounds using the same approach.

The strategic approach applicable to the construction of materials based on other POMs. Future efforts aim at the synthesis and isolation of silver(I)-purine-W(VI)-, Nb(V)- and Ta(V)-POMs. Especially materials based on POMs of the heavier elements of the fifth group of the periodic table will be in focus, as no Ag(I)-Nb(V) or –Ta(V) POM has been isolated so far.

2.5 Experimental Section

All starting materials were purchased from commercial sources. The phase purities of bulk samples of compounds **2.2-7** were verified by X-ray powder diffraction on a STOE STADI transmission powder diffractometer (Cu-K_α radiation, λ = 1.5406 Å, see Figures 2.16 – 2.21 for measured and simulated spectra). FT-IR spectra were recorded on a Bruker IFS v/s spectrophotometer using KBr pellets. UV/Vis measurements were accomplished on a Varian Cary 5E spectrophotometer using KBr pellets as well. DTA and TG analyses were performed on a Netzsch STA 409 thermal analyzer. Elemental analyses were carried out on a HEKAtech Euro EA 3000 elemental analyser. The same equipment was used to characterize the compounds described in subsequent chapters unless stated otherwise.

Despite structural conformation by powder X-ray diffraction, the calculated and found values of the elemental analyses of the compounds **2.3-7** do not match exactly. The found values for C are always too low. This fact can be explained by minor inorganic impurities (e. g. $NaClO_4$) not observable in the noise of the powder X-ray diffractograms.

The stock solution of theobromine for the synthesis of the compounds **2.4**, **2.6**, **2.7** and **2.8** was prepared as follows: theobromine (180 mg, 1.00 mmol) was suspended in 50 ml of H_2O and brought into solution by addition of 6 ml of $HClO_4$ (60%). The pH was adjusted to the desired values by addition of roughly 12.5 ml of NaOH-solution (15%). pH values were controlled by a Bischof pH24 pH-meter calibrated in the buffer solutions immediately before use. All pH adjustments described below were accomplished upon addition of $HClO_4$ (60%) or NaOH (15%) solutions.

2.5.1 Synthetic Procedures

$[Ag(thb)_2]ClO_4$ (**2.2**): Theobromine (122 mg, 0.68 mmol) was dissolved in methanol (MeOH), (36 mL) by addition of $HClO_4$ (60%, 4 mL). $AgClO_4$ (70 mg, 0.34 mmol) in MeOH (34 mL) was added to this solution without stirring. The solution was left open in the dark and yielded colourless crystals within ten days. The mother liquor was filtered off; the crystals were washed twice with 10 ml portions of ice-cold MeOH and dried overnight over $CaCl_2$ in a desiccator. Yield: 120 mg (0.21 mmol, 62%). Elemental analysis calcd. (%) for $C_{14}H_{16}AgN_8O_8$: C 29.72, H 2.49, N 19.80; found: C 29.32, H 2.94, N 20.38; IR: ν (cm^{-1}) = 3470 (m), 3153 (m), 3123 (s),

3027 (s), 2883 (w), 2826 (s), 2750 (m), 2639 (m), 1697 (s), 1599 (s), 1551 (s), 1503 (s), 1458 (s), 1427 (s), 1365 (s), 1324 (m), 1289 (m), 1231 (s), 1201 (s), 1175 (s), 1102 (s), 1075 (s), 936 (w), 863 (m), 793 (m), 763 (m), 747 (m), 735 (m), 682 (s), 625 (s), 607 (m), 516 (s), 452 (s), 435 (m); UV/Vis: λ (nm) = 201, 216, 277.

$[Ag(thb)_2(H_2O)]ClO_4$ (**2.3**): Theobromine (180 mg, 1.00 mmol) was dissolved in 50 mL of water by addition of 6 ml of 60%-$HClO_4$. $AgClO_4$ (104 mg, 0.50 mmol) in water (50 mL) was added to this solution with stirring all at once. The solution was left open for two months, after which the mother liquor was filtered off and the obtained colourless crystals washed twice with 10 mL portions of cold water. 95 mg of 3 were obtained after drying overnight over $CaCl_2$ in a desiccator. Yield: 95 mg (0.16 mmol, 32%). Elemental analysis calcd. (%) for $C_{14}H_{18}AgClN_8O_9$: C 29.60, H 2.82, N 19.73; found: C 28.25, H 3.00, N 19.72; IR: ν (cm^{-1}) = 3582 (m), 3522 (m), 3371 (w), 3240 (s), 3122 (s), 3123 (s), 3070 (m), 2957 (w), 2827 (w), 2779 (w), 1695 (s), 1595 (s), 1551 (s), 1501 (s), 1464 (s), 1414 (m), 1366 (s), 1315 (w), 1285 (w), 1221 (s), 1082 (s), 937 (w), 874 (w), 789 (m), 744 (s), 681 (m), 615 (s), 515 (m), 449 (s).

$[Ag(thb)_2]_2[H_4V_{10}O_{28}]\cdot 3H_2O$ (**2.4**): $NaVO_3$ (400 mg, 3.28 mmol) was suspended in 80 ml of the stock solution of theobromine (180 mg, 1.00 mmol) of pH 4.0 and diluted with 12 ml of water. The suspension was heated to 55°C and the resulting pH of 5.4 was decreased to 2.6 by addition of 1.8 ml of aqueous $HClO_4$ solution (2%). The red suspension was allowed to cool to 40°C with stirring and the resultant pH of 3.4 was decreased to 2.9 by addition of further 0.1 ml of aqueous $HClO_4$ solution (2%). The yellow solution was separated from the red solid by filtration through medium-porosity filter paper. 50 ml of the aqueous solution of $AgClO_4$ (104 mg, 0.50 mmol) were added very slowly to the reaction mixture. Orange crystals appeared after eight days in the closed reaction vessel. Yield: 290 mg (0.15 mmol, 60% based on $AgClO_4$). Elemental analysis calcd. (%) for $C_{28}H_{42}Ag_2N_{16}O_{39}V_{10}$: C 17.23, H 2.17, N 11.48; found: C 18.63, H 2.22, N 11.96; IR: ν (cm^{-1}) = 3420 (br, s), 3165 (w), 3115 (m), 3032 (m), 2827 (m), 1695 (s), 1670 (s), 1593 (m), 1548 (s), 1487 (m), 1454 (m), 1367 (m), 1294 (m), 1225 (s), 1141 (s), 1112 (s), 1090 (s), 970 (m), 960 (m), 847 (m), 827 (m), 763 (w), 750 (w), 732 (w), 682 (m), 627 (m), 509 (w), 455 (m), 422 (w); UV/Vis: λ (nm) = 207, 217, 277.

$[Ag(thb)_2]_2[Cr_2O_7]\cdot 0.5H_2O$ (**2.5**): Theobromine (180 mg, 1.00 mmol) was dissolved in 50 mL of water by addition of 5 ml of 60%-$HClO_4$. $Na_2Cr_2O_7$ (262 mg, 1.00 mmol) was dissolved in

35 ml of water and added to the theobromine solution. $AgClO_4$ (207 mg, 1.00 mmol) in water (50 mL) was added to the reaction mixture without stirring. After one day orange block-shaped crystals precipitated. The mother liquor was decanted after one week, the crystals dried overnight over $CaCl_2$ in a desiccator. Yield: 120 mg (0.10 mmol, 40% based on theobromine). Elemental analysis calcd. (%) for $C_{28}H_{33}Ag_2Cr_2N_{16}O_{15.5}$: C 28.75, H 2.74, N 19.17; found: C 27.70, H 3.14, N 19.53; IR: ν (cm^{-1}) = 3601 (w), 3526 (w), 3119 (m), 3028 (s), 2826 (w), 2791 (m), 1707 (s), 1672 (s), 1601 (m), 1549 (s), 1468 (w), 1414 (w), 1363 (m), 1313 (m), 1288 (m), 1231 (m), 1198 (m), 1141 (m), 1082 (w), 1043 (w), 935 (s), 878 (w), 845 (w), 677 (m), 744 (m), 609 (m), 515 (m), 449 (m). UV/Vis: λ (nm) = 205, 276, 380.

$[Ag(thb)_2(H_2O)]_2(H_3O)[Ag(\beta\text{-}Mo_8O_{26})]\cdot 4H_2O$ (**2.6**): 45 ml of the stock solution of theobromine (108 mg, 0.60 mmol) of pH 3.1 was added to the solution of Na_2MoO_4 (443 mg, 1.8 mmol) in 60 ml of water at pH 4.5. $AgClO_4$ (124 mg, 0.6 mmol) dissolved in 6 ml water was added over the course of 15 min to the reaction mixture. The final pH was adjusted to 4.0. The yellow solution was filtered after 5 hours. The yellow residue was discarded. The reaction mixture was left in the fume hood closed by perforated PARAFILM® for three weeks, after which the product crystallized in yellow blocks. Yield: 42 mg (0.02 mmol, 13% based on theobromine). Elemental analysis calcd. (%) for $C_{28}H_{47}Ag_3Mo_8N_{16}O_{41}$: C 14.28, H 2.01, N 9.52; found: C 13.32, H 2.11, N 8.95; IR: ν (cm^{-1}) = 3458 (br, s), 3121 (w), 3036 (w), 2837 (m), 1693 (br, s), 1597 (w), 1553 (m), 1497 (m), 1456 (w), 1425 (w), 1367 (m), 1292 (w), 1227 (m), 1199 (w), 1144 (s), 1117 (s), 1089 (s), 943 (m), 912 (m), 837 (m), 715 (br, m), 685 (w), 627(m), 555 (w), 515 (m), 455 (w), 411 (w). UV/Vis: λ (nm) = 208, 222, 288.

$[Ag(thb)]_2[Ag(Cr(OH)_6Mo_6O_{18})]\cdot 2H_2O$ (**2.7**): The pH value of the stock solution of theobromine (180 mg, 1.00 mmol, 69 ml) was brought to 4.5, while heating the solution to 80°C. $Na_2MoO_4\cdot 2H_2O$ (730 mg, 2.97 mmol) was added to the solution and the pH was readjusted to 4.5 with $HClO_4$ (2%). $Cr(NO_3)_3$ (120 mg, 0.50 mmol) in 10 mL of water was added to the solution, after which $AgClO_4$ (338 mg, 1.50 mmol) was added in 15 mL of water. A yellow solid precipitated, which was filtered off twice through a 2 μm porosity filter. The yellow solid (160 mg) could not be identified by powder XRD and was discarded. A rose-coloured crystalline product precipitated within a week; the mother liquor was filtered off through a Büchner funnel with suction. Yield: 430 mg (0.25 mmol, 50%). Elemental analysis calcd. (%) for

$C_{14}H_{26}Ag_3CrN_8Mo_6O_{30}$: C 9.68, H 1.51, N 6.45; found: C 8.87, H 1.81, N 5.35; IR: ν (cm^{-1}) = 3470 (br, s), 3167 (br, w), 3115 (w), 3036 (w), 2827 (w), 1693 (s), 1670 (s), 1595 (m), 1551 (s), 1487 (m), 1454 (m), 1412 (w), 1366 (m), 1294 (m), 1225 (m), 1142 (s), 1113 (s), 1087 (s), 943 (s), 889 (s), 636 (s), 575 (w), 511 (w), 413 (s). UV/Vis: λ (nm) = 218, 272.

$[Ag(thb)_2]_2(H_3O)_3[Ni(OH)_6Mo_6O_{18}](HCO_3)\cdot 14H_2O$ (**2.8**): Neat $NiCO_3\cdot 2Ni(OH)_2\cdot 4H_2O$ (7.5 mg, 0.02 mmol) and Na_2MoO_4 (99 mg, 0.4 mmol) were added to 9 ml of the stock solution of theobromine (27 mg, 0.15 mmol) of pH 3.5. The pH was adjusted to 4.5 and the solid was dissolved upon mild heating. $AgClO_4$ (31 mg, 0.15 mmol) in 1.5 ml water was added to the reaction mixture. After three weeks and several cycles of filtration one yellow crystal was obtained of sufficient quality for a single-crystal X-ray diffraction measurement. Despite several attempts to upscale the reaction the isolation of a sufficient amount of material for further analysis could not be accomplished.

2.5.2 Powder X-Ray Diffractograms

All measurements accomplished with Cu-K_α-radiation, λ = 1.5406 Å.

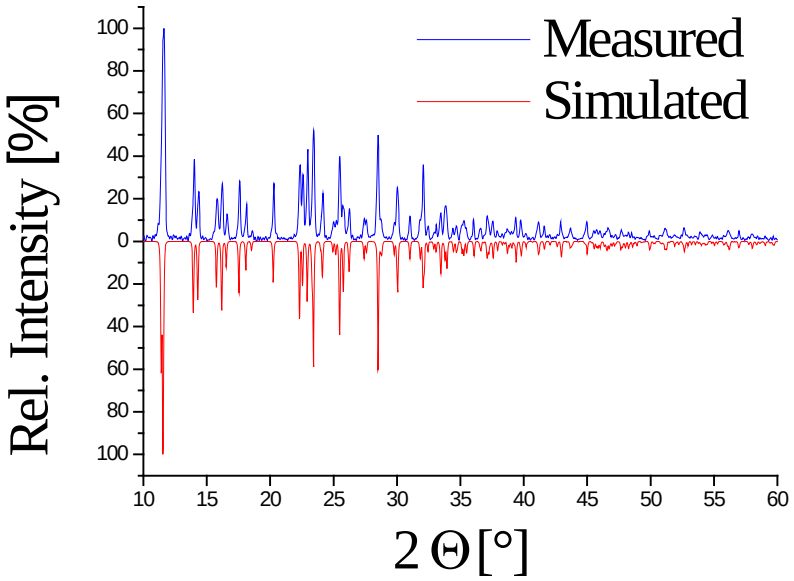

Figure 2.16: Powder X-ray diffractogram of **2.2.**

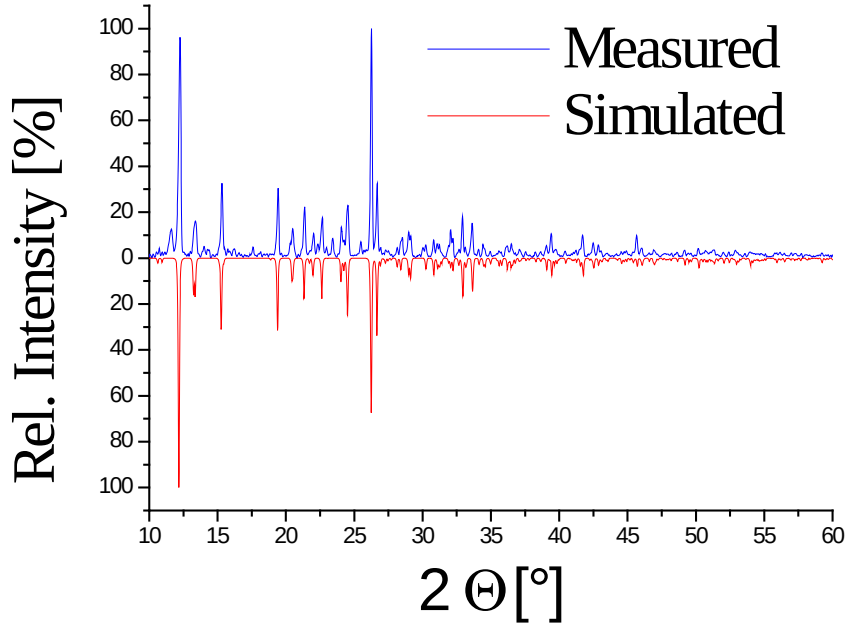

Figure 2.17: Powder X-ray diffractogram of **2.3**.

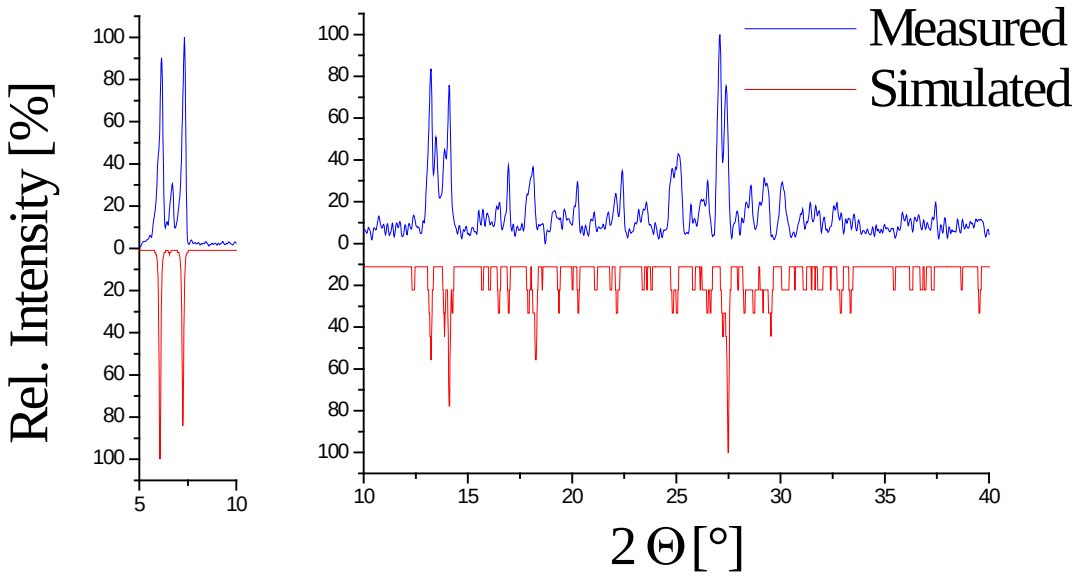

Figure 2.18: Powder X-ray diffractogram of **2.4.** The simulated and measured diffractograms for 2 Θ = 5-10° were normalized separately, as the measured relative intensities of the most intensive peaks are considerably lower than the simulated.

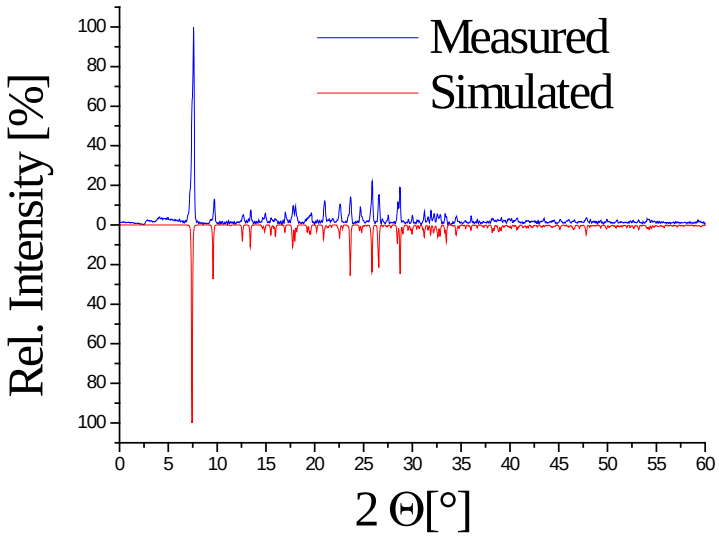

Figure 2.19: Powder X-ray diffractogram of **2.5.**

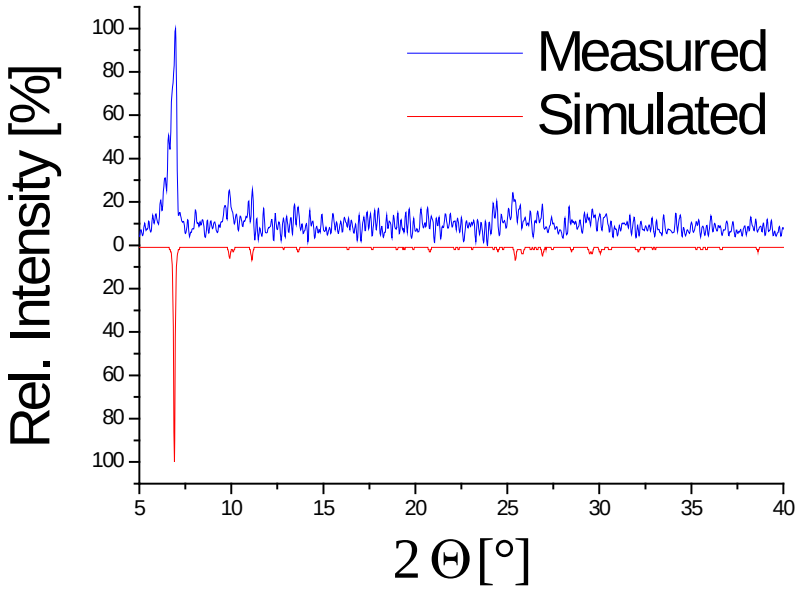

Figure 2.20: Powder X-ray diffractogram of **2.6.**

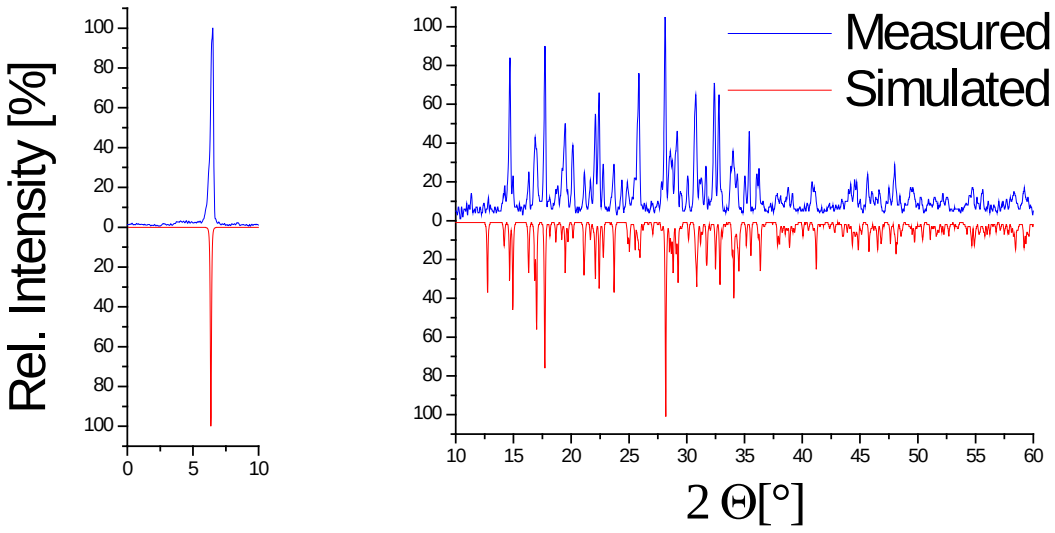

Figure 2.21: Powder X-ray diffractogram of **2.7**.The simulated and measured diffractograms for 2 Θ = 0-10° were normalized separately, as the measured relative intensities of the most intensive peaks are considerably lower than the simulated.

2.5.3 DTA/TG Measurements

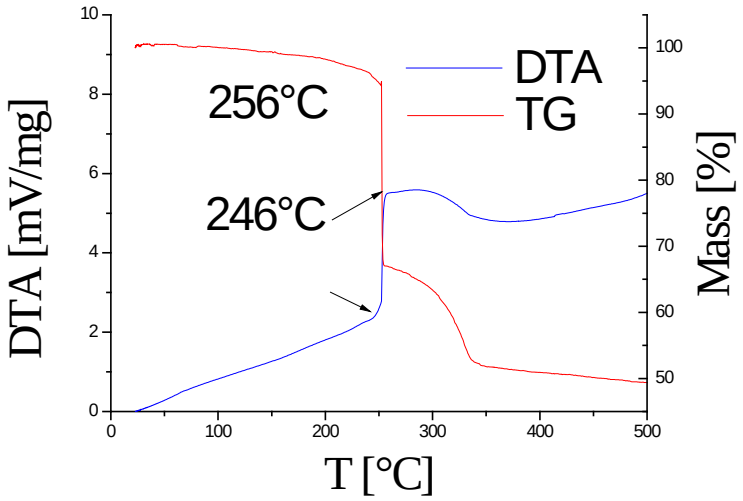

Figure 2.22: DTA/TG of **2.4.**

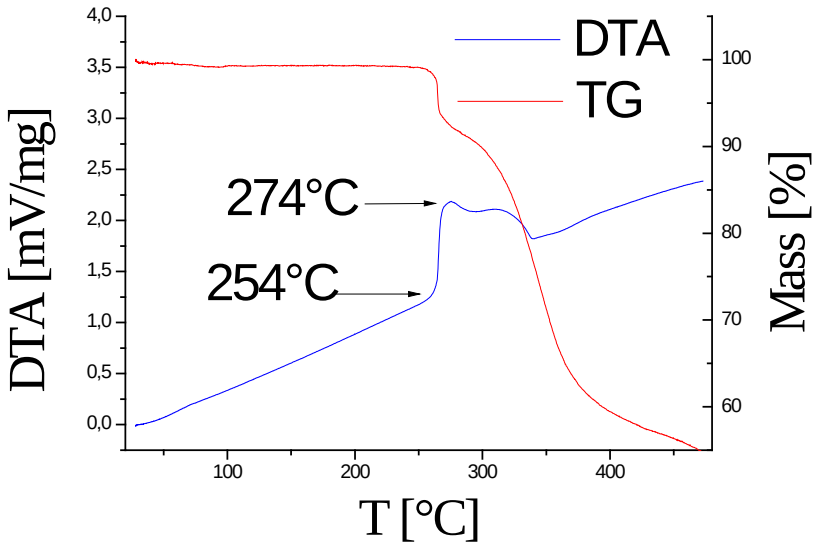

Figure 2.23: DTA/TG of **2.5.**

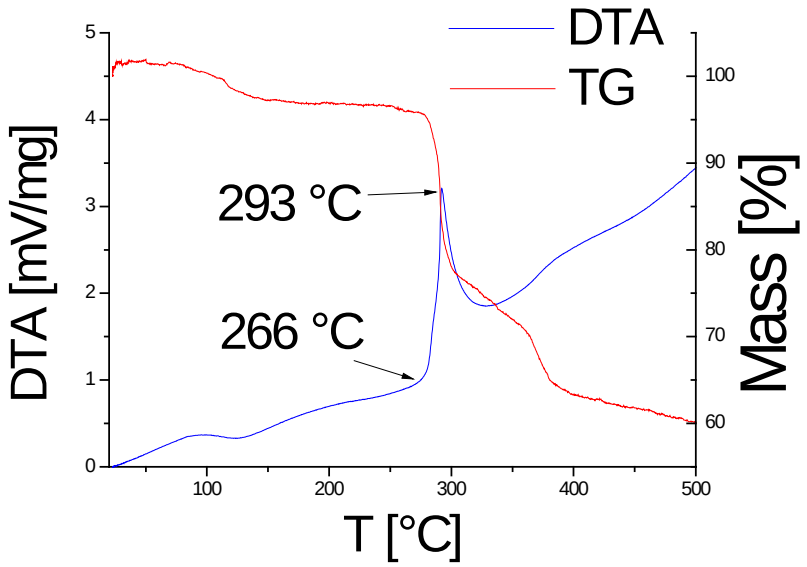

Figure 2.24: DTA/TG of **2.6.**

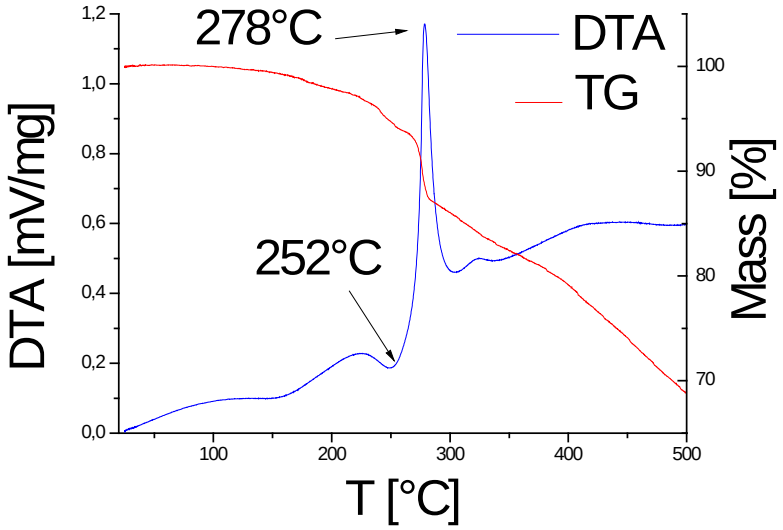

Figure 2.25: DTA/TG of **2.7.**

2.5.4 X-Ray Crystallographic Studies

The experimental details for crystallographic data collection described below are applicable to the Experimental Sections in all subsequent chapters.

Intensity data were measured at temperatures given in Table 2.3 on an image-plate diffractometer, STOE IPDS I and STOE IPDS II, respectively ($\lambda(Mo_{K\alpha})$ = 0.71073 Å, graphite monochromator). Structure solutions and refinements were performed using the program package WinGX,[23] which includes the programs SHELX[24] and Platon.[24-25] Spherical and numerical absorption corrections were accomplished with the X-red and X-shape software (STOE Darmstadt). The crystal structure solution of **5** at room temperature indicated highly disordered oxygen atoms at dichromate anions. Accordingly, the atomic displacement parameters (ADPs) were quite poor. The low fraction of high-angle reflections is to be explained by the measurement on the IPDS I diffractometer and difficulties in positioning the crystal for data collection. Nevertheless, the error values R1 and wR2 are quite acceptable (Table 2.3) and the measured and simulated X-ray diffraction patterns are matching (Figure 2.19). The respective argumentation regarding the ADPs applies to the low temperature phase of the compound.

Crystallographic data as well as structure solution and refinement details are summarized in Table 2.3 and have been deposited in more detail with the Cambridge Crystallographic Data Centre as supplementary publications Nos. CCDC 906234 - 906241. Copies of the data can be

obtained, free of charge, on application to CHGC, 12 Union Road, Cambridge CB2 1EZ, UK (fax: +44 1223 336033 or e-mail: deposit@ccdc.cam.ac.uk).

Table 2.3. Crystallographic data for compounds **2.2** to **2.8**.

	2.2	**2.3**	**2.4**	**2.5(RT)**	**2.5(100K)**	**2.6**	**2.7**	**2.8**
empirical formula	$C_{14}H_{16}AgN_8O_8$	$C_{14}H_{18}AgN_8O_9$	$C_{28}H_{42}Ag_2N_{16}O_{39}V_{10}$	$C_{28}H_{33}Ag_2Cr_2N_{16}O_{15.5}$	$C_{28}H_{33}Ag_2Cr_2N_{16}O_{15.5}$	$C_{28}H_{47}Ag_3Mo_8N_{16}O_{41}$	$C_{14}H_{26}Ag_3CrN_8Mo_6O_{30}$	$C_{29}H_{76}Ag_2Mo_6N_{16}NiO_{52}$
M [g/mol]	532.19	585.67	1951.80	1161.39	1161.39	2353.02	1737.75	2191.11
crystal system	monoclinic	monoclinic	triclinic	triclinic	triclinic	monoclinic	monoclinic	triclinic
space group	C2/c	C2/c	$P\bar{1}$	$P\bar{1}$	$P\bar{1}$	C 2/c	C 2/c	$P\bar{1}$
a [Å]	11.914(2)	7.4803(8)	7.2094(4)	7.157(1)	12.8296(4)	21.7118(6)	28.079(1)	10.469(1)
b [Å]	10.714(2)	16.162(3)	14.3947(8)	12.098(2)	14.2400(4)	17.8399(4)	6.3957(1)	12.135(1)
c [Å]	16.176(2)	16.974(2)	15.5978(9)	12.256(2)	22.0804(6)	18.8061(5)	21.3742(8)	14.498(1)
α [°]	90	90	69.658(4)	80.03(2)	90.268(2)	90	90	85.470(8)
β [°]	109.43(1)	101.210(8)	83.836(4)	79.18(2)	98.412(2)	122.236(2)	98.857(3)	77.104(8)
γ [°]	90	90	86.800(4)	87.79(2)	94.089(2)	90	90	77.693(8)
$\rho_{calc.}$ [g/cm³]	19.362	193.241	214.387	187.768	193.647	252.215	303.588	217.154
V [Å^3]	1947.2(5)	2013.0(5)	1503.9(2)	1026.6(3)	3979.9(2)	6161.5(3)	3792.7(2)	1753.1(3)
Z	4	4	1	1	4	4	4	1
$\mu(Mo_{K\alpha})$ [mm^{-1}]	1.238	1.204	2.224	1.544	1.592	2.611	3.814	1.966
T [K]	293	293	293	293	100	293	293	170
reflns measured	18722	13917	20424	12388	55579	46531	25775	27173
independent reflns	2737	2819	6357	4589	16820	6545	5103	7629
parameters	165	167	444	331	1360	446	305	550
R1 (I>4σ)	0.0381	0.034	0.0440	0.0381	0.0537	0.0372	0.0309	0.0383
R1 (all data)	0.0753	0.0457	0.0667	0.0890	0.0769	0.0441	0.0412	0.0406
wR2 (all data)	0.1094	0.1018	0.1444	0.0871	0.1573	0.1227	0.0806	0.1017

2.6 References

(1) Kulikov, V.; Meyer, G. *Cryst. Growth. & Des.* **2013**, *13*, 2916.

(2) a) Ford, K. A.; Ebisuzaki, Y.; Boyle, P. D. *Acta Cryst. C* **1998**, *54*, 1980; b) Biradha, K.; Samai, S.; Maity, A. C.; Goswami, S. *Cryst. Growth. & Des.* **2010**, *10*, 937.

(3) Lippert, B. In *Nucleic Acid-Metal Ion Interactions*; Hud, N. V., Ed.; The Royal Society of Chemistry: 2009, p 39.

(4) a) Crans, D. C.; Smee, J. J.; Gaidamauskas, E.; Yang, L. *Chem. Rev.* **2004**, *104*, 849; b) Holleman, A. F.; Wiberg, E.; Wiberg, N. *Lehrbuch der Anorganischen Chemie*; Walter de Gryuter & Co.: Berlin, 2007; c) Alam, T. M.; Nyman, M.; Cherry, B. R.; Segall, J. M.; Lybarger, L. E. *J. Am. Chem. Soc.* **2004**, *126*, 5610; d) Krishnan, C. V.; Garnett, M.; Hsiao, B.; Chu, B. *Int. J. Electrochem. Sci.* **2007**, *2*, 29.

(5) Wery, A. S. J.; Gutiérrez-Zorrilla, J. M.; Luque, A.; Ugalde, M.; Román, P.; Lezama, L.; Rojo, T. *Acta Chem. Scand.* **1998**, *52*, 1194.

(6) Hoogsten, K. *Acta. Cryst.* **1963**, *16*, 907.

(7) a) Bondi, A. *J. Phys. Chem.* **1964**, *68*, 441; b) Chang, R. *Physical Chemistry for the Chemical and Biological Sciences*; 3 ed.; University Science Books: United States of America, 2000.

(8) a) Ilie, A.; Raţ, C. I.; Scheutzow, S.; Kiske, C.; Lux, K.; Klapötke, T. M.; Silvestru, C.; Karaghiosoff, K. *Inorg. Chem.* **2011**, *50*, 2675; b) Thakur, T. S.; Desiraju, G. R. *J. Mol. Struct.: THEOCHEM* **2007**, *810*, 143.

(9) Steiner, T. *Angew. Chem.* **2002**, *114*, 50.

(10) Schottel, B. L.; Chifotides, H. T.; Dunbar, K. R. *Chem. Soc. Rev.* **2008**, *37*, 68.

(11) Massa, W. *Kristallstrukturbestimmung*; B. G. Teubner Verlag: Wiesbaden, 2007.

(12) a) Abbas, H.; Pickering, A. L.; Long, D.-L.; Kögerler, P.; Cronin, L. *Chem. Eur. J.* **2005**, *11*, 1071; b) Abbas, H.; Streb, C.; Pickering, A. L.; Neil, A. R.; Long, D.-L.; Cronin, L. *Cryst. Growth. & Des.* **2008**, *8*, 635.

(13) See all silver(I)-POM related publlications referenced in the introduction.

(14) Guerra, C. F.; Bickelhaupt, F. M.; Snijders, J. G.; Baerends, E. J. *J. Am. Chem. Soc.* **2000**, *122*, 4117.

(15) Henry, M. *ChemPhysChem* **2002**, *3*, 561.

(16) The PACHA software was obtained from the URL http://www-chimie.u-strasbg.fr/~lcmes/fichiers/soft.htm on the 02.10.2012.

(17) Henry, M.; Hosseini, M. W. *New J. Chem.* **2004**, *28*, 897.

(18) Hobza, P. *Phys. Chem. Chem. Phys.: Themed issue "Stacking Interactions"* **2008**, *10*, 2561.

(19) Callahan, M. P.; Gengeliczki, Z.; Svadlenak, N.; Valdes, H.; Hobza, P.; de Vries, M. S. *PCCP* **2008**, *10*, 2819.

(20) Kool, E. T. *Annu. Rev. Biophys. Biomol. Struct.* **2001**, *30*, 1.

(21) Quiñonero, D.; Garau, C.; Rotger, C.; Frontera, A.; Ballester, P.; Costa, A.; Deyà, P. M. *Angew. Chem. Int. Ed.* **2002**, *41*, 3389.

(22) Egli, M.; Sarkhel, S. *Acc. Chem. Res.* **2006**, *40*, 197.

(23) Farrugia, L. *J. Appl. Crystallogr.* **1999**, *32*, 837.

(24) Sheldrick, G. *Acta Cryst. A* **2008**, *64*, 112.

(25) Spek, A. *Acta Cryst. D* **2009**, *65*, 148.

3. New Organoamine Silver(I) Decatungstate Frameworks: Remarkable Chemoselectivity and Employment as Precursors for Potential Functional Materials. A Related β-Octamolybdate Compound

3.1 Synthesis and Crystal Structures of Materials Consisting of Organoamine Silver(I) Complexes and Decatungstate

Inorganic-organic frameworks based on silver(I)-polyoxotungstates were shown to be useful for the directed synthesis of silver nanomaterials.[1] A viable approach to the fine-tuning of these frameworks by variation of polyoxoanions and organoamine ligands under hydrothermal conditions was developed.[2] In this chapter a less energy-intensive fine-tuning approach is reported, allowing different inorganic-organic network architectures by subtle changes of the reaction conditions as well as structures and further characteristics of the resulting new compounds. Implications of the structural changes for the chemical composition of materials generated upon temperature induced decomposition of the synthesized compounds are also reported.

Despite repetitive attempts to extend the row of hybrid materials of silver(I)-theobromine complexes and polyoxometalates to polyoxotungstates, the application of the strategy as described in chapter 2 was not successful. Different inorganic sodium and silver(I) para-dodecatungstates containing different amounts of hydration water precipitated instead. They were identified by the determination of the unit cell for compounds described in the literature or solving the crystal structures for new compounds. The quality of the crystal structures was not satisfactory; their discussion here is therefore omitted.

Cronin et al. were successful in the application of acetonitrile as a solvent for the isolation of silver(I)-polyoxotungstate compounds.[1,3] The compounds they isolated are mentioned in chapter 1. They consist of acetonitrile silver(I)-complexes bearing a little amount of solvent molecules, thus comprising essentially inorganic frameworks. An attempted reaction of the tetrabutylammonium decatungstate with silver(I) and theobromine under similar conditions led to the isolation of $[Ag(MeCN)_3]_2[Ag(MeCN)_2]_2[W_{10}O_{32}]$ which was characterized by Cronin et al.[1] Hence, theobromine was assessed as not strong enough a ligand to displace acetonitrile from

the coordination sphere. A different solvent was therefore needed. It should exhibit similarly strong ability to dissolve purine bases but weaker coordination tendency towards silver(I). Benzonitrile satisfied these criteria being a weaker σ-donor than acetonitrile due to the aromatic ring stabilizing the electron pairs of the nitrile moiety.

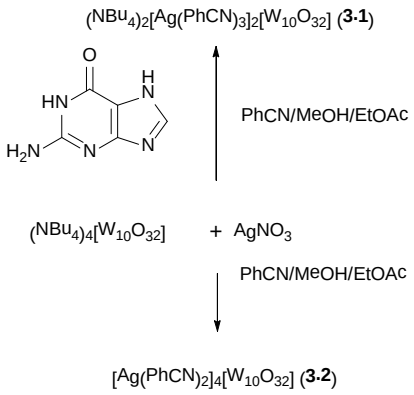

Scheme 3.1: Influence of guanine on the outcome of the reaction of $AgNO_3$ and $(NBu_4)_2[W_{10}O_{32}]$.

In accordance with this idea, $AgNO_3$ and $(NBu_4)_2[W_{10}O_{32}]$ were reacted with guanine in benzonitrile. Unexpectedly, the X-ray diffraction study of the isolated crystals from the reaction did not show any guanine in the product. Rather, the compound was identified as $(NBu_4)_2[(Ag(PhCN_3)]_2[W_{10}O_{32}]$ (**3.1**) (Scheme 3.1).

The defining influence of guanine on the reaction products was confirmed by performing the same reaction without the nucleic base. Under these conditions $[(Ag(PhCN_3)]_4[W_{10}O_{32}]$ (**3.2**) was obtained. Both reactions are highly selective based on elemental analysis and powder XRD (Figure 3.9 and 3.10).

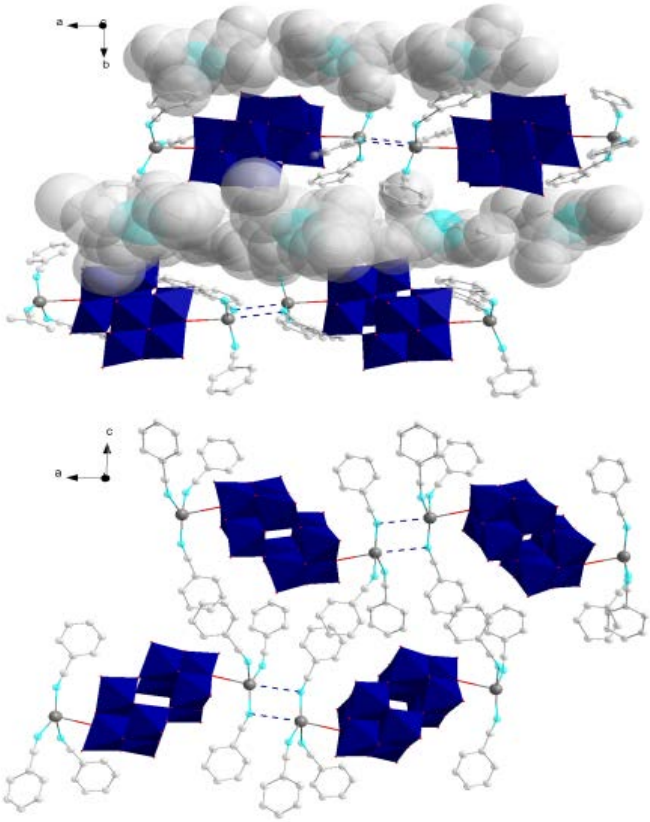

The defining aspect of the crystal structure of **3.1** are coordination polymers consisting of dimers of $[Ag(PhCN)_3]^+$ complexes interlinking decatungstate anions (Figure 3.1). The dimers display a central rectangle of Ag and N atoms, with side lengths of 2.19(1) and 3.46(1) Å. The lengths of the shorter side lies within a typical Ag(I)-N coordinative bond length.[4] On the contrary, a distance of 3.46(1) Å between Ag(I) and N of neighbouring complexes is barely less than the sum of the van der Waals radii.[5] Accordingly these

Figure 3.1: Crystal structure of $(NBu_4)_2[(Ag(PhCN)_3]_2[W_{10}O_{32}]$ (**3.1**). Colour scheme: C light grey, Ag silver, N light blue, O red, W dark blue, H omitted for clarity. Subsequent illustrations follow the same scheme.

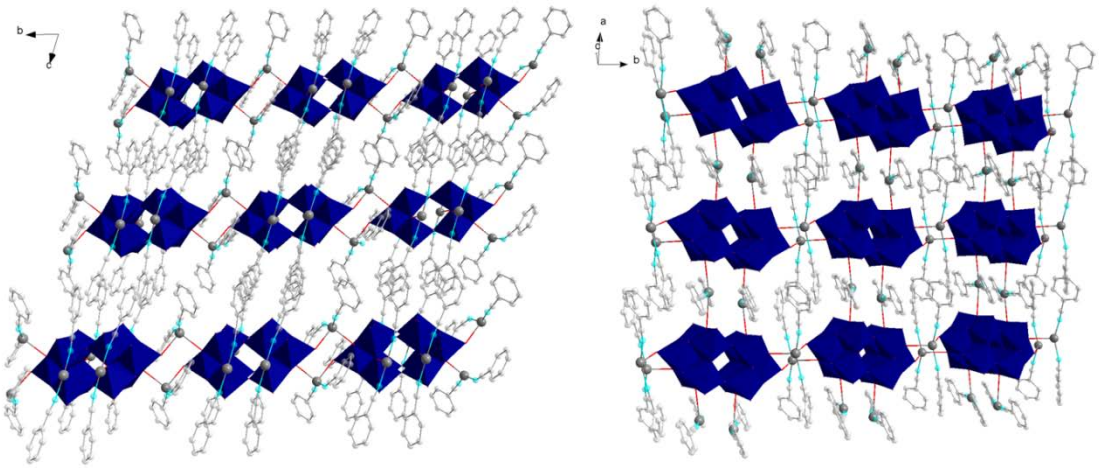

Figure 3.2: Crystal structure of **3.2**.

interactions are indicated with dashed instead of solid lines in Figure 3.1.

The coordination polymers built by the dimers and decatungstates alternate with layers of tetrabutylammonium cations along the crystallographic b-axis. Coulombic interactions between the negatively charged chains and the organic cations must contribute decisively to the crystal structure formation, in analogy to silver(I)-octamolybdate based compounds.[6]

Compound **3.2** displays completely different building units of the crystal structure as well as complex geometries. Each decatungstate anion is surrounded by eight Ag(I) ions sharing them with neighbouring POMs. Accordingly a two-dimensional coordinative framework consisting of Ag(I) and decatungstates is built up (right part of the Figure 3.2). These layers alternate with layers of aromatic moieties of benzonitrile ligands in the direction of the crystallographic c-axis (left part of the Figure 2). The steric surrounding of Ag(I) now allows coordination of only two benzonitrile ligands (as opposed to three in **3.1**) in trans-position to each other.

$[Ag(PhCN)_2(thb)]_4[W_{10}O_{32}]\cdot PhCN$ (thb = theobromine) (**3.3**) is prepared under similar conditions as **3.1** and **3.2**, but thb is employed as the supporting purine ligand instead of guanine. Contrary to **3.1**, the purine base now acts as a ligand for Ag(I) in the crystal structure.

The silver(I) ions now display two PhCN ligands and thb in their coordination sphere (Figure 3.3a). They are located in two crystallographically different positions, coordinated by one and two oxygen atoms of the decatungstate, respectively. Accordingly one of the silver(I) ions shows a tetrahedral and the other one a strongly distorted pentagonal-bipyramidal surrounding. The strong distortion is most likely induced by the decatungstate framework and by anion-π-interactions between the theobromine ligand and the decatungstate.

The Ag(I)-O bond lengths of the silver(I) ion between two terminal oxygen atoms of decatungstate (Figure 3.3a, in the distorted pentagonal bipyramidal environment) are 2.80(1) and 2.842(9) Å. These distances are rather long (see tables 1.1, 1.2 and 1.3 in the Introduction). The respective bond lengths in the tetrahedral silver(I) complex are 2.52(1) Å, which is in the usual range for Ag(I)-O bonding distances. This discrepancy suggests that the coordination geometry is influenced by the decatungstate framework quite profoundly.

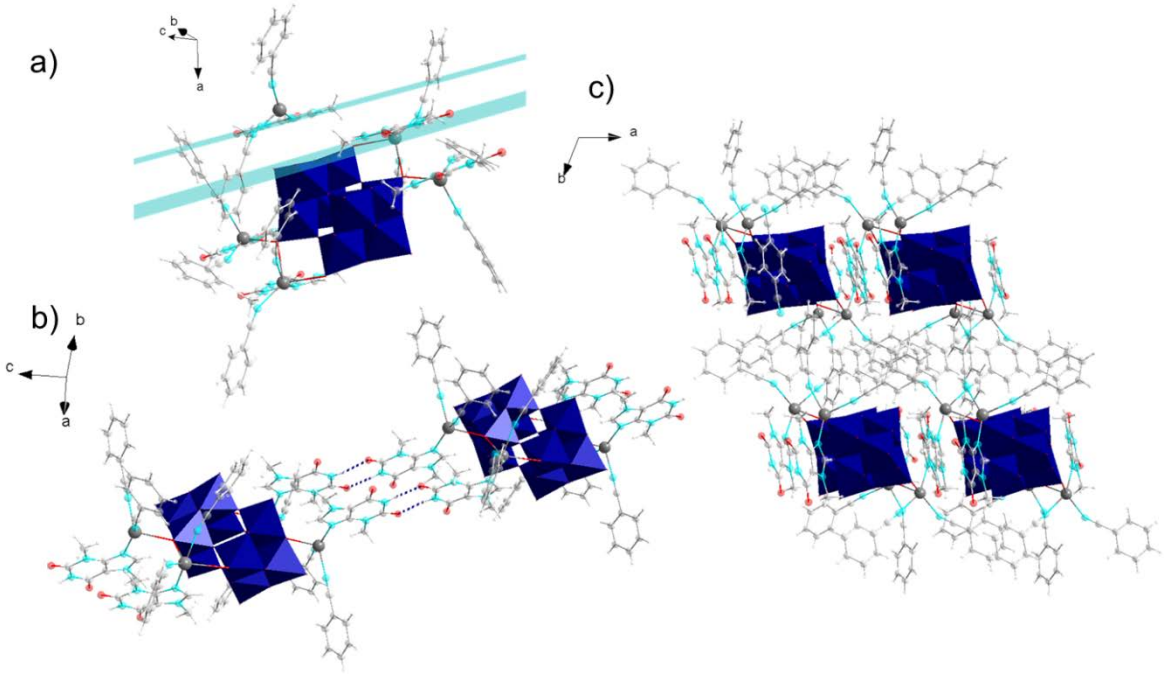

Figure 3.3: Crystal structure of **3.3**: a) Formula unit with two additional Ag(I)-complexes interacting with POM via anion-π interactions. The planes of one of the theobromine ligands and one of the faces of decatungstate are shown in light blue. The H-atoms are not omitted to indicate non-covalent interactions. b) Interconnection of the POM-units by amide-to-amide theobromine dimers. c) Overview of the crystal structure with hydrophobic and anion-π interactions.

Contrary to the previously described compounds, the crystal structure of **3.3** is not defined by a network of coordination polymers. The units are connected by diverse non-covalent interactions (Fig. 3.3). These are H-bonds between the self-pairing theobromine molecules (Figure 3.3b), anion-π-stacking interactions between the theobromine ligands and decatungstate (Figure 3.3a indicated by blue planes) and hydrophobic interactions between the benzonitrile ligands (Figure 3.3c).

The strongest of these interactions are most likely amide-to-amide bonds between the theobromine molecules and anion-π-interactions between the organic ligands and the POM. This

assumption is supported by the H-bond donor-acceptor distances of 2.75(2) and 2.84(2) Å[7] as well as the interplanar distance between theobromine and the parallel face of the decatungstate of only 2.85(8) Å.[8]

Silver nanoparticles are applied as photocatalysts as well as parts of optical, electrical and sensing devices.[9] Tungsten oxides and tungsten oxide bronzes with inserted hydrogen display fascinating photochromic and electrochromic properties.[10] The combination of both materials made it possible to couple proton-coupled electron transfer to photoelectronic excitation processes.[11] The possibility of careful adjustment of the H/Ag/WO_3 ratio might be helpful for the construction of photosensitive semiconducting materials, for instance for use in solar cells.

As compounds **3.1**-**3** contain Ag(I), W(VI) and reducing agents in form of organic ligands, the construction of such materials by inducing an intramolecular redox-reaction was attempted. The reaction was induced by gradual heating of the materials and the reaction products were scrutinized by powder XRD (Figure 3.4).

According to the DTA/TG results the redox reactions occur in all compounds between 100 and 400 °C in several steps accompanied by strong mass loss and energy release (Figures 3.13 – 3.15). Both observations can be attributed to the oxidation of the organic part to gaseous products such as CO_2, H_2O and NO_x. Concomitantly the inorganic part is reduced. The residue contains elemental silver and tungsten oxides in various oxidation states (Figure 3.4).

The similarities between the residues of **3.1** and **3.2** are quite striking. Both contain WO_3 and H_xWO_3 as well as Ag. The differences in composition are minimal. The powder pattern of the residue of **3.3** is markedly different. The POM was reduced all the way to WO_2, no sign of any higher oxidized tungsten compounds is present. This difference can be accounted for by the different organic parts employed. Whereas **3.1** and **3.2** contain benzonitrile molecules, which are labile and easily removed, **3.3** contains theobromine ligands having much higher melting and decomposition points.[12] Accordingly it is capable of gradual reduction of the inorganic moiety, which results in a lower oxidation state of the resulting tungsten oxide. Another reason for the quantitative reduction of the POM to WO_2 could be the crystal structure, in which every polyoxoanion is surrounded by organic molecules from all sides (Figure 3.3a), thus facilitating the redox reaction.

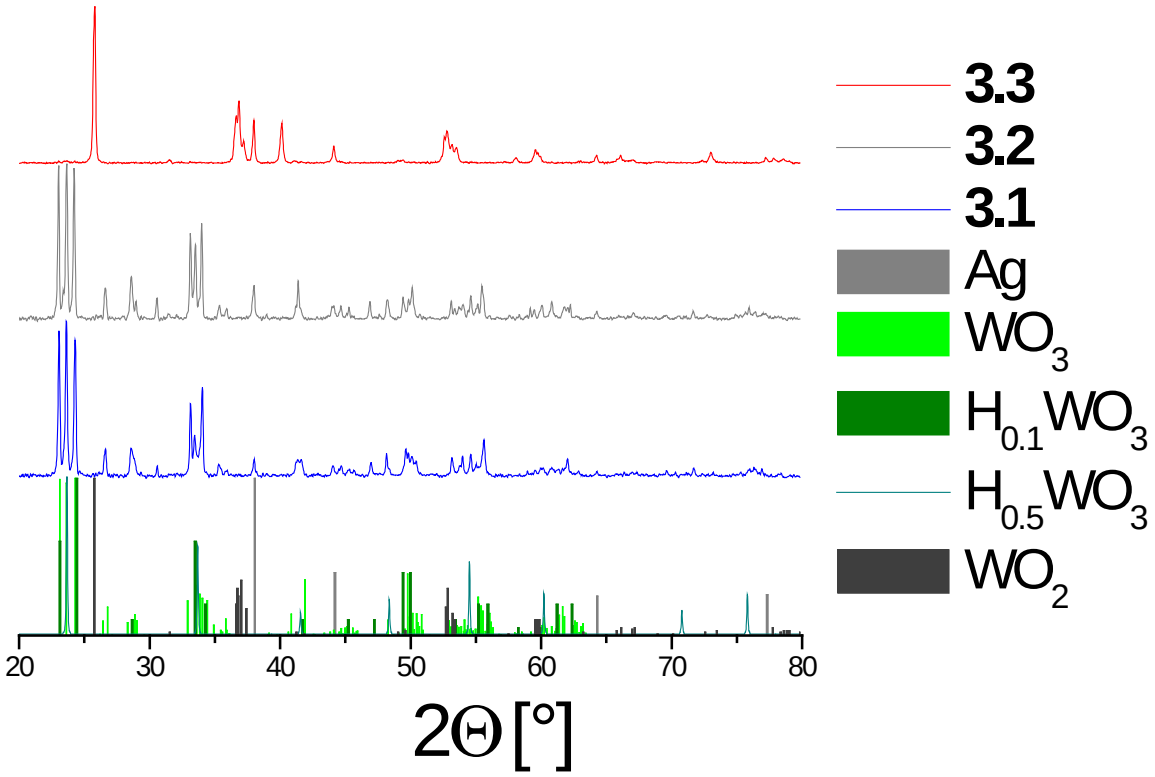

Figure 3.4: Powder X-ray diffractograms of the DTA residues of synthesized compounds and respective matching species.[13]

3.2 Structural and Chemical Influence of the Replacement of Decatungstate by Octamolybdate

The chemical reactivity of polyoxomolybdates resembles that of polyoxotungstates. Nonetheless several remarkable distinctions are observable in the reaction behaviour of both anions. Among these is the preference for different levels of agglomeration and stability in organic solvents. The most common polyoxotungstate anions are the hexa-, deca- and dodecatungstate. The most common polyoxomolybdates are hexa- and octamolybdate. Polyoxotungstates reacting with transition metals are usually stable in organic solvents regardless of the nature of the reaction partner. Thus, reacting decatungstate anion with silver(I) yields a decatungstate containing product, as exemplified in the section 3.1. Polyoxomolybdates reacting with silver are, on the other hand, unstable: the reaction product of a polyoxomolybdate

with silver(I) in organic solvents always contains octamolybdate regardless of the level of agglomeration of the starting material. The reason is the stability of the $[Ag_2Mo_8O_{26}]^{2-}$ fragment shown by Cronin et al.[14] and discussed in the Introduction to this thesis.

In order to prove the validity of these concepts silver(I) nitrate, theobromine and hexamolybdate were brought to reaction under the same conditions, as the ones employed for the synthesis of **3.3**. This reaction led to the isolation of **3.4**. The stoichiometric equation is displayed in the Scheme 3.2. As expected the hexamolybdate anion is transformed into octamolybdate upon reaction with silver(I). $Ag_2Mo_2O_7$ is deliberately taken into parentheses as it is not the actual species existing in solution. There are rather different polyoxoanions dynamically transforming into one another which react with Lindqvist-molybdate.[14] These reactions lead to the net addition of $Ag_2Mo_2O_7$.

The resulting material – $[Ag(PhCN)(thb)]_4[Mo_8O_{26}](PhCN)_2$ (**3.4**) – contains β-octamolybdate anions each of which is surrounded by six $[Ag(PhCN)(thb)]^+$-complexes. The central cations are situated in two different crystallographic environments (Figure 3.5). Ag2 is

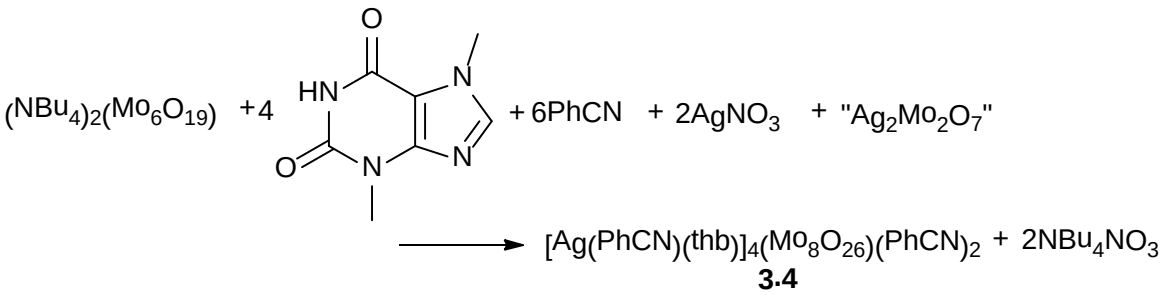

Scheme 3.2: Transformation of hexamolybdate into octamolybdate upon reaction with silver(I) nitrate and thb in benzonitrile.

coordinated to two chelating terminal oxygen atoms belonging to one β-octamolybdate with respective coordinative distances of 2.584(5) and 2.565(4) Å. Ag1 displays three oxygen atoms from two different octamolybdates in the coordination sphere. The respective coordination distances amount to 2.502(5), 2.696(4) and 2.802(4) Å. The two shorter coordinative bonds are between the Ag^+ and chelating oxygen atoms of one octamolybdate. The longer one is the coordination bond to the

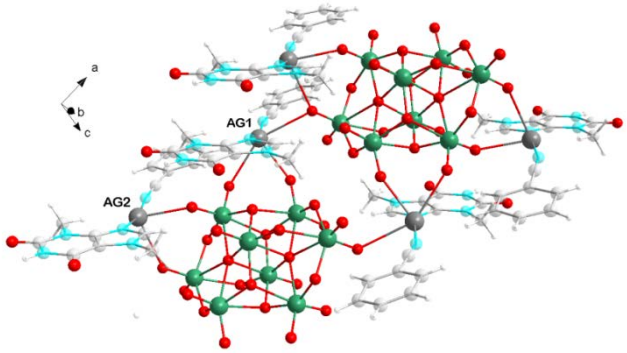

Figure 3.5: Network of coordination bonds of $[Ag(PhCN)(thb)]^+$-complexes and octamolybdates in **3.4**.

neighbouring octamolybdate. Hence this Ag^+ ion connects two adjacent octamolybdates along the crystallographic a-axis.

The ladder-like chains of octamolybdate anions coordinating organoamine silver(I) complexes are built along the crystallographic a-axis (Figure 3.6). They are interconnected by amide-to-amide theobromine dimers similar to **3.3**. The thb ligands are arranged antiparallel to one another with an interplanar distance of 3.22(1) Å. Accordingly we can conclude stabilizing stacking interactions reinforced by dipole-dipole attraction between the carbonyl groups and nitrogen atoms of the pyrimidine ring (Figure 3.6).[15]

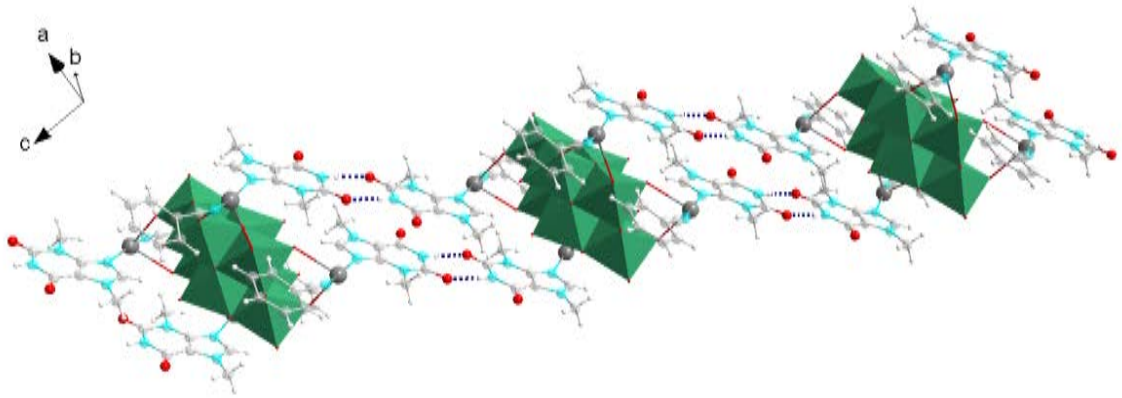

Figure 3.7: Coordination polymers of $[Ag(PhCN)(thb)]^+$-complexes and β-octamolybdates interconnected by self-pairing theobromine dimers in **3.4**. H-bonds are indicated by dashed lines.

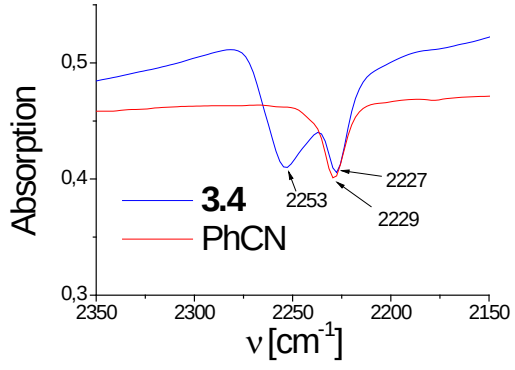

Figure 3.6: Nitrile absorption bands in the IR spectra of **3.4** and PhCN.

The IR-Spectrum of **3.4** is consistent with its crystal structure. There are two absorption bands in the nitrile region (2227-2253 cm^{-1}; Figure 3.7). One of the absorption bands is virtually at the same position as the one of free benzonitrile (2229 cm^{-1}). It most likely belongs to the benzonitrile molecule incorporated into crystal structure. The other absorption band displays a hypsochromic shift of 26 cm^{-1}, indicative of the coordination bond to silver(I).

The DTA/TG curves are quite reminiscent of the ones measured for **3.1**-**3.3**. The remarkable difference is the lower fractional mass remaining after decomposition and evaporation of the

organic parts (Figure 3.16). Around 70% of the mass of tungsten containing compounds remain after the reactions as opposed to around 50% of mass remaining of compound **3.4**. This is consistent with the molar mass of Mo being lower than that of W and according lower fractional mass.

The DTA residue of **3.4** corresponds to the one of **3.3**. The octamolybdate is fully reduced to MoO_2 and the silver(I) cations to elemental silver (Figure 3.8).[13c,16]

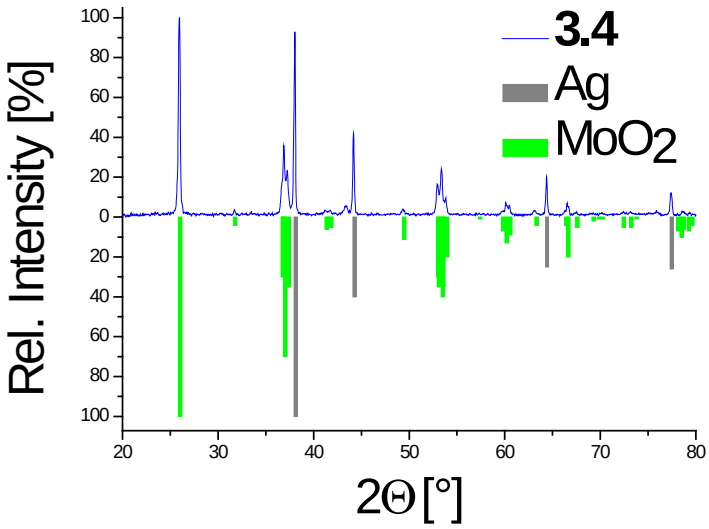

Figure 3.8: Powder X-ray diffractograms of the DTA residue of **3.4** and respective matching species.

3.3 Conclusions

In conclusion, three new inorganic-organic hybrid silver(I) decatungstates (Figure 3.9) and one respective octamolybdate were synthesized. Remarkable is the chemical behaviour of the nucleic base guanine, which serves as reaction modifier but is not encountered in the reaction product, when reacted with silver(I) nitrate and decatungstate. The thermolysis residues of all three materials were determined by powder XRD and demonstrated that they contain mixtures of tungsten oxides and elemental silver. Further investigations could be directed towards the exploration of physico-chemical properties of the inorganic materials such as photo- and electrochromism as well as conducting properties.

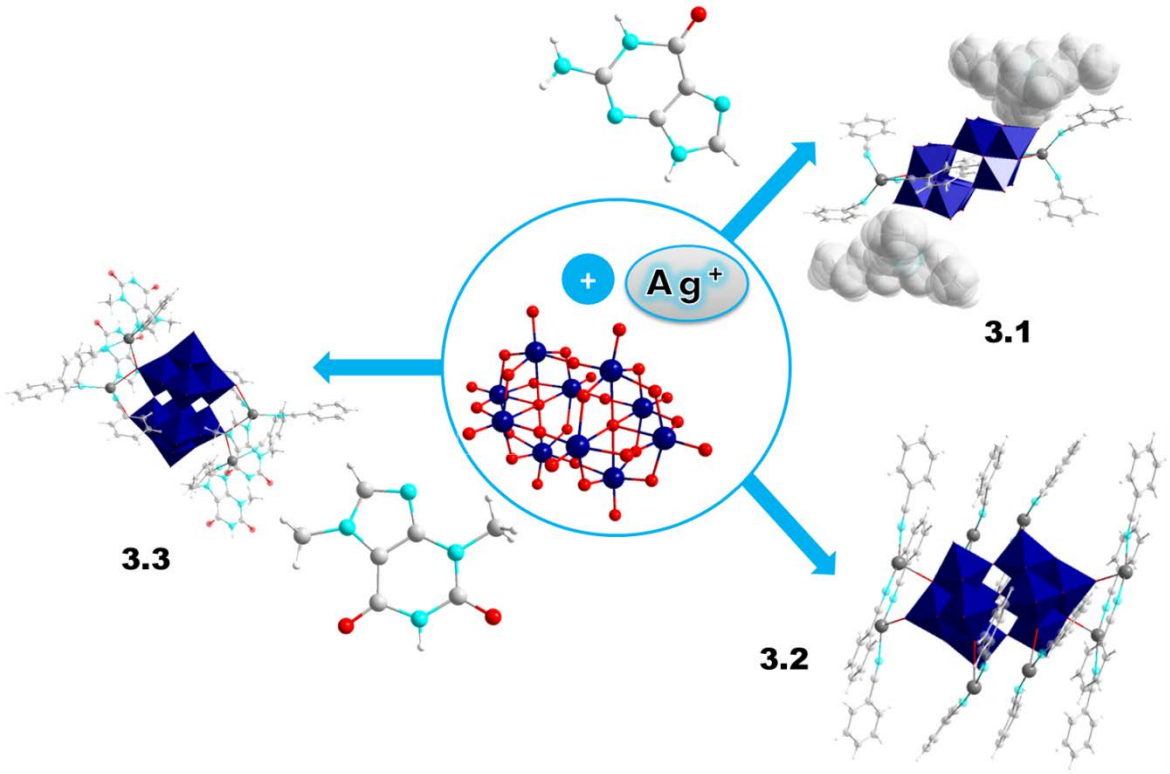

Figure 3.9: Overview of reactions of silver(I) cations and decatungstate with purine bases in benzonitrile.

To compare the reactivity of polyoxomolybdates and –tungstates under similar synthetic conditions, an octamolybdate containing material was synthesized. Both materials containing theobromine-silver(I)-complexes - $[Ag(PhCN)_2(thb)]_4[W_{10}O_{32}]\cdot PhCN$ (thb = theobromine) (**3.3**) and $[Ag(PhCN)(thb)]_4[Mo_8O_{26}]\cdot PhCN$ (**3.4**) – display a number of similarities but also quite a few of marked differences. The similarities are in the intermolecular interactions which are largely determined by self-pairing theobromine molecules and hydrophobic interactions of benzonitrile ligands. The thermolysis products correspond exactly to one another: Ag and WO_2 in the case of compound **3.3** and Ag and MoO_2 in the case of **3.4**. The major difference is the overall crystal structure: **3.3** consists of separated formula units interacting with one another only by weak intramolecular interactions, whereas the octamolybdates of the compound **3.4** are interconnected with one another via O-Ag coordinative bonds.

3.4 Experimental Section

3.4.1 Synthetic Procedures

$(NBu_4)_4[W_{10}O_{32}]$ and $(NBu_4)_2[Mo_6O_{19}]$ were synthesized according to the published procedures.[17] All other chemicals were purchased from commercial sources. The phase purities of the bulk samples of all compounds were verified by X-ray powder diffraction on a STOE STADI transmission powder diffractometer (see Figures 3.10 – 3.13 for measured and simulated powder patterns).

$(NBu_4)_2[Ag(PhCN)_3]_2[W_{10}O_{32}]$ (3.1): $(NBu_4)_2[W_{10}O_{32}]$ (1.00 g, 0.33 mmol) was dissolved in PhCN (120 ml). The solution was heated to 50 °C and neat guanine (0.18 g, 1.20 mmol) was added creating a white suspension. The reaction mixture was gradually heated to 107 °C during a period of 80 min. $AgNO_3$ (0.41 g, 2.43 mmol) in 24 ml MeOH was added to the hot suspension under vigorous stirring, causing strong boiling of the reaction mixture. The suspension was allowed to cool to room temperature and was filtered. The dried filter residue (0.14 g) was identified as guanine by powder XRD and discarded. The filtrate became cloudy upon EtOAc diffusion over the period of four weeks. Colourless block crystals of **3.1** precipitated one day after filtration. They were washed with EtOAc (3×5 ml) and dried in membrane vacuum (20 mbar) overnight. Yield: 0.71 g, 58.6 % based on $(NBu_4)_2(W_{10}O_{32})$. Elemental analysis found: C 24.1, H 2.8, N 3.0. Calc. for $C_{74}H_{102}Ag_2N_8O_{32}W_{10}$: C 24.2, H 2.8, N 3.05%. Characteristic IR bands (KBr): ν (cm^{-1}) = 3581 (w), 3085 (w), 3037(w), 2960 (s), 2933(s), 2875(s), 2246 (shoulder, s), 2233 (s), 1984 (w), 1915 (w), 1828 (w), 1789 (w), 1699 (w), 1617 (m), 1595 (s), 1486 (s), 1446 (s), 1381 (s), 1344 (w), 1292 (m), 1195 (m), 1176 (m), 1153 (m), 1104 (w), 1070 (w), 1026 (w), 996 (m), 958 (s), 889 (s), 800 (br, s), 759 (m), 688 (s), 624 (w), 581 (br, m), 552 (s), 434 (s), 401 (s), 334 (s), 258 (m), 183 (m), 67(w); UV/Vis (KBr): λ (nm) = 210, 223, 272, 329.

$[Ag(PhCN)_3]_4[W_{10}O_{32}]$ (3.2): $(NBu_4)_2[W_{10}O_{32}]$ (0.33 g, 0.10 mmol) was dissolved in PhCN (20 ml). $AgNO_3$ (0.14 g, 0.83 mmol) in 8 ml MeOH was added causing a slight turbidity of the solution. A white partly crystalline product precipitated from the solution upon EtOAc diffusion after a week. The mother liquor was filtered off and the product was dried one day in air and one day in membrane vacuum (20 mbar). Yield: 0.21 g, 58.2% based on $(NBu_4)_2[W_{10}O_{32}]$.

Elemental analysis found: C 18.3, H 1.1, N 3.1. Calc. for $C_{56}H_{40}Ag_4N_8O_{32}W_{10}$: C 18.65, H 1.1, N 3.1%. Characteristic IR bands (KBr): ν (cm^{-1}) = 3579 (m), 3501 (br, s), 3064 (w), 2281 (m), 2229 (s), 1978 (w), 1902 (w), 1772 (w), 1618 (s), 1596 (s), 1487 (s), 1447 (s), 1291 (m), 1195 (m), 1175 (m), 1071 (w), 1003 (m), 963 (s), 893 (s), 793 (s), 758 (shoulder, w), 684 (m), 585 (br, m), 548 (s), 424 (br, s). UV/Vis (KBr): λ (nm) = 205, 223, 271, 277, 320.

$[Ag(PhCN)_2(thb)]_4[W_{10}O_{32}]\cdot PhCN$ (3.3): $(NBu_4)_2[W_{10}O_{32}]$ (0.83 g, 0.25 mmol) and theobromine (0.18 g, 1.00 mmol9 were dissolved in PhCN (100 ml) upon heating to 115 °C. $AgNO_3$ (0.34 g, 2.00 mmol) in 20 ml MeOH was added causing strong boiling and temperature drop to 80 °C. The reaction mixture was allowed to cool to 30°C and filtered. A yellow solid precipitated upon EtOAc diffusion after one day. It was separated from the reaction mixture, washed with acetone (5×10 ml). It was dried in air and washed with PhCN (2×10 ml) and EtOAc (10 ml), than dried in air again. Yield: 0.10 g, 11.1 % based on $(NBu_4)_2(W_{10}O_{32})$. Characteristic IR bands (KBr): ν (cm^{-1}) = 3483 (br, s), 3167 (m), 3121 (w), 3038 (w), 2832 (m), 2242 (s), 2226 (s), 1694 (br, vs), 1596 (m), 1553 (s); 1504 (m), 1489 (m), 1456 (shoulder, w), 1447 (m), 1419 (w), 1367 (s), 1330 (w), 1291 (m), 1231 (s); 1204 (m), 1178 (w), 1142 (m), 1069 (w), 1045 (w), 998 (w), 960 (br, s), 890 (s), 799 (br, vs), 761 (shoulder, w), 687 (s), 608 (m), 589(br, m), 549 (m), 515 (m), 452 (shoulder, w), 434 (s), 425 (s). UV/Vis (KBr): λ (nm) = 208, 223, 278, 326.

$[Ag(PhCN)(thb)]_4[Mo_8O_{26}](PhCN)_2$ (3.4): $(NBu_4)_2[Mo_6O_{19}]$ (0.34 g, 0.25 mmol) was added to the suspension of thb (0.09 g, 0.5 mmol) in PhCN (50 ml). The reactants dissolved upon heating the reaction mixture to 103 °C. $AgNO_3$ (0.17 g, 1.00 mmol) in MeOH (10 ml) was added to the solution causing strong boiling. The reaction mixture was allowed to cool to the room temperature, upon which an additional portion of $AgNO_3$ (0.17 g, 1.00 mmol) in MeOH (10 ml) was added and the reaction vessel closed. The product precipitated as a white powder upon standing at room temperature for two weeks. It was washed with acetone (2×10 ml) and dried in air for a day. Yield: 0.19 g, 55.3% based on thb. Elemental analysis found: C 24.4, H 2.1, N 10.35. Calc. for $C_{56}H_{52}Ag_4Mo_8N_{20}O_{34}$:[18] C 24.5, H 1.9, N 10.2%. Characteristic IR bands (KBr): ν (cm^{-1}) = 3480 (br, s), 3185 (m), 3116 (s), 3035 (m), 2822 (m), 2253 (s), 2227 (s), 1717 (shoulder, s), 1690 (vs), 1597 (m), 1547 (s), 1491 (m), 1449 (w), 1415 (w), 1365 (m), 1324 (w), 1288 (m), 1227 (m), 1198 (w), 1176 (w), 1137 (w), 1085 (w), 1042 (w), 1025 (w), 946 (s), 913 (shoulder, s), 895 (s), 837 (s), 795 (w), 758 (w), 740 (m), 705 (m), 684 (m), 662 (shoulder, m), 609 (m), 548 (m), 514 (m), 475 (w), 451 (m), 438 (shoulder, w), 408 (m). UV/Vis (KBr): λ_{max}

(nm) = 207, 218, 278.

3.4.2 Powder X-Ray Diffractograms

All measurements accomplished with Cu-K_α radiation, λ = 1.5406 Å, at room temperature unless stated otherwise.

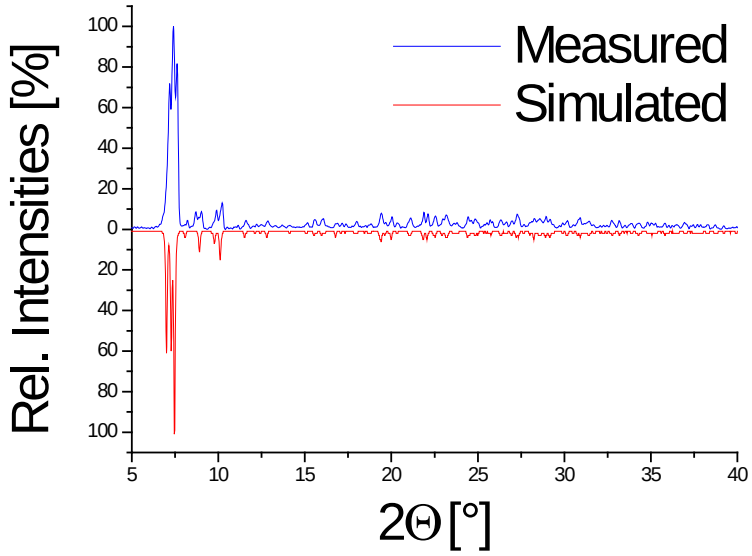

Figure 3.10: Powder X-ray diffractogram of $(NBu_4)_2[Ag(PhCN)_3]_2[W_{10}O_{32}]$ (**3.1**).

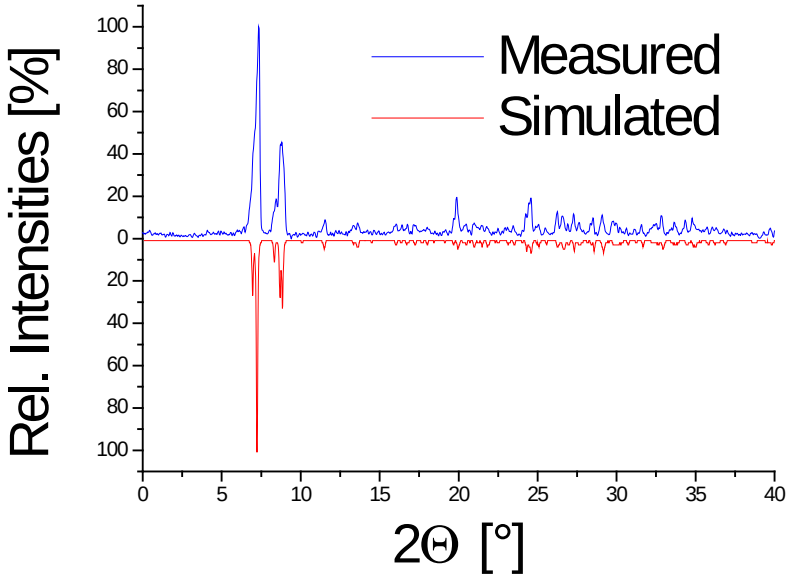

Figure 3.11: Powder X-ray diffractogram of $[Ag(PhCN)_3]_4[W_{10}O_{32}]$ (**3.2**).

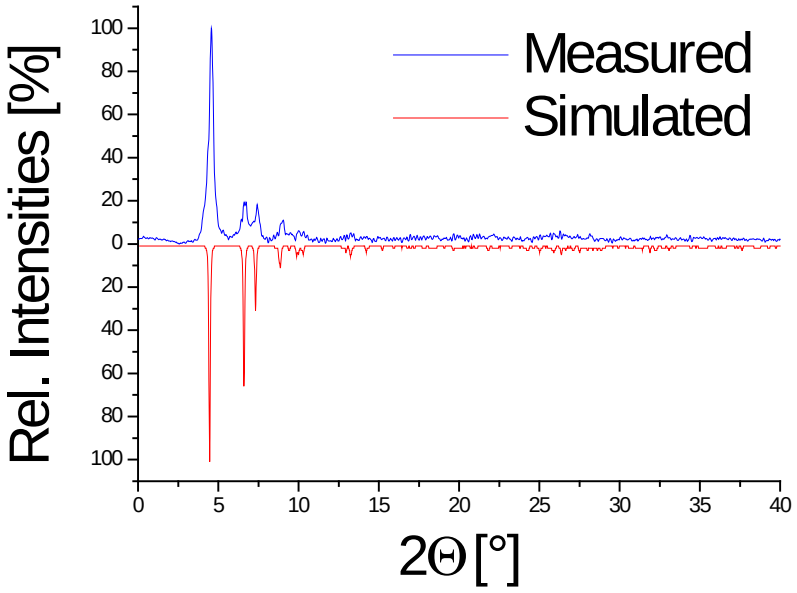

Figure 3.12: Powder X-ray diffractogram of $[Ag(PhCN)_2(thb)]_4[W_{10}O_{32}]\cdot PhCN$ (**3.3**). The simulated diffractogram is based on the crystal structure at 170(2) K.

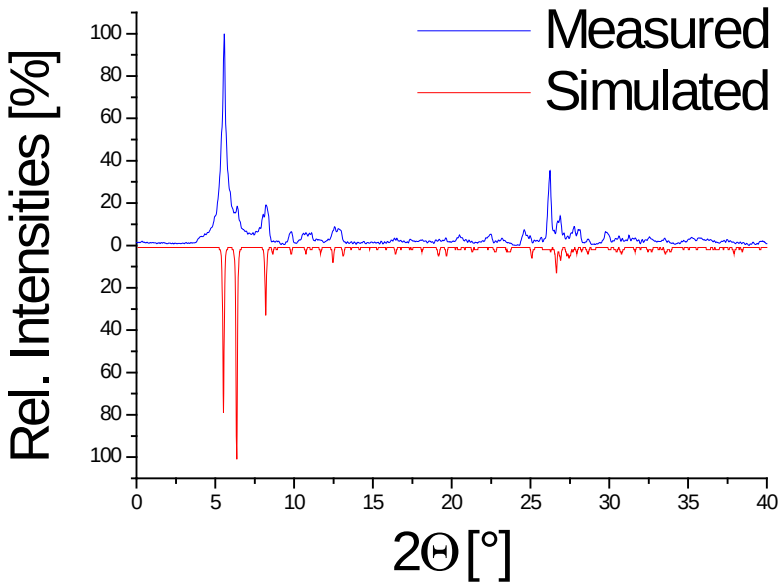

Figure 3.13: Powder X-ray diffractogram of $[Ag(PhCN)(thb)]_4[Mo_8O_{26}]\cdot PhCN$ (**3.4**). The simulated diffractogram is based on the crystal structure at 170(2) K.

3.4.3 DTA/TG Measurements

The DTA/TG measurements were accomplished on a Netzsch STA 409 thermal analyzer with a heating rate of 20°C/min.

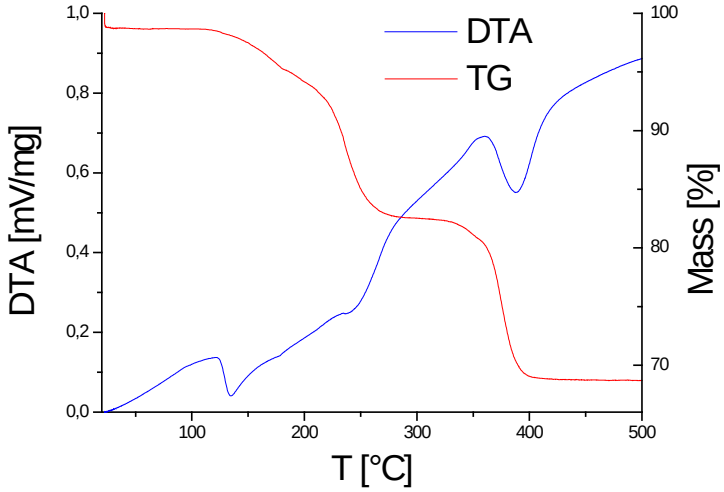

Figure 3.14: DTA/TG of $(NBu_4)_2[Ag(PhCN)_3]_2[W_{10}O_{32}]$ (**3.1**).

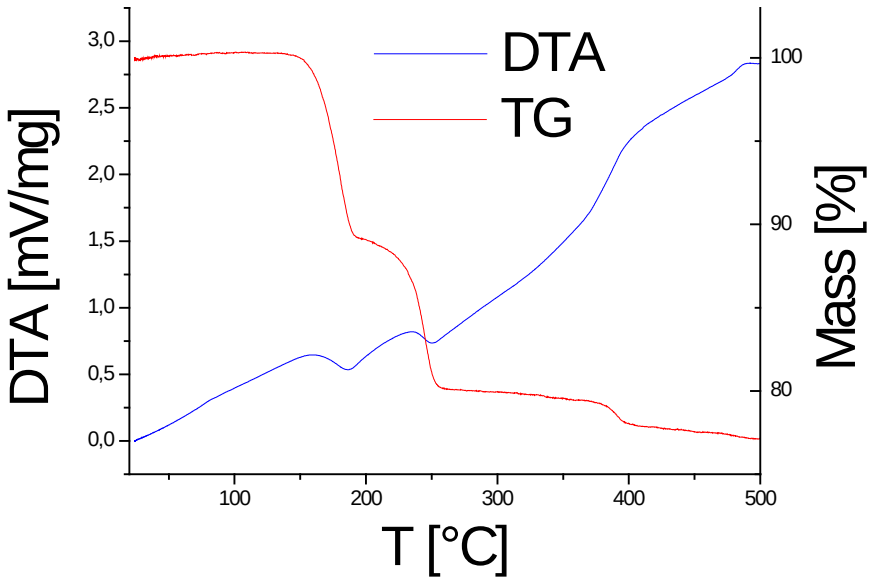

Figure 3.15: DTA/TG of $[Ag(PhCN)_3]_4[W_{10}O_{32}]$ (**3.2**).

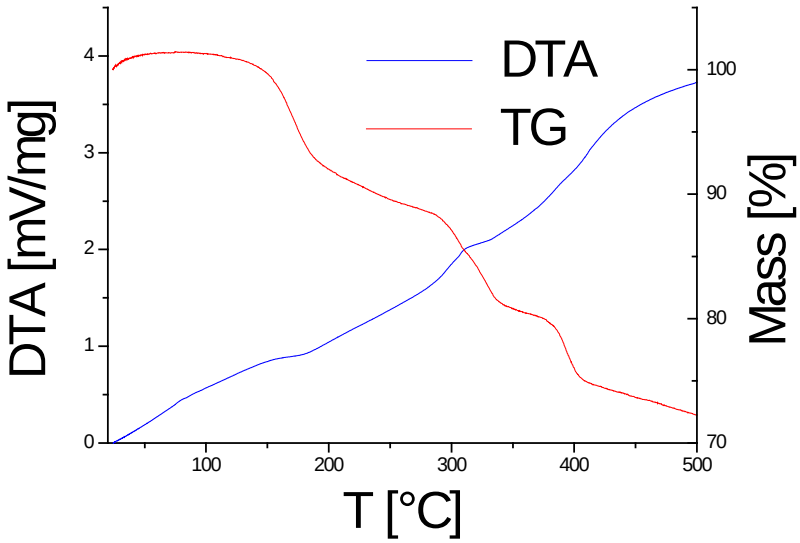

Figure 3.16: DTA/TG of $[Ag(PhCN)_2(thb)]_4[W_{10}O_{32}]\cdot PhCN$ (**3.3**).

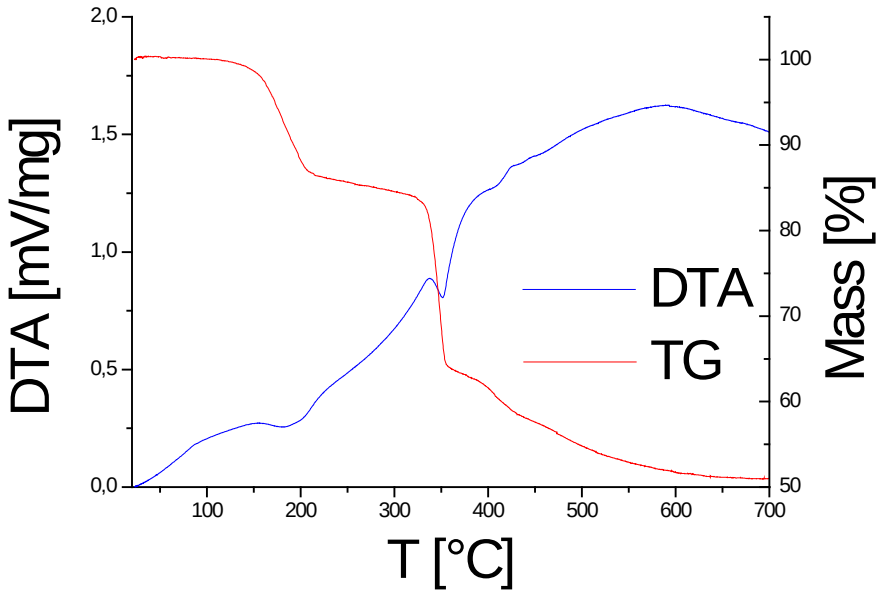

Figure 3.17: DTA/TG of $[Ag(PhCN)(thb)]_4[Mo_8O_{26}]\cdot PhCN$ (**3.4**).

3.4.4 Single Crystal X-Ray Crystallography

X-Ray crystallography: The single crystals suitable for X-ray diffraction of **3.4** were obtained with the filtrate of the solution described in the experimental procedure. The C, H and N atoms

of the embedded solvent molecule were refined isotropically and their positions were split with relative occupancies of 67.3 and 32.7 % due to the disorder. The C and H atoms of the disordered aromatic ring of one of the benzonitrile ligands were also refined isotropically and split in two positions with relative occupancies of 62.2 and 37.8 %. Crystallographic data (excluding structure factors) have been deposited with the Cambridge Crystallographic Data Centre, CCDC, 12 Union Road, Cambridge CB21EZ, UK. Copies of the data can be obtained free of charge on quoting the depository numbers CCDC 943409-943411 (**3.1-3**) and CCDC 947921 (**3.4**). (Fax: +44-1223-336-033; E-Mail: deposit@ccdc.cam.ac.uk, http://www.ccdc.cam.ac.uk).

Table 3.1: Crystallographic data for compounds **3.1** – **3.4**.

	3.1	**3.2**	**3.3**	**3.4**
empirical formula	$C_{84}H_{102}Ag_2N_8O_{32}W_{10}$	$C_{56}H_{40}Ag_4N_8O_{32}W_{10}$	$C_{91}H_{77}Ag_4N_{25}O_{40}W_{10}$	$C_{70}H_{62}Ag_4Mo_8N_{22}O_{34}$
M [g/mol]	3789.88	3606.94	4430.76	2954.41
crystal system	orthorhombic	triclinic	triclinic	triclinic
space group	*Pbca*	$P\bar{1}$	$P\bar{1}$	$P\bar{1}$
a [Å]	16.0555(6)	11.0972(4)	10.7971(5)	10.0221(4)
b [Å]	24.2744(9)	13.3970(5),	14.5000(6)	13.9136(6)
c [Å]	25.214(1)	14.0088(5	20.1073(8)	16.1648(7)
α [°]	90	71.514(3)	97.929(3)	92.764(4)
β [°]	90	66.534(3)	93.069(3)	97.678(3)
γ [°]	90	85.406(3)	110.612(3)	91.800(3)
V [Å^3]	9827.0(7)	1809.30(11)	2900.5(2)	2229.6(2)
Z	4	1	1	1
T [K]	293(2)	293(2)	170(2)	170(2)
reflns measured	149947	25537	44202	27993
unique reflns	11088	7649	12299	9450
R_{int}	0.0694	0.0798	0.1092	0.0807

$R_1(I>4\sigma)$	0.0468	0.0301	0.0467	0.0428
wR_2(all data)	0.1327	0.0767	0.1181	0.1099

3.5 References

(1) McGlone, T.; Streb, C.; Busquets-Fité, M.; Yan, J.; Gabb, D.; Long, D.-L.; Cronin, L. *Cryst. Growth Des.* **2011**, *11*, 2471.

(2) a) Wang, X.; Peng, J.; Alimaje, K.; Shi, Z.-Y. *CrystEngComm* **2012**, *14*, 8509; b) Wang, X.; Peng, J.; Liu, M.-G.; Wang, D.-D.; Meng, C.-L.; Li, Y.; Shi, Z.-Y. *CrystEngComm* **2012**, *14*, 3220; c) Zhang, P.-p.; Peng, J.; Pang, H.-j.; Sha, J.-q.; Zhu, M.; Wang, D.-d.; Liu, M.-g. *CrystEngComm* **2011**, *13*, 3832.

(3) Streb, C.; Ritchie, C.; Long, D.-L.; Kögerler, P.; Cronin, L. *Angew. Chem.* **2007**, *119*, 7723.

(4) Meyer, G.; Pantenburg, I. In *Design and Construction of Coordination Polymers* Hong, M.-C., Chen, L., Eds.; John Wiley and Sons: 2009, p 1.

(5) Bondi, A. *J. Phys. Chem.* **1964**, *68*, 441.

(6) Wilson, E.; Abbas, H.; Duncombe, B.; Streb, C.; Long, D.-L.; Cronin, L. *J. Am. Chem. Soc.* **2008**, *130*, 13876.

(7) Steiner, T. *Angew. Chem.* **2002**, *114*, 50.

(8) Schottel, B. L.; Chifotides, H. T.; Dunbar, K. R. *Chem. Soc. Rev.* **2008**, *37*, 68.

(9) a) Reddy, V. R.; Currao, A.; Calzaferri, G. *J. Phys.: Conf. Ser.* **2007**, *61*, 960; b) Hong-Yan, S.; Bo, H.; Xiao-Chun, Y.; Rong-Li, Z.; Xi-Feng, R.; Shi-Lin, L.; Jian-Wei, L.; Mei, F.; An-Wu, X.; Shu-Hong, Y. *Adv. Funct. Mater.* **2010**, *20*, 958; c) Gao, X.; Jin, L.; Wu, Q.; Chen, Z.; Lin, X. *Electroanalysis* **2012**, *24*, 1771.

(10) Tritthart, U.; Gey, W.; Gavrilyuk, A. *Electrochim. Acta* **1999**, *44*, 3039.

(11) Gavrilyuk, A. I. *Sol. Energy Mater. Sol. Cells* **2009**, *93*, 1885.

(12) Wesołowski, M.; Szynkaruk, P. *J. Therm. Anal. Calorim.* **2001**, *65*, 599.

(13) a) Glemser, O.; Naumann, C. *Z. Anorg. Allg. Chem.* **1951**, *265*, 288; b) *Natl. Bur. Stand. (U. S.), Monogr. 25* **1981**, *18*, 74; c) *Natl. Bur. Stand. (U.S.), Circ. 539* **1953**, *I*, 23; d) Woodward, P. M.; Sleight, A. W.; Vogt, T. *J. Phys. Chem. Solids* **1995**, *56*, 1305.

(14) Wilson, E. F.; Abbas, H.; Duncombe, B. J.; Streb, C.; Long, D.-L.; Cronin, L. *J. Am. Chem. Soc.* **2008**, *130*, 13876.

(15) Kulikov, V.; Meyer, G. *Cryst. Growth Des.* **2013**, *13*, 2916.

(16) *Natl. Bur. Stand. (U. S.), Monogr. 25* **1981**, *18*, 44.

(17) Fournier, M. In *Inorg. Synth.*; Ginsberg, A. P., Ed.; John Wiley & Sons, Inc.: New York, Chichster, Brisbane, Toronto, Singapore, 1990; Vol. 27, p 74.

(18) The simulated reflexes are moved, due to temperature difference of simulated vs. measured sample (170K vs. room temperature). The values of calculated elemental composition without the embedded PhCN molecule matched the found ones (see section 3.4). The lack of the embedded PhCN molecule might have led to changes in the crystal structure and respective reflections. PhCN was most likely washed away with acetone.

4. Polyoxotungstates Packed in Molecular “Boxes” of Purine Bases

4.1 Introduction

One of the most promising potential application fields of POMs is pharmacology. A multitude of different polyoxoanions was tested in vitro and in vivo, showing partly strong antiviral and antitumor activity.[1]

Several groups accomplished extensive research of the antiviral activity of polyoxotungstates.[2] The effectivity of the compounds was determined with several virus strains ranging from herpes simplex to HIV. Some of the effective polyoxotungstates were shown to hinder viral proliferation at the initial stage - during the cell entry. The experiments with these compounds *in vitro* indicated competitive inhibition of the viral proteins responsible for the cell binding and membrane fusion as a likely mechanistic pathway. For other polyoxotungstates exhibiting antiviral activity, biochemical experiments indicated the inhibition at later stages of the viral proliferation, mechanistic details of which remain obscure. Hexa- and decatungstate were both tested on their anti-HIV activity. Decatungstate showed a promising effectivity value and concomitant comparatively low toxicity.[3]

Based on these results, the viral RNA can be considered one of the possible targets of the polyoxotungstates. It consists of a series of purine and pyrimidine bases interconnected by ribose/phosphate backbone and H-bonds.[4] In the hope to assist medical research in the area a compound containing one of the constituent purine bases - guanine and decatungstate was synthesized. The respective interactions were investigated by means of single crystal X-ray diffraction.

Other purine bases such as theobromine are of high biological and partly pharmacological importance.[5] Accordingly the crystal structures of their salts are of continuing scientific interest. Compounds containing theobromine and polyoxotungstates were synthesized and characterized in order to expand the structural knowledge and to compare the respective interactions with the guanine counterpart.

4.2 Results and Discussion

There are two basic intermolecular interactions stabilizing all presented compounds: H-bonding and Coulombic cation-anion interactions. H-bonding is illustrated by guaninium and theobrominium dimers (Figure 4.1). Both dimers are centrosymmetric. The guaninium dimer is stabilized by interactions between protonated and deprotonated N atoms, while the

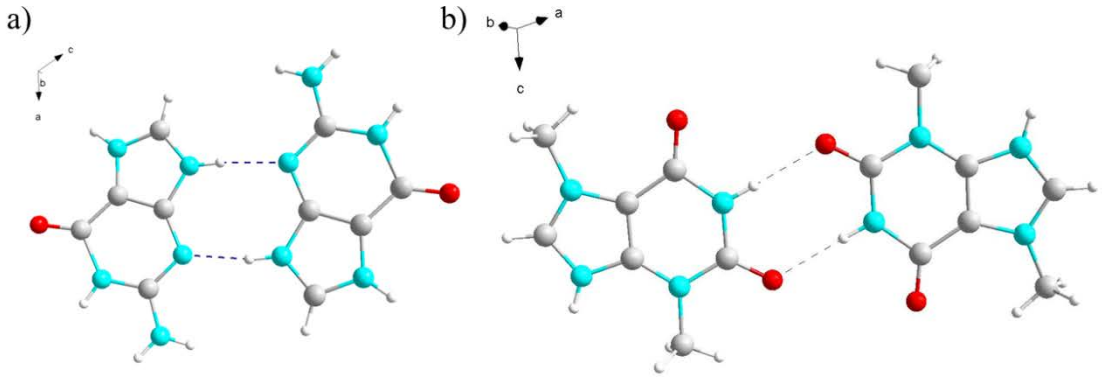

Figure 4.1: Guaninium and theobrominium dimers. C grey, H white, O red. This color scheme is used throughout the text.

theobrominium counterpart is stabilized by amide-to-amide H-bonds reminiscent of the adenine-thymine base pair in the duplex nucleic acids.[6] The H-bond donor-acceptor distances (N···N 2.90(2) Å) and the directionality (N-H···N = 157.3(9)°) indicate medium strength interactions for the guaninium dimer.[7] The same is true for the theobrominium dimer (N···O 2.87(1) Å; N-H···N = 169.1(8)°).

The Coulombic interactions are rather similar in all compounds. The organic cations lie parallel to the faces of the POM anions. Thus, the positive charge delocalized over the purinium ring can be optimally stabilized by the negatively charged decatungstate face. The decatungstate anions are surrounded by two guaninium dimers and two single guaninium ions on the opposite sides in the crystal structure of $(guaH)_4[W_{10}O_{32}]\cdot 4H_2O\cdot MeCN$ (**4.1**) (Gua = guanine; Figure 4.2a). The planes of the single guaninium ions and the dimers build a right angle with each other. This arrangement resembles a box limited by water molecules additionally stabilizing the framework on the vertices. The guaninium dimers are shared with the neighbouring decatungstates along the crystallographic b-axis. The single guaninium ions belong to one

polyoxoanion only. Accordingly the interplanar distance from the dimers to decatungstate is roughly 0.3 Å shorter than the respective distance from the single guaninium ions (Figure 4.2a). Both distances are shorter than the interplanar distances between the homoaromatic organic molecules conducting π-π stacking interactions published previously.[8]

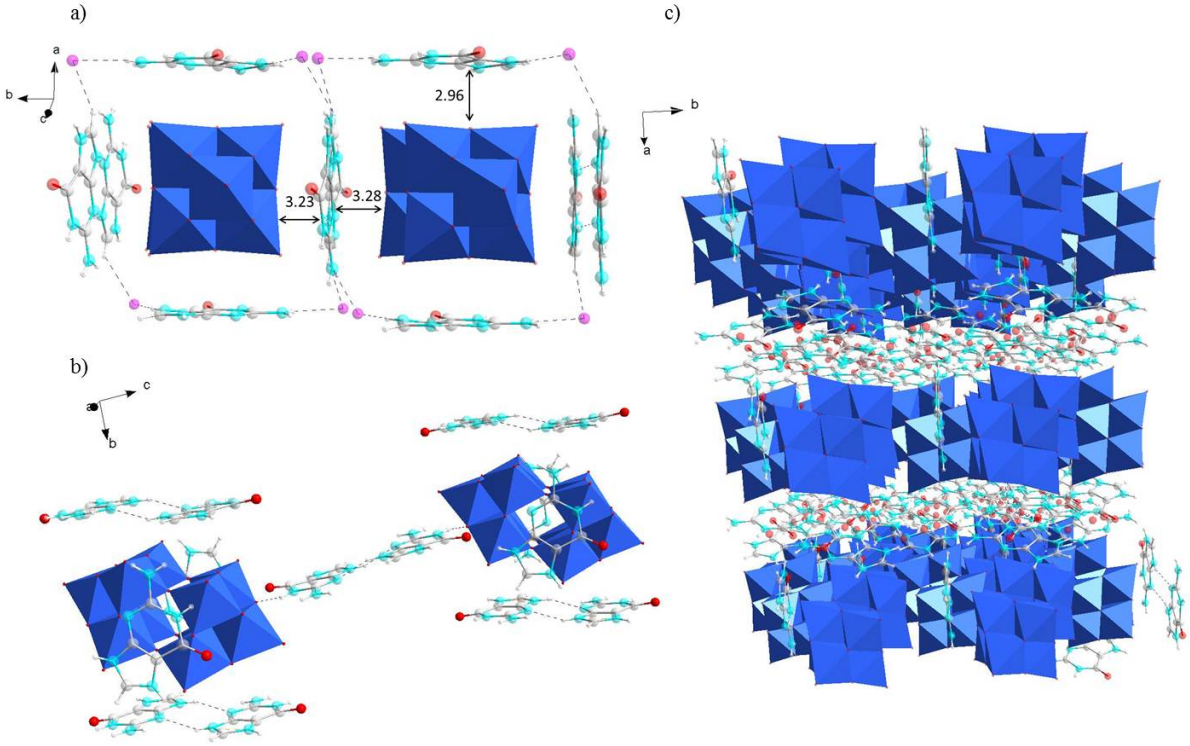

Figure 4.2: Crystal structure of $(guaH)_4[W_{10}O_{32}]\cdot 4H_2O\cdot MeCN$ (**4.1**). a) Molecular "boxes" of organic cations connecting decatungstate anions into chains. The distances were determined from the nearest decatungstate oxygens and are given in Å. b) H-bond connection of two decatungstates via a guaninium dimer. c) Layers of guaninium/water framework and decatungstate anions. Tungstate - light blue polyhedra, half occupied water positions – magenta. This color scheme is used throughout the text.

The guaninium dimers additionally interconnect $[W_{10}O_{32}]^{4-}$ units along the crystallographic c-axis by H-bonding between the amide protons and POM oxygen atoms (Figure 4.2b). Again, the geometry suggests interactions of medium strength (N···O 2.95(3) Å; N-H···N = 158.2(2)°). The resulting crystal structure consists of alternating layers of POMs / guaninium dimers and single guaninium molecules / water molecules running along the crystallographic b-axis (Figure 4.2c).

A little different crystallographic arrangement is encountered in the crystal structure of $(thbH)_3(H_3O)[W_{10}O_{32}]\cdot 7.5H_2O$ (**4.2**) (thb = theobromine). Now the molecular "boxes" run along the face diagonals of every plane of the unit cell (Figure 4.3a,c). Each decatungstate is

surrounded by six theobrominium ions sharing them with neighbouring POMs. Again the planes of the theobrominium ions are perpendicular to one another and the individual cations are connected by H-bonding either through water molecules or directly by the H-bonds between the protonated heterocyclic nitrogen and carbonyl group of theobromine (Figure 4.3a).

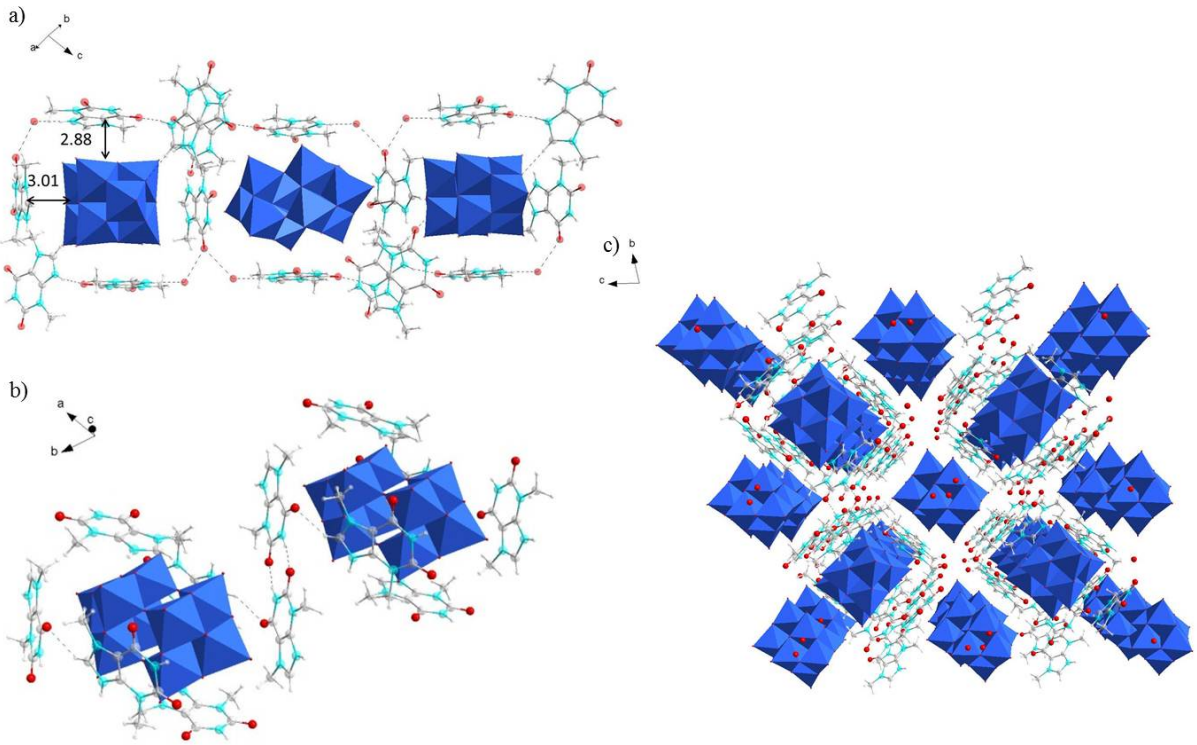

Figure 4.3: Crystal structure of $(thbH)_3(H_3O)[W_{10}O_{32}]\cdot 7.5H_2O$ (**4.2**). a) Molecular "boxes" of organic cations connecting decatungstate anions into chains. b) H-bond connection of two decatungstates via theobrominium dimer. c) View along the crystallographic a-axis onto the molecular "boxes".

The theobrominium dimers additionally strengthen the framework by amide-to-amide H-bonding (Figure 4.3b). The overall framework resembles a grid of the molecular "boxes" connected in [110], [101] and [011] directions (Figure 4.3c).

Contrary to **4.1** and **4.2**, $(thbH)_2[W_6O_{19}]\cdot 2H_2O$ (**4.3**) does not contain decatungstate but the Lindqvist tungstate anion of higher symmetry. Accordingly, it displays a crystal structure of higher symmetry than **4.1** and **4.2**. The interplanar distances between the faces of the hexatungstate and the organic cations are equal to every face (Figure 4.4a). The planes of the theobromine molecules are not perpendicular to one another as in the previous compounds, but all of the organic cations are crystallographically equivalent.

Each Lindqvist tungstate is connected to neighbours via H-bonding through two water

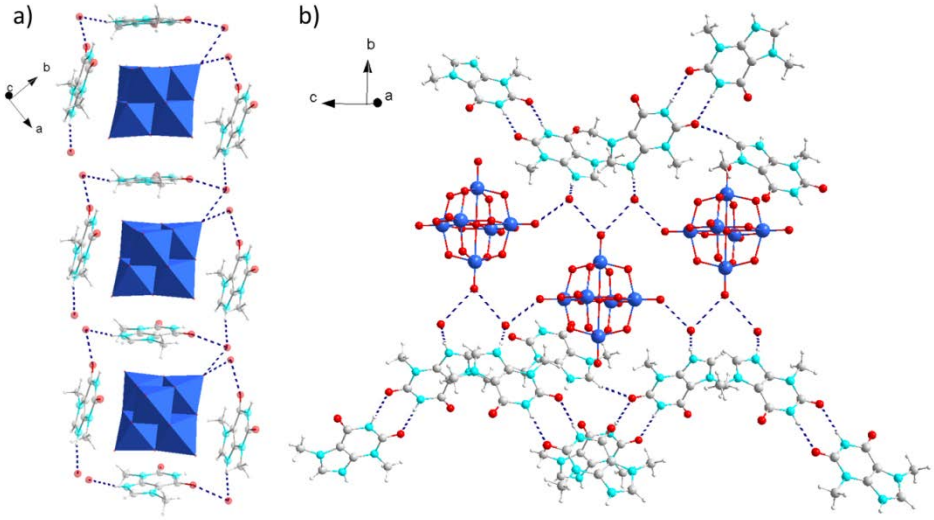

Figure 4.4: Crystal structure of $(thbH)_2[W_6O_{19}]\cdot 2H_2O$ (**4.3**). Molecular "boxes" of organic cations connecting Lindqvist anions into chains. b) H-bond framework of Lindqvist anions, water molecules and theobrominium dimers.

molecules (Figure 4.4a). The distances between the terminal oxygen atoms of the hexatungstate and water molecules are just above 3 Å. This indicates H-bonds of intermediate to low strength. The anions and water molecules build chains running along the crystallographic c-axis. The chains are interconnected via H-bonding between water molecules and theobrominium amide-to-amide dimers (Figure 4.4b).

4.3 Thermolysis Results

The behaviour of **4.2** and **4.3** upon heating to high temperatures was scrutinized in N_2-atmosphere by DTA and TG (Figures 4.7 and 4.8). Both compounds exhibit exothermic reactions and emission of heat in the temperature ranges 100-350°C and 150-400°C respectively. This thermal behaviour can be explained by redox reactions, in course of which the organic parts are oxidized to volatile products such as CO_2 and H_2O, whereas the polyoxotungstates(VI) are reduced to tungsten oxides in lower oxidation states.

Indeed, the powder X-ray diffraction experiments showed presence of tungsten(IV) oxide in both thermolysis residues (Scheme 4.1 and Figure 4.11 and 4.12). The measurements were undertaken in an alumosilicate crucible. The black residue stuck firmly at the bottom of the

crucible; hence some of the crucible material was scratched off with a spatula together with the sample (Figure 4.11).

In order to explore the possibilities to obtain tungsten oxides of different oxidation states, heating of **4.2** to 1000°C was performed in a Ni crucible (Scheme 4.1). A mixture of tungsten oxides and different hydrogen tungsten oxide bronzes could be obtained upon heating the material to this temperature (Figure 4.9). Unfortunately, the material reacted also with the crucible, which yielded a quantitative conversion to $NiWO_4$ upon calcination at 1000°C (Figure 10).

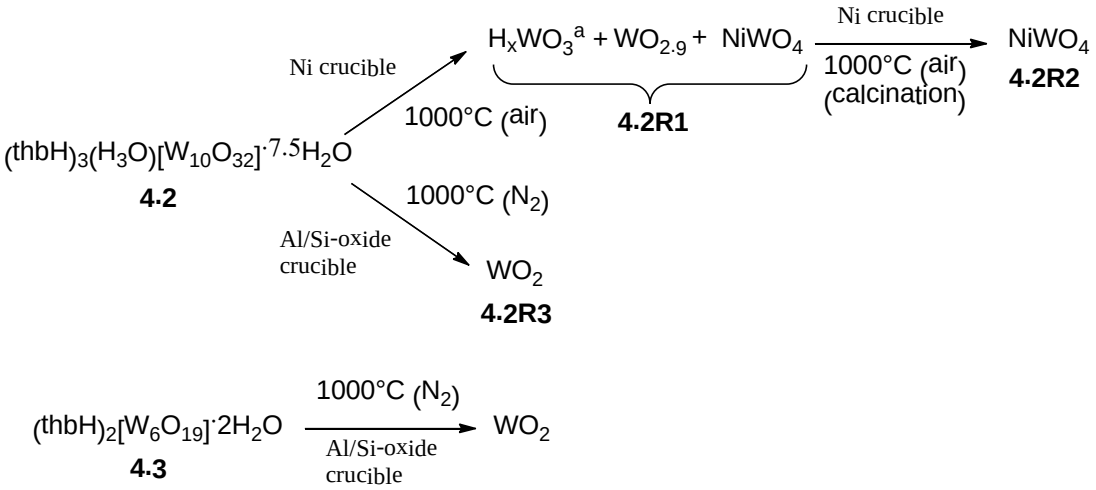

Scheme 4.1: Thermolysis of **4.2** and **4.3**.

4.4 Conclusion

Three compounds containing protonated guanine and theobromine as cations and polyoxotungstates as anions were characterized crystallographically. The organic cations lie parallel to the faces of the POMs in all characterized compounds. This arrangement can be attributed to the delocalization of the positive charge throughout the aromatic system of the organic molecules and negative charge throughout the oxygen framework of the anions. Both purine bases are encountered in the protonated forms in the synthesized compounds, which is unlikely under physiological conditions. Hence, it cannot be concluded, whether the same geometric arrangement would be encountered *in vivo*. Nevertheless, the crystal structures serve

as a hint on the type of possible interactions between POMs and biomolecules containing purine bases.

The organic cations reduce the polyoxotungstates upon heating to tungsten oxides of different oxidation states. One of the compounds was calcinated at 1000°C in air, which resulted in reaction with nickel crucible.

4.5 Experimental Section

4.5.1 Synthetic Procedures

The precursors $(NBu_4)_2[W_6O_{19}]$ and $(NBu_4)_4[W_{10}O_{32}]$ were prepared according to literature procedures.[9] The phase purities of the bulk samples of **4.2** and **4.3** were verified by X-ray powder diffraction on a STOE STADI transmission powder diffractometer (Figures 4.5 and 4.6). DTA and TG analyses were performed on a Netzsch STA 409 thermal analyzer.

$(guaH)_4[W_{10}O_{32}]\cdot 4H_2O\cdot MeCN$ (4.1). Guanine (45 mg, 0.3 mmol) was dissolved in a mixture of 26 ml of acetonitrile and 8 ml of 27% nitric acid. $(NBu_4)_4[W_{10}O_{32}]$ (200 mg, 0.06 mmol) was dissolved in 8 ml of acetonitrile and added to the reaction mixture. The reaction mixture was filtered after stirring for 1.5 hrs. Yellow crystals precipitated after 2 weeks. The amount of material obtained was too low for any further investigations. Attempts to upscale the reaction failed.

$(thbH)_3(H_3O)[W_{10}O_{32}]\cdot 7.5H_2O$ (4.2). Theobromine (270 mg, 1.50 mmol) was dissolved in a mixture of 130 ml acetonitrile and 40 ml of 27% nitric acid. $(NBu_4)_4[W_{10}O_{32}]$ (996 mg, 0.3 mmol) dissolved in 40 ml acetonitrile was added to the solution. After addition of 20 ml of MeOH the reaction mixture was kept in a closed vessel for two weeks. The rest of the yellow crystalline product was washed twice with 5 ml portions of acetone and dried in air for a day. Obtained: 540 mg, 0.18 mmol, 60% based on decatungstate (product 1). Elemental analysis calcd. (%) for $C_{21}H_{45}N_{12}O_{46.5}W_{10}$: C 8.27, H 1.49, N 5.51; found: C 9.09, H 1.49, N 5.76. IR (KBr): $\tilde{\upsilon}$ (cm^{-1}) = 3450 (br, s), 3161 (w), 3045 (w), 2826 (w), 2611 (w), 1699 (s), 1651 (s), 1580 (m), 1549 (m), 1476 (w), 1437 (m), 1393 (m), 1363 (w), 1304 (w), 1279 (m), 1211 (w), 1167 (m), 1030 (m), 964 (s), 895 (s), 795 (br, s), 677 (m), 604 (s), 513 (m), 432 (m), 401 (m). UV/Vis (KBr): λ (nm) = 203, 273, 326.

$(thbH)_2[W_6O_{19}]\cdot 2H_2O$ (4.3). Theobromine (540 mg, 3.00 mmol) was dissolved in a mixture of 130 ml acetonitrile and 40 ml of 27% nitric acid. $(NBu_4)_2[W_6O_{19}]$ (1.135 mg, 0.6 mmol) dissolved in 40 ml acetonitrile was added to the solution. After addition of 20 ml of MeOH, the reaction mixture was kept in a closed vessel for five days. The product was obtained as white crystalline powder and dried over $CaCl_2$ in a desiccator under dynamic vacuum (20 mbar) for a day. Yield: 960 mg, 0.51 mmol, 85% based on hexatungstate. Elemental analysis calcd. (%) for $C_{14}H_{22}N_8O_{25}W_6$: C 9.31, H 1.23, N 6.21; found: C 8.80, H 1.27, N 5.99. IR: $\tilde{\upsilon}$ (cm^{-1}) = 3578 (m), 3524 (m), 3141 (m), 3053 (m), 2852 (w), 1728 (s), 1684 (s), 1576 (m), 1545 (m), 1487 (w), 1437 (m), 1385 (s), 1323 (w), 1275 (m), 1211 (w), 1163 (m), 1088 (w), 1038 (m), 978 (s), 804 (br, s), 681 (w), 608 (w), 584 (m), 511 (w), 444 (s). UV/Vis: λ (nm) = 206, 275.

4.5.2 X-Ray Diffractograms

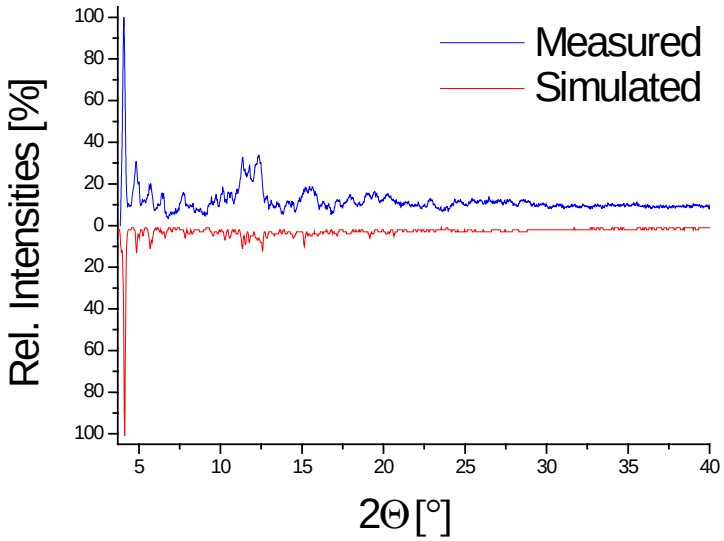

Figure 4.5: Powder X-ray diffractogram of $(thbH)_3(H_3O)[W_{10}O_{32}]\cdot 7.5H_2O$ (**4.2**). Mo-K_α radiation, λ = 0.7107 Å.

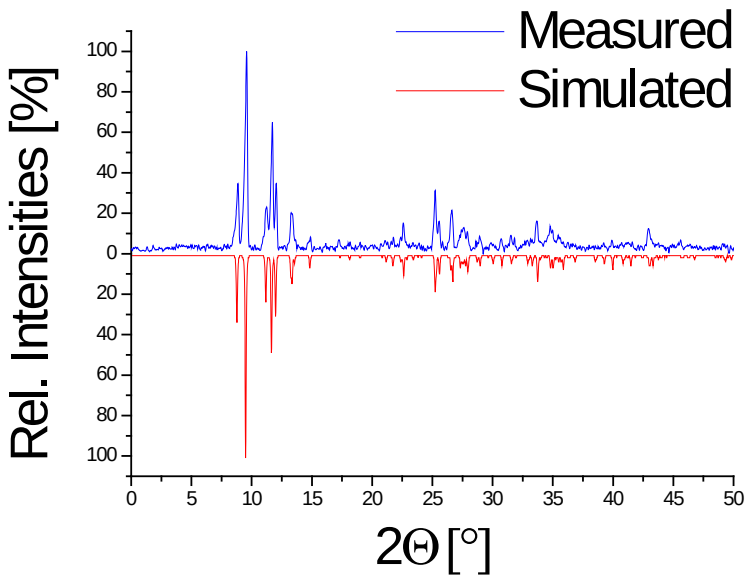

Figure 4.6: Powder X-ray diffractogram of $(thbH)_2[W_6O_{19}]\cdot 2H_2O$ (**4.3**). (Cu-K_α radiation, $\lambda = 1.5406$ Å).

4.5.3 DTA/TG Curves

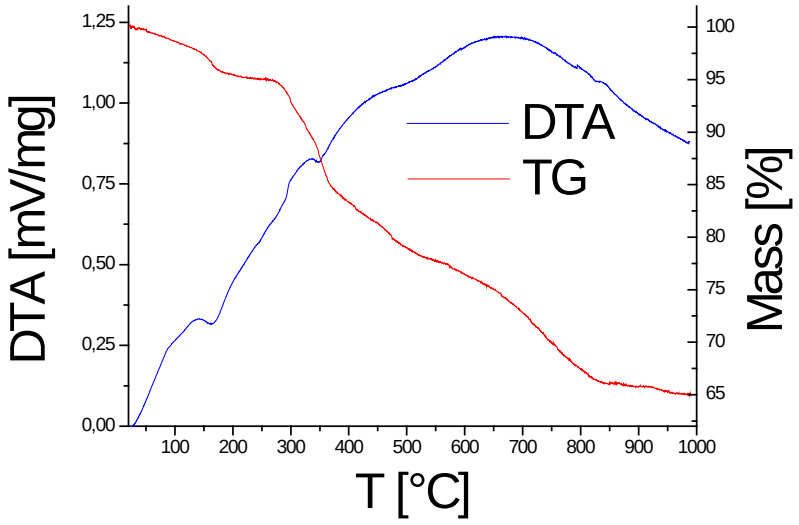

Figure 4.7: DTA/TG of $(thbH)_3(H_3O)[W_{10}O_{32}]\cdot 7.5H_2O$ (**4.2**). Heating rate: 10°C/min.

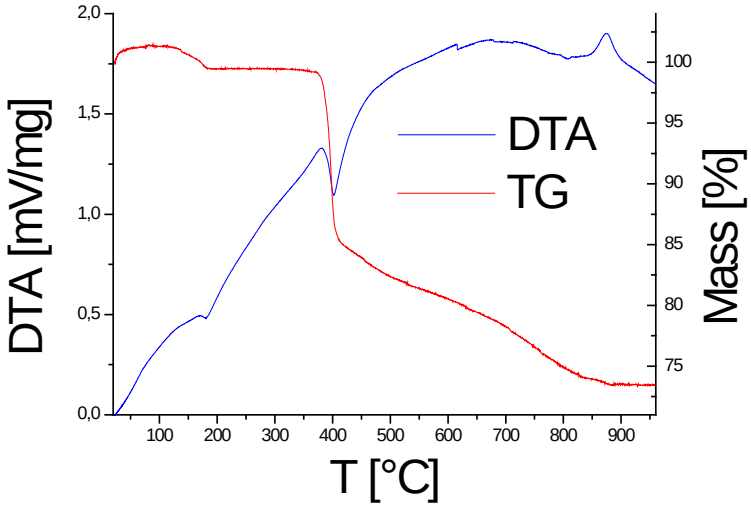

Figure 4.8: DTA/TG of $(thbH)_2[W_6O_{19}]\cdot 2H_2O$ **(4.3)**. Heating rate: 10°C/min.

4.5.4 X-Ray Powder Patterns of Thermolysis Residues

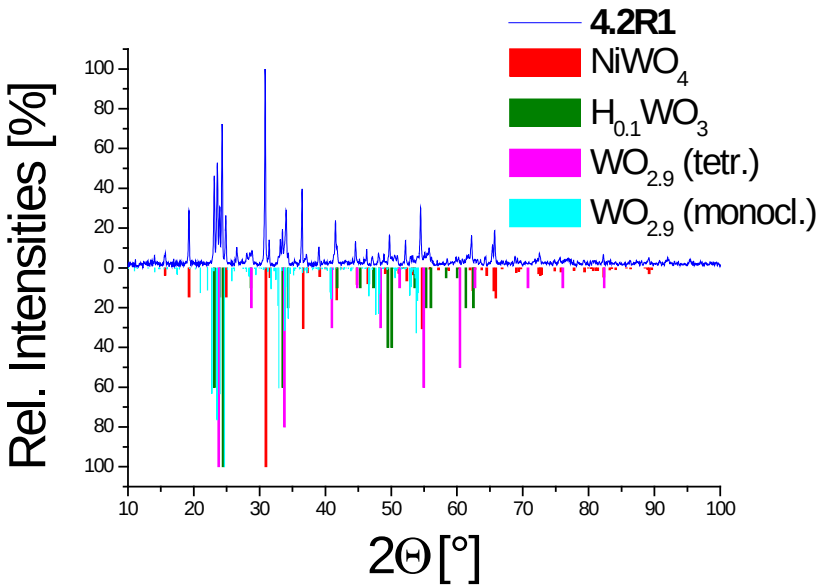

Figure 4.9: X-Ray powder pattern of the thermolysis residue (Ni crucible) of $(thbH)_3(H_3O)[W_{10}O_{32}]\cdot 7.5H_2O$ (**4.2**) – labeled **4.2R1**. (Cu-K_α radiation, λ = 1.5406 Å).[10] Temperature program: 20°C→1000°C (10°C/min).

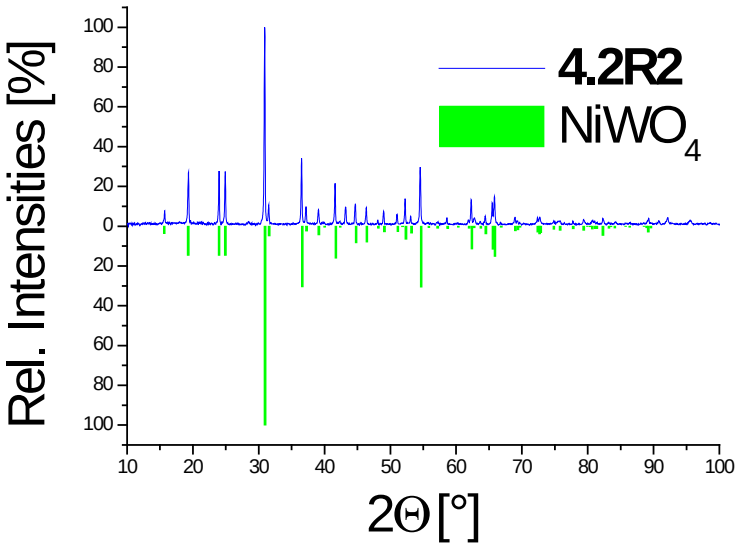

Figure 10: X-Ray powder pattern of the thermolysis residue (Ni crucible) of $(thbH)_3(H_3O)[W_{10}O_{32}]\cdot 7.5H_2O$ (**4.2**) – labeled **4.2R2**. (Cu-K_α radiation, λ = 1.5406 Å).[10a] (Calcination at 1000°C for 10 hrs.).

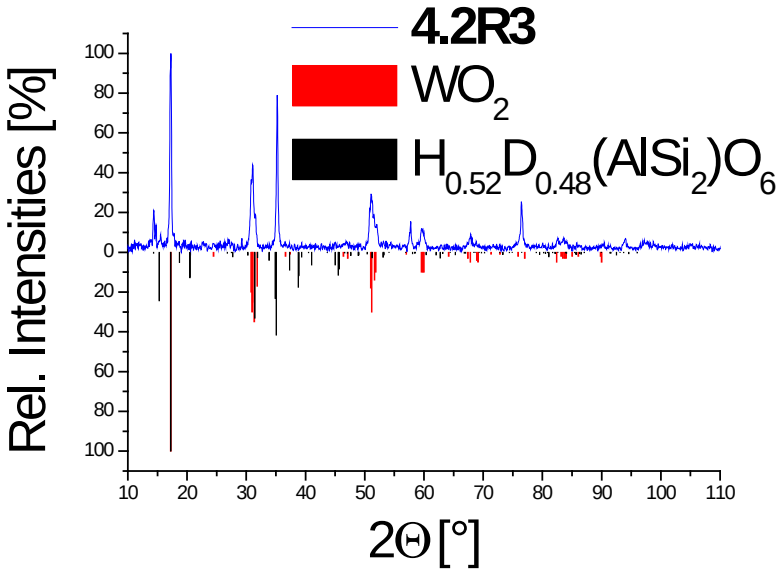

Figure 4.11: X-Ray powder pattern of the DTA residue of $(thbH)_3(H_3O)[W_{10}O_{32}]\cdot 7.5H_2O$ (**4.2**) labeled **4.2R2**. (Cu-K_α radiation, λ = 1.5406 Å).[11]

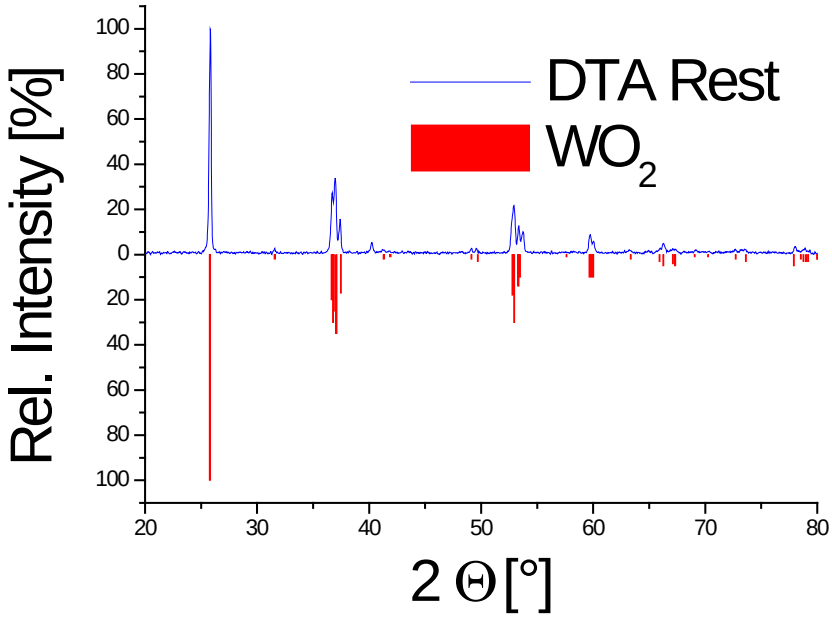

Figure 4.12: X-Ray powder pattern of the DTA residue of $(thbH)_2[W_6O_{19}]\cdot 2H_2O$ (**4.3**) (Cu-K_α radiation, $\lambda = 1.5406$ Å).[11]

4.5.5 Single Crystal X-Ray Diffraction Studies

Intensity data were measured at temperatures given in on an image-plate diffractometer, STOE IPDS I and STOE IPDS II, respectively (λ(MoKα) = 0.71073 Å, graphite monochromator). Structure solutions and refinements were performed using the program package WinGX,[12] which includes the programs SHELX and Platon.[13] Spherical and numerical absorption corrections were accomplished with the X-red and X-shape software (STOE Darmstadt).[14]

All of non-hydrogen atoms, except for several atoms of the embedded solvent molecules were refined anisotropically. H-atom positions were calculated using the riding model.

Crystallographic data as well as structure solution and refinement details are summarized in Table 4.1 and have been deposited in more detail with the Cambridge Crystallographic Data Centre as supplementary publications Nos. CCDC 949335-949337. Copies of the data can be obtained, free of charge, on application to CHGC, 12 Union Road, Cambridge CB2 1EZ, UK (fax: +44 1223 336033 or e-mail: deposit@ccdc.cam.ac.uk).

Table 4.1: Crystallographic data for **4.1-3**.

	4.1	**4.2**	**4.3**
empirical formula	$C_{22}H_{37}N_{20}O_{41}W_{10}$	$C_{21}H_{45}N_{12}O_{46.5}W_{10}$	$C_{14}H_{22}N_8O_{25}W_6$
M [g/mol]	3076.2	3048.2	1805.47
crystal system	monoclinic	triclinic	monoclinic
space group	*P* $2_1/c$	*P* $\bar{1}$	*C 2/c*
a [Å]	14.477(1))	13.491(1)	16.810(3)
b [Å]	10.8678(9)	15.171(1)	13.051(2)
c [Å]	21.627(2)	17.069(2)	15.676(3)
α [°]	90	79.594(8)	90
β [°]	122.780(6)	89.386(8)	109.73(1)
γ [°]	90	70.001(7)	90
ρcalc. [g/cm³]	3.526	3.057	3.6960
V [$Å^3$]	2860.8(4)	3223.8(6)	3237.2(9)
Z	2	2	4
$\mu(MoK_\alpha)$ [mm^{-1}]	20.131	17.86	21.35
T [K]	170(2)	293(2)	293(2)
reflns measured	33411	41410	21383
independent reflns	6202	14242	3590
parameters	443	767	242
R_1 (I>4σ)	0.0434	0.0347	0.0361
R_1 (all data)	0.0612	0.0590	0.1037
wR_2 (all data)	0.1316	0.0950	0.0745

4.6 References

(1) Rhule, J. T.; Hill, C. L.; Judd, D. A.; Schinazi, R. F. *Chemical Reviews* **1998**, *98*, 327.

(2) a) Shigeta, S.; Mori, S.; Yamase, T.; Yamamoto, N.; Yamamoto, N. *Biomed. & Pharmacother.* **2006**, *60*, 211; b) Witvrouw, M.; Weigold, H.; Pannecouque, C.; Schols, D.; De Clercq, E.; Holan, G. *J. Med. Chem.* **2000**, *43*, 778; c) Barnard, D. L.; Hill, C. L.; Gage, T.; Matheson, J. E.; Huffman, J. H.; Sidwell, R. W.; Otto, M. I.; Schinazi, R. F. *Antivir. Res.* **1997**, *34*, 27.

(3) Hill, C. L.; Weeks, M. S.; Schinazi, R. F. *J. Med. Chem.* **1990**, *33*, 2767.

(4) Voet, D.; Voet, J. G. *Biochemistry*; 4 ed.; John Wiley & Sons, Inc.: United States of America, 2011.

(5) Biradha, K.; Samai, S.; Maity, A. C.; Goswami, S. *Cryst. Growth. & Des.* **2010**, *10*, 937.

(6) Hoogsten, K. *Acta. Cryst.* **1963**, *16*, 907.

(7) Steiner, T. *Angew. Chem.* **2002**, *114*, 50.

(8) Roesky, H. W.; Andruh, M. *Coord. Chem. Rev.* **2003**, *236*, 91.

(9) Fournier, M. In *Inorg. Synth.*; Ginsberg, A. P., Ed.; John Wiley & Sons, Inc.: New York, Chichster, Brisbane, Toronto, Singapore, 1990; Vol. 27, p 74.

(10) a) Weitzel, H. *Z. Kirstallogr.* **1976**, *144*, 238; b) Glemser, O.; Weidelt, J.; Freund, F. *Z. Anorg. Allg. Chem.* **1964**, *332*, 299; c) Glemser, O.; Naumann, C. *Z. Anorg. Allg. Chem.* **1951**, *265*, 288.

(11) Palmer, D. J.; Dickens, P. G. *Acta Cryst. B* **1979**, *35*, 2199.

(12) Farrugia, L. *J. Appl. Crystallogr.* **1999**, *32*, 837.

(13) a) Sheldrick, G. *Acta Cryst. A* **2008**, *64*, 112; b) Spek, A. *Acta Cryst. D* **2009**, *65*, 148.

(14) a) GmbH, S. C.; 1.06 ed.; STOE & Cie GmbH: Darmstadt, 1999, "Crystal Optimization for Numerical Absorption Correction"; b) GmbH, S. C.; 1.22 ed.; STOE & Cie GmbH: Darmstadt, 2001.

5. Agglomeration of a Guanosine-Polyoxometalate Hybrid and its Helical Crystal Structure

5.1. Introduction

Guanosine derivatives are biomolecules of unparalleled significance. They play a central role in the composition and regulation of nucleic acids[1] as well as in the energy metabolism[2] and intracellular signalling.[3] In addition to their biological importance these compounds show fascinating physico-chemical properties as low molecular weight gelators,[4] ionophores[5] as well as building blocks for nanodevices.[6] A considerable amount of research was directed towards covalent organic modification of guanosine derivatives, mostly in order to obtain quadruplex structures.[5,7]

Strandberg anions are polyoxometalates (POMs), consisting of a ring of five condensed molybdate(VI) anions and two phosphate groups opposing each other above and below the plane of the ring.[8] The self-assembly of covalently modified Strandberg-type anions from phosphorylated organic molecules and molybdates(VI) have already been known for nearly four decades.[9] Quite a few phosphorylated biomolecules covalently attached to this POM were synthesized.[10] These compounds were usually characterized only by means of spectroscopy and elemental analysis. A few compounds containing nucleosides covalently bound to Strandberg anion or other hybrid-type POMs were isolated and analytically characterized.[10a,11] Two adenine-POM hybrids were characterized structurally.[12]

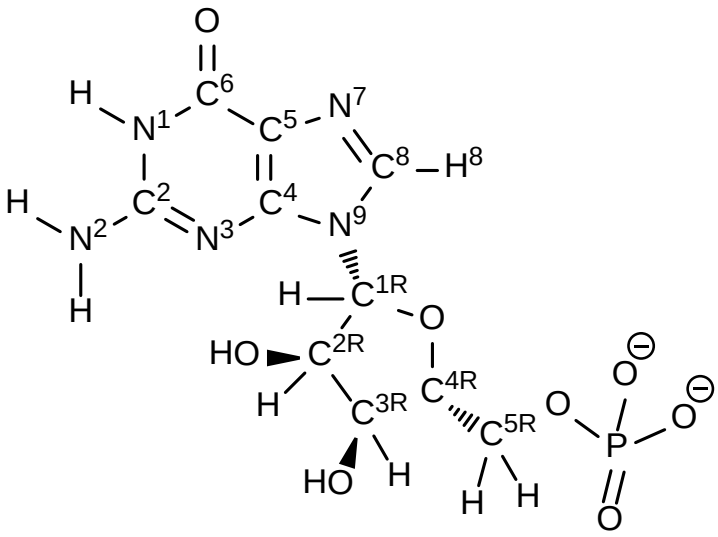

Figure 5.1: Atom numbering in guanosine monophosphate (GMP).

5.2. Results and Discussion

The synthesis, crystal structure as well as solution and agglomeration properties of $Na_2[(HGMP)_2Mo_5O_{15}]\cdot 7H_2O$ (GMP = guanosine monophosphate) (**5.1**) are described below. It was synthesized by reaction of Na_2MoO_4 with GMP under acidic conditions. The formation of **5.1** can easily be verified by ^{31}P-NMR spectroscopy (Figure 5.2). The ^{31}P nucleus is coupled to the H^{5R}-protons of the ribose ring (indicated by blue circles in Figure 5.2, see Figure 5.1 for atom numbering). Due to the chirality of both GMP and **5.1** these protons are diastereotopic. This

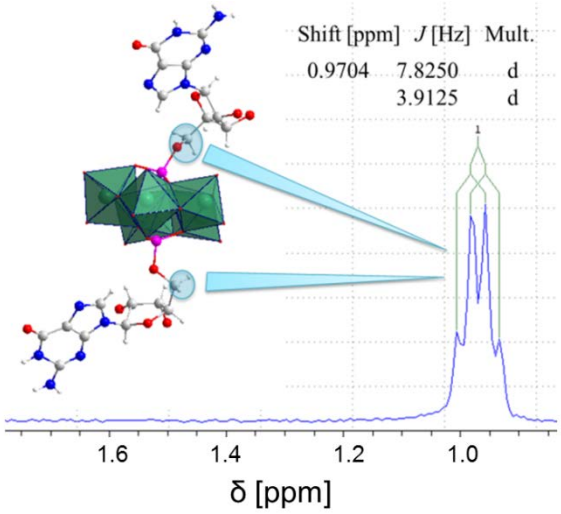

Figure 5.3:. Diastereotopic protons of **5.1** and corresponding ^{31}P resonance (162 MHz). C light grey, H white, O red, P magenta, Mo sea green. The same colour scheme applied in subsequent illustrations.

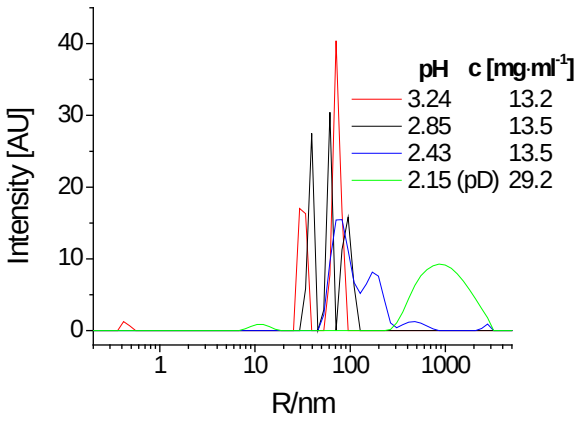

Figure 5.2: DLS size distributions at different pH/pD values and concentrations

diastereotopicity has no effect on the ^{31}P-resonance of GMP, as the coupling constants are averaged by rotation around the C^{5R}-O^{5R} bond. Accordingly, the respective ^{31}P signal is split into a triplet. This rotation around the C^{5R}-O^{5R}-bond is hindered by the ring plane of the polyoxoanion in **5.1**, such that the ^{31}P resonance appears as doublet of doublets in the NMR spectrum.

The NMR samples at pD ≈ 3 and concentrations of **5.1** of higher than 5 mg/mL turned into clear gels upon standing for several hours at room temperature. The transformation was noticeable as the sample did not flow when the NMR tube was turned upside down. This sample behaviour was not unexpected, as both Strandberg anions and GMP readily build organo- and hydrogels.[4,13]

Gelation is a process related to agglomeration of molecules.[14] The size of the agglomerated particles can be assessed by determination of the hydrodynamic radius by the DLS (dynamic light scattering) technique.[15] DLS measurements confirmed the agglomeration of compound **5.1** with increasing acidity of the solution, a property also displayed by GMP.[16] A small peak at 0.45 nm is observable at pH = 3.25 (Figure 5.3). This value corresponds to the hydrodynamic radius of GMP surrounded by five water molecules.[17] Accordingly, we can assume that **5.1** partly disintegrates into the GMP and molybdate anions at that pH value at the indicated concentrations. Increasing the hydrodynamic radius of the particles is clearly observable with decreasing pH. It reaches 1000 nm in size at the pD value of 2.15 at slightly elevated concentrations.

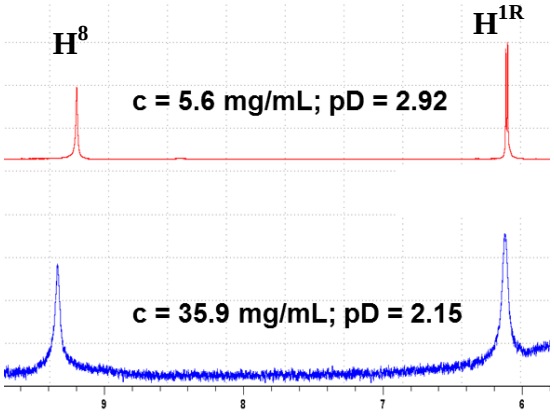

Figure 5.4: Part of the 1H NMR spectrum of **5.1** at different pD-values and concentrations.

The results of ^{1}H NMR measurements are consistent with the DLS results (Figure 5.4). They show noticeable deshielding of the guanine ring proton H^{8} with increasing concentration and acidity. Concomitantly the signal to noise ratio becomes lower resulting in the poorer spectrum. The first observation indicates the agglomeration of **5.1**, the second one indicates increased spin-lattice relaxation, which is consistent with the increased gelation of the sample. Nonetheless any splitting of the H^{8} signal peak is observable, which would hint at the quadruplex formation.[4] Accordingly it can be assumed, that the agglomeration is accomplished via stacking of the monomers.

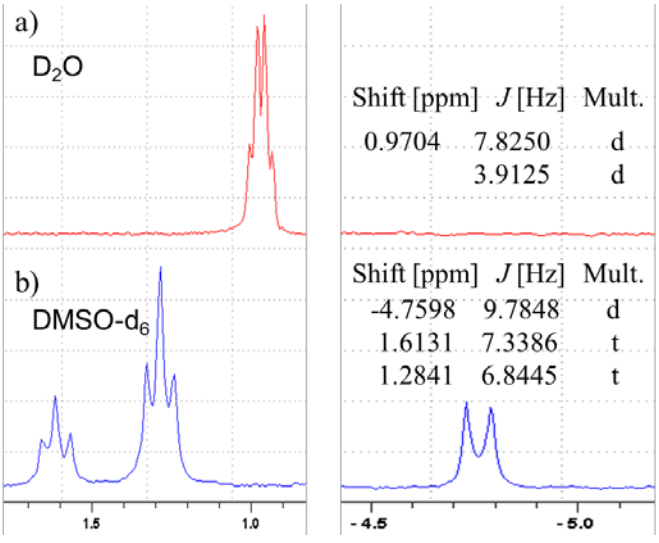

Figure 5.5: a) c = 5.6 mg/ml; pD = 2.92; b) c = 53 mg/ml.

5.1 exhibits quite interesting behaviour in organic solvents. Based on the ^{31}P NMR spectrum it can be concluded, that the compound disintegrates into three

different species in DMSO (Figure 5.5). The nature of the species could not be determined. Further experiments, especially single crystal X-ray diffraction can be expected to bring some light into the composition of the reaction products.

Based on the crystal structure (*vide infra*), the hydrodynamic radius of a monomer of **5.1** can be assessed to amount to between 1 and 2 nm. As peaks in the range between 0.5 nm and 10 nm are absent in the analysed pH range, it can be concluded that no monomers of **5.1** exist in solution, they rather agglomerate directly to higher non-covalently bound aggregates.

The crystal structure of **5.1** consists of guanosine-Strandberg anions with Na^+ cations balancing the charge including several water molecules. It is stabilized by a series of non-covalent interactions such as coordinative bonds, stacking interactions and H-bonds (Figure 5.6). The guanosine moieties of the hybrid anions are interconnected with each other via hydrogen bonding between the N^3 atoms of the purine ring and the OH groups of the sugar of the neighbouring anion. Further interconnection is accomplished by coordination of Na^+ through the oxygen atoms of the ribose rings of the neighbouring guanosine Strandberg anions. Additional hydrogen bonds between amino groups of the guanosine residue and adjacent Strandberg anions reinforce the crystal structure.

Stacking interactions between the guanine rings are quite similar to the ones encountered in the duplex DNA.[18] The planes of the pairwise interlinked guanosine moieties are virtually parallel to one another and display an interplanar distance of 3.4(1) Å, which corresponds to the average distance between the stacked nucleotides in the B-DNA (planes 1 and 2 in Figure 5.6). The dimers are crystallographically equivalent and can be converted into one another by translation along the crystallographic c-axis (1/6 of the unit cell length) and subsequent 60° rotation around it. The interplanar angle of the adjacent dimers (the angle between the planes 2 and 3 in Figure 5.6) is 7.089°. Thus the ring planes of the guanine residues of the stacked dimers are slightly tilted to one another. The respective interplanar distance is 3.5(2) Å.

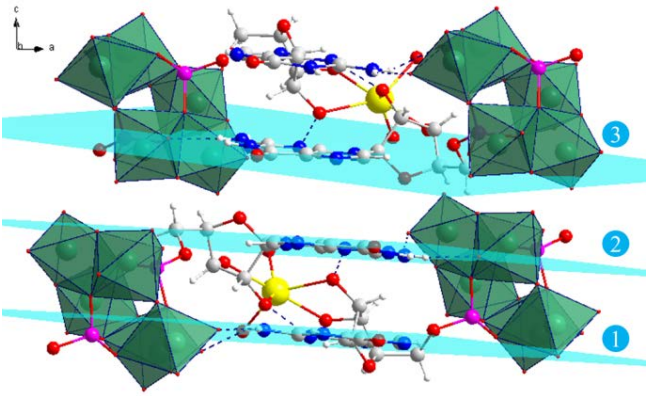

Figure 5.6: Stacked dimers of **1**.The planes of purine rings are numbered and indicated in blue. Na yellow.

The space group $P6_522$ includes a six fold left handed screw axis as the central symmetry element. Accordingly, the crystal structure of **5.1** can be described as consisting of a number of helices with the pitch size corresponding to one unit cell length along the crystallographic c-axis (Figure 5.7). The helix rise per pair of stacked guanosine Strandberg dimers is 1/6 of the unit cell length along the c-axis (≈ 7.1 Å). This value corresponds to the van-der-Waals thickness of the dimers of around 6.9(3) Å. The helix turn per dimer is 60°, consistent with the crystal symmetry. Contrary to the DNA, the building units of **5.1** are not interconnected by a covalent backbone. This fact implies the conclusion, that the helical symmetry of the DNA is not defined by the phosphate-ribose backbone, but by the nucleosides.

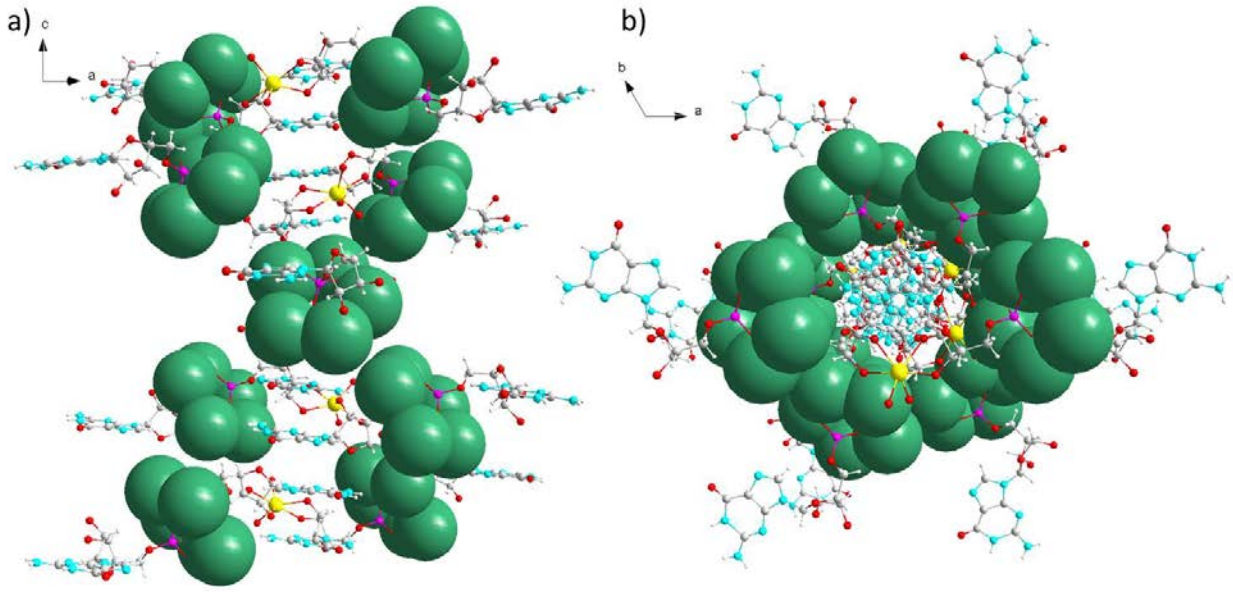

Figure 5.7: Crystal structure of **5.1**. a) View along the crystallographic b-axis; b) View along the crystallographic c-axis. Water molecules are omitted for clarity. Space-filling model was used for molybdate fragments to illustrate helicity/homochirality.

Atomic Force Microscopy (AFM) can provide valuable information regarding the morphology of hydrogels. Because AFM looks into surface interactions, the data obtained are complementary to those obtained by DLS (in solution) and diffractometry (in solid state). The three techniques combined therefore provide a global understanding of guanosine self-assembly.

AFM data were obtained from drop casting 10 µL of a solution of **5.1** on a freshly cleaved mica surface. The sample has then been left at ambient conditions overnight to dry.

Table 5.1. Crystal and structure refinement data for $Na_2[(HGMP)_2(Mo_5O_{15})]•7H_2O$ (**5.1**).

	$Na_2(HGMP)_2[Mo_5O_{15}]·7H_2O$ (**5.1**)		
formula	$C_{20}H_{40}Mo_5N_{10}Na_2O_{38}P_2$	ρ_{calcd} [g•cm^{-3}]	1.686
M_r	1616.24	μ [mm-1]	9.304
T [K]	150(2)	Refl. collected/unique	75586/4943
space group	*P6$_5$22*	R_{int}	0.0394
crystal system	hexagonal	Refined parameters	357
a [Å]	16.0517(3)	GooF	1.045
c [Å]	42.8082(7)	$R_1(I>2\sigma)$	0.0887
V [Å^3]	9552.1(4)	wR_2(all)	0.2600
Z	6	Flack x-Parameter[a]	0.001(8)

[a] H. Flack, Acta Cryst. A **1983**, *39*, 876-881.

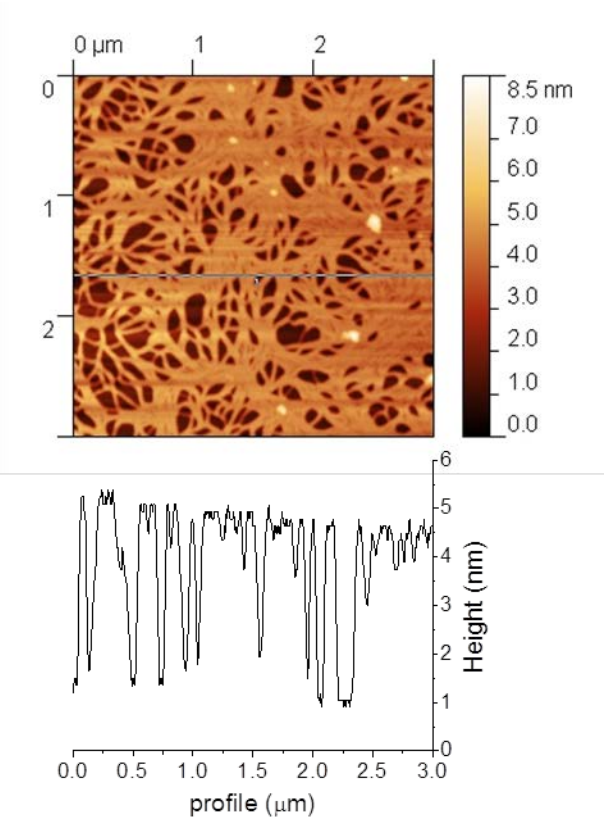

Figure 5.8: Height AFM picture of the agglomerates of the compound **5.1** on mica surface, taken in the semi-contact mode under air.

As previously reported in other hybrid systems,[19] the features seen on the surface by AFM depend highly on local concentration. In some areas a tight network of fibers is observed (see Figure 5.8) systematically highlighting a height of around 3.5 nm. Guanosine self-assembly has already been studied by AFM and is known to form fiber-like structures on mica.[20] However in most reports the height of these fibers is between 1.5-2.0 nm. The difference with the 3.5 nm measured in this study is the consequence of the presence of the inorganic core, and is consistent with the helicoidal diameter measured on the crystal structure (3.85 nm). Because the freshly cleaved mica surface is negatively charged, it is expected that the structure will not grow from a dimer of hybrids POM-guanosine, as this would require the anion to interact directly with the surface, but that the guanosine moiety not involved in the dimerization would interact with the surface. The

slight difference between the height of the fibers and the diameter of the helix could be explained by the guanosine interacting not only *via* its free amine group, but lying flat on the surface in order to maximize the stabilizing interaction, leading to a more compact structure.

5.3. Experimental Section

NMR experiments: The NMR spectra were measured on a Bruker 400MHz spectrometer. The samples were prepared from D_2O/H_2O (1/10) solutions, the pD/pH adjusted by DCl/D_2O (0.2 M).The NMR spectra are referenced to the peaks of 3-(trimethylsilyl)propionic-2,2,3,3-d_4 acid (87 mM, δ (H, C of the TMS-group) = 0.0 ppm) and D_3PO_4 (1 mM, δ = 0.0 ppm) in D_2O. The assignment of ^1H and ^{13}C NMR signals was verified by $^1H,^1H$-COSY and $^{13}C,^1H$-HSQC measurements.

DLS experiments: DLS measurements were accomplished on Zetasizer Nano-ZS (Malvern Instruments). The aqueous DLS samples were allowed to equilibrate for 20 min, the heavy water ones for 1 hr. after filtration through 0.2 μm syringe filter. pH values were adjusted by HCl (1.1 M), the pD values were adjusted by DCl (0.2 M).

AFM experiments: The AFM pictures were taken in semi-contact mode using the NTEGRA Spectra platform of NTMDT. The cantilevers used were purchased from NTMDT (NSG10, resonant frequency 140-390 kHz, force constant 3.1-37.6 N/m). The samples were prepared by drop cast 10 μl of the solution of 1 (0.1 mg/mL, pH = 1.95 adjusted by 1 M HCl, matured for 6 days) on a freshly cleaved mica surface.

Elemental analyses: Performed on the Vario EL analysing machine (Elementaranalysesysteme GmbH).

Synthesis: The starting materials for the synthesis of **5.1** were purchased from commercial sources and used without further purification.

$Na_2(HGMP)_2[Mo5O15]•7H_2O$ (5.1): $Na_2MoO_4•2H_2O$ (0.72 g, 3.04 mmol) and $Na_2GMP•yH_2O$ (0.61 g, 1.50 mmol(if y = 0)) were dissolved in H_2O (10 ml). 1.0 M HCl (7.2 ml) was added upon vigorous stirring over the course of 15 min adjusting the pH to 3.24. H_2O (6 ml) was added after further 50 min of stirring to the reaction mixture. The stirring was continued for further 30 min. A white solid was obtained upon MeOH vapour diffusion after a week. The white product was separated from the gelatinous reaction mixture via centrifugation (1600 rpm, 1 hr.) and washed 3 times with 20 ml portions of MeOH. 0.70 g (0.43 mmol, 58%) of the product

was obtained after drying for two days in air and two hours under dynamic vacuum (0.02 mbar). ^{1}H NMR (400 MHz, c = 28 mg/ml, pD = 2.60, ppm): 4.48 (m, 1H, H^{4R}), 4.53 (m, 1H, H^{5R}), 4.60 (m, 1H, H^{5R}), 4.72 (m, 1H, H^{3R}), 4.96 (m, 1H, H^{2R}), 6.00 (d, $^{3}J_{H1RH2R} \approx 6.3$ Hz, 1H, H^{1R}), 8.68 (s, 1H, H^{8}). ^{13}C NMR (101 MHz, c = 28 mg/ml, pD = 2.60, ppm): 68.0 (d, $^{2}J_{C5RP} \approx 4.4$ Hz, C^{5R}), 73.9 (C^{3R}), 77.0 (C^{2R}), 87.6 (d, $^{3}J_{C4RP} \approx 9.7$ Hz, C^{4R}), 90.3 (C^{1R}), 140.2 (C8), 154.0, 157.3, 160.3 (C^{2}, C^{4}, C^{6}). ^{31}P NMR (162 MHz, c = 5.6 mg/ml, pD = 2.92, ppm): 0.97 (dd, $^{3}J_{PH5R} \approx 3.9$ Hz, $^{3}J_{PH5R} \approx 7.8$ Hz). IR (KBr): ν (cm^{-1}) = 3350 (very broad, vs, 2938 (w), 1696 (s), 1635 (s), 1599 (s), 1533 (m), 1480 (w), 1411 (w), 1361 (m), 1250 (w), 1139 (s), 1073 (s), 993 (s), 932 (s), 907 (s), 798 (w), 681 (broad, vs), 526 (w), 496 (w). Elemental Analysis (%): Calc. for $C_{20}H_{40}Mo_5N_{10}Na_2O_{38}P_2$: C 14.86, H 2.49, N 8.67; found: C 15.05, H 2.31, N 8.77.

X-Ray Crystallography: Single crystals suitable for X-ray diffraction studies were obtained from a similar reaction mixture upon addition of 1 eq. of NBu_4Br to the centrifugate and subsequent methanol diffusion. Suitable single crystals of **5.1** were attached to a thin glass fibber by using Fomblin YR-1800 oil and mounted on a goniometer head in a general position. All data were collected at 150 K on an Oxford Gemini A Ultra diffractometer, with graphite monochromated X-radiation (MoK_{α}, λ = 0.71073Å), running under the CrysAlisPro software. The corrections for the incident and diffracted beam absorption effects were applied using analytical methods.[21] Structures were solved using direct methods with SHELXS-97[22] using WinGX routines.[23] Structure refinement was accomplished by full matrix least-squares on F^2 via SHELXL-2013.[22] Non-hydrogen atoms except O-atoms of water, O^6 of the carbonyl group of guanosine and Na^+ were refined anisotropically. Hydrogen atom positions were calculated using standard geometric criteria and refined on riding model. All data manipulation and presentation were performed using WinGX.[23]

Table 5.2: Atomic coordinates ($\times 10^{-4}$) and equivalent temperature coefficients U_{eq} (10^{-4} pm^2) of **5.1**.

Atom	x	y	z	U_{eq}
Mo(1)	5510(1)	6836(1)	360(1)	113(1)
Mo(2)	6078(1)	5096(1)	463(1)	109(1)
Mo(3)	3654(1)	6346(1)	833	130(1)
P(1)	3800(2)	4435(2)	550(1)	102(1)
Na(1)	-1500(2)	1500(2)	833	87(2)
Na(2)	670(20)	-3130(20)	135(8)	112(10)
Na(3)	6043(8)	2774(9)	14(3)	118(4)

Na(4)	5211(9)	5456(9)	-410(3)	125(4)
O(1)	7272(4)	5828(5)	565(1)	130(3)
O(2)	5679(4)	4321(4)	833	104(3)
O(3)	6182(5)	4352(5)	194(1)	130(3)
O(4)	4461(4)	4216(4)	373(1)	101(2)
O(5)	5878(4)	5930(4)	201(1)	112(2)
O(6)	4020(4)	5470(4)	502(1)	104(2)
O(7)	5023(6)	6919(5)	36(1)	142(3)
O(8)	3619(6)	7047(6)	1116(2)	155(3)
O(9)	4915(5)	7227(4)	675(1)	122(3)
O(10)	6620(5)	7844(4)	356(1)	132(3)
O(11)	3824(3)	4200(4)	894(1)	94(2)
O(12)	2748(4)	3705(4)	447(1)	118(2)
O(13)	1014(5)	2262(4)	152(1)	117(3)
O(14)	-221(5)	2830(5)	558(2)	137(3)
O(15)	103(4)	1695(4)	928(1)	112(2)
O(16)	1587(6)	-1553(6)	420(2)	164(3)
O(18)	-2501(8)	1735(8)	482(3)	109(3)
O(19)	0	6634(19)	1667	109(8)
O(20)	7687(18)	0	0	138(9)
O(21)	3913(11)	900(12)	435(4)	93(5)
O(22)	-732(12)	-3695(13)	625(4)	129(5)
O(23)	1375(17)	-3610(17)	597(6)	136(8)
O(24)	5940(30)	740(30)	-481(11)	158(15)
O(24')	5760(30)	1290(30)	-352(12)	172(16)
O(25)	4343(14)	2493(14)	58(5)	94(6)
O(25')	4326(15)	2243(16)	462(5)	81(6)
O(27)	3680(18)	5676(18)	-394(6)	96(7)
N(1)	1029(6)	966(5)	386(1)	110(3)
N(2)	2144(5)	568(6)	368(2)	124(3)
N(3)	-422(5)	-572(4)	451(1)	100(3)
N(4)	45(5)	-1833(5)	488(2)	126(3)
N(5)	-1600(7)	-2166(6)	534(2)	146(4)
C(1)	2253(6)	3972(7)	231(2)	124(4)
C(2)	1158(6)	3182(7)	244(2)	128(3)
C(3)	777(6)	3062(7)	570(2)	112(4)
C(4)	800(6)	2212(6)	687(2)	99(3)
C(5)	601(6)	1550(6)	394(2)	107(3)
C(6)	1980(5)	1268(6)	369(2)	92(3)
C(7)	537(7)	10(7)	419(2)	118(4)
C(8)	1249(6)	-281(7)	406(2)	113(3)
C(9)	1057(7)	-1234(6)	429(2)	112(3)
C(10)	-658(6)	-1457(7)	486(2)	143(5)

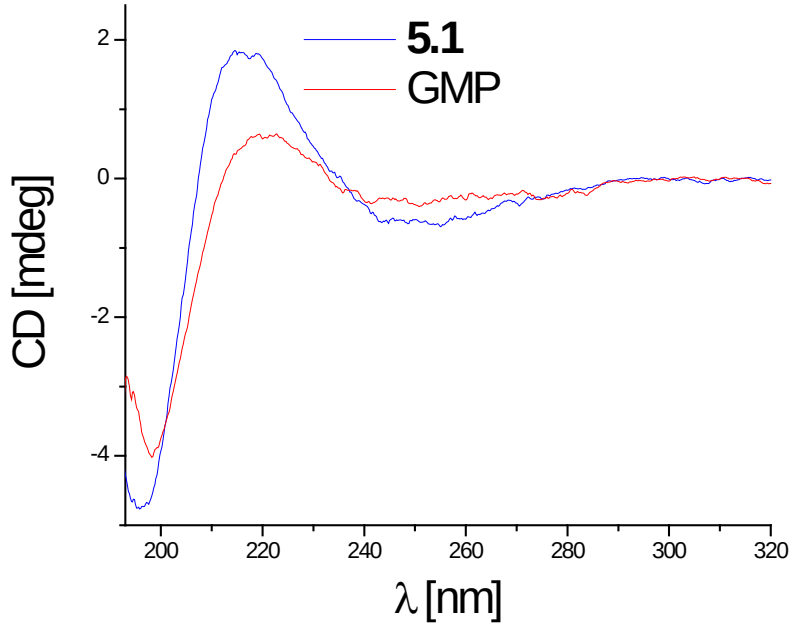

Figure 5.10: Near/Far UV circular dichroism spectra of GMP and compound **5.1**. c(GMP) = $3.7 \cdot 10^{-5}$ M, pH = 3.5; c(**1**) = $3.5 \cdot 10^{-5}$M, pH = 3.4. Spectra were recorded in a JASCO J810 spectropolarimeter in cells of pathlength 1cm (**5.1**) and 0.5cm (GMP) using the following parameters: Bandwidth 1cm; Response 2 sec; Scan rate 10nm/min, data pitch 0.2nm.

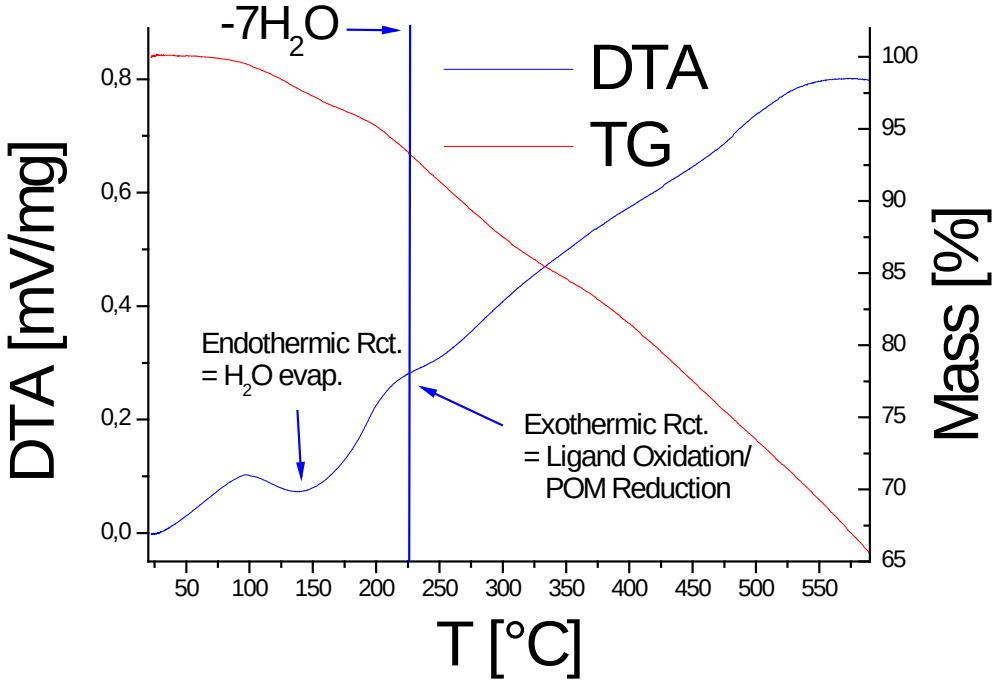

5.4. References

(1) Biffi, G.; Tannahill, D.; McCafferty, J.; Balasubramanian, S. *Nature Chem.* **2013**, *5*, 182.

(2) Voet, D.; Voet, J. G. In *Biochemistry*; 4 ed.; Recta, P., Ed.; John Wiley & Sons, Inc.: United States of America, 2011, p 789.

(3) Pierce, K.; Premont, R.; Lefkowitz, R. *Nature Rev. Mol. Cell Biol.* **2002**, *3*, 639.

(4) Wong, A.; Ida, R.; Spindler, L.; Wu, G. *J. Am. Chem. Soc.* **2005**, *127*, 6990.

(5) González-Rodríguez, D.; van Dongen, J.; Lutz, M.; Spek, A.; Schenning, A.; Meijer, E. *Nature Chem.* **2009**, *1*, 151.

(6) Alberti, P.; Mergny, J.-L. *Proc. Nat. Acad. Sci. U. S. A.* **2003**, *100*, 1569.

(7) Davis, J. T. *Angew. Chem. Int. Ed.* **2004**, *43*, 668.

(8) Strandberg, R. *Acta Chem. Scand.* **1973**, *27*, 1004.

(9) Kwak, W.; Pope, M. T.; Scully, T. F. *J. Am. Chem. Soc.* **1975**, *97*, 5735.

(10) a) Katsoulis, D. E.; Lambrianidou, A. N.; Pope, M. T. *Inorg. Chim. Acta* **1980**, *46*, L55; b) Geraldes, C. F. G. C.; Castro, M. M. C. A. *J. Inorg. Biochem.* **1988**, *33*, 47.

(11) Hill, L. M. R.; George, G. N.; Duhme-Klair, A.-K.; Young, C. G. *J. Inorg. Biochem.* **2002**, *88*, 274.

(12) aInoue, M.; Yamase, T. *Bull. Chem. Soc. Jpn.* **1996**, *69*, 2863; bHe, Z.; Yan, Y.; Li, B.; Ai, H.; Wang, H.; Li, H.; Wu, L. *Dalton Trans.* **2012**, *41*, 10043.

(13) Carraro, M.; Sartorel, A.; Scorrano, G.; Maccato, C.; Dickman, M.; Kortz, U.; Bonchio, M. *Angew. Chem. (Int. Ed. Engl.)* **2008**, *47*, 7275.

(14) Loo, K.; Degtyareva, N.; Park, J.; Sengupta, B.; Reddish, M.; Rogers, C. C.; Bryant, A.; Petty, J. T. *J. Phys. Chem. B* **2010**, *114*, 4320.

(15) The hydrodynmic radius is a physical quantity, which is calculated based on the approximation of spheric particles in solution (Stokes-Einstein relation). This approximation is not valid for the real systems, but the hydrodynamic radius gives an indication of the size of the dissolved particles.

(16) Eimer, W.; Dorfmueller, T. *J. Phys. Chem.* **1992**, *96*, 6790.

(17) Jurga-Nowak, H.; Banachowicz, E.; Dobek, A.; Patkowski, A. *J. Phys. Chem. B* **2004**, *108*, 2744.

(18) Voet, D.; Voet, J. G. In *Biochemistry*; 4 ed.; Recta, P., Ed.; John Wiley & Sons, Inc.: United States of America, 2011, p 1145.

(19) a) Musumeci, C.; Luzio, A.; Pradeep, C. P.; Miras, H. N.; Rosnes, M. H.; Song, Y.-F.; Long, D.-L.; Cronin, L.; Pignataro, B. *J. Phys. Chem. C* **2011**, *115*, 4446; b) Hutin, M.; Yvon, C.; Yan, J.; Macdonell, A.; Long, D.-L.; Cronin, L. *CrystEngComm* **2013**, *15*, 4422.

(20) a) Kunstelj, K.; Federiconi, F.; Spindler, L.; Drevenšek-Olenik, I. *Colloids and Surf. B* **2007**, *59*, 120; b) Oliveira Brett, A. M.; Chiorcea Paquim, A. M.; Diculescu, V.; Oretskaya, T. S. *Bioelectrochemistry* **2005**, *67*, 181; c) Li, Y.; Dong, M.; Otzen, D. E.; Yao, Y.; Liu, B.; Besenbacher, F.; Mamdouh, W. *Langmuir* **2009**, *25*, 13432.

(21) a) Clark, R. C.; Reid, J. S. *Acta Cryst. A* **1995**, *51*, 887; b) Blessing, R. *Acta Cryst. A* **1995**, *51*, 33.

(22) Sheldrick, G. *Acta Cryst. A* **2008**, *64*, 112.

(23) Farrugia, L. *J. Appl. Crystallogr.* **1999**, *32*, 837.

6. Summary and Conclusions

6.1 The types of compounds obtained

The present work is the first thorough exploration of the chemistry of the systems comprising purine bases and POMs. Different modes of interplay of these chemical species were employed in order to design and synthesize new compounds. The obtained materials can be divided into the

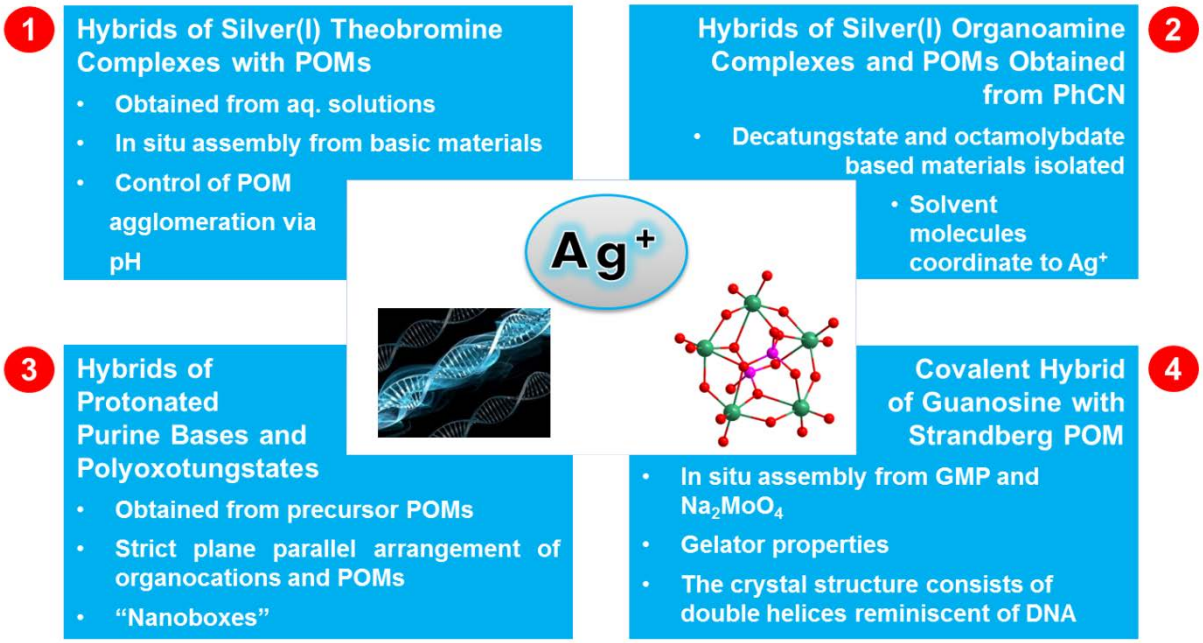

Figure 6.1: Four types of materials described in the present work and their key remarkable traces presented as bullet points.

four different types displayed in Figure 6.1. A chapter of the present thesis was dedicated to each type.[1]

1. The first type comprises the largest number of compounds and consists majorly of materials in which polyoxoanions are interconnected by ditheobromine silver(I) complexes. The target materials are readily obtained from aqueous solutions. The convenient feature of the experimental procedure is the possibility of obtaining the desired POM from the basic materials by adjustment of the pH value of the reaction mixture. A ubiquitous structural trait of the target materials are the one-dimensional coordination polymers consisting of the polyoxoanions interconnected by $[Ag(thb)_2]^+$-complexes. These chains are interconnected by a framework

consisting of hydrogen bonding and stacking interactions between the self-pairing theobromine molecules and between the theobromine molecules and the POMs. Materials containing polyoxoanions based on vanadium, chromium and molybdenum could be obtained by this strategy, but not the ones based on tungsten. Reactions, in which Na_2WO_4 was employed as starting material yielded an inorganic paratungstate containing compound with variable Na^+ and H_2O content.[2] The most likely reason for this difference in chemical behaviour between tungsten and its lighter homologues is the more pronounced affinity of paratungstate to sodium cations than that of the polyoxoanions of vanadium, chromium and molybdenum.

2. As these attempts to extend the row of theobromine silver(I)-POM compounds to polyoxotungstates were unsuccessful, different reaction conditions had to be employed. Benzonitrile proved to be the solvent of choice for the synthesis of $[Ag(PhCN)_2(thb)]_4[W_{10}O_{32}]\cdot PhCN$ (**3.3**), which contained theobromine as the ligand for silver(I) and decatungstate. The compound obtained was nonetheless quite different from the ones obtained from aqueous reaction mixtures. The most striking difference was the silver(I) coordination by the solvent molecules. Benzonitrile partly displaced theobromine from the coordination sphere of the metal. Hence a pronouncedly different crystal structure resulted. It did not display exclusively the polar H-bonding and stacking interactions framework determined by the theobromine ligands but also showed some hydrophobic faces consisting of the phenyl rings of the benzonitrile ligands.

Two other compounds containing organoamine silver(I) complexes and decatungstate anions were obtained using the same approach demonstrating its generality. A related compound, in which decatungstate was replaced by octamolybdate, was obtained via a similar experimental procedure. This allowed for comparison of the organic-inorganic compounds containing different polyoxoanions.

3. The protonated purine bases could also be employed for crystal engineering of organic-inorganic materials containing polyoxotungstates. The aromatic cations are arranged parallel to the faces of the POMs in all of the resulting crystal structures. This arrangement is most likely the optimal one for Coulombic interactions between the organic cation and the inorganic anion. The polyoxotungstates are contained in distinctive compartments by the organic framework. Accordingly the arrangement was named “nanoboxes” reflecting the size of the units.

4. Only one compound obtained in the course of the research described in the present thesis contained a purine derivative covalently bound to a polyoxometalate. $Na_2(HGMP)_2[Mo_5O_{15}]\bullet 7H_2O$ (**5.1**) shows several remarkable gelator properties and crystallizes in space group $P6_522$, which implies a helical structure in the solid state. The crystal structure consists of guanosine Strandberg anions interconnected by a network of coordinative, H-bonding and stacking interactions.

There are several intriguing aspects of this crystal structure which allows for the following observations:

- The helical structure of the DNA is most likely determined by the nucleosides. The phosphate moieties or even a covalent backbone are not necessary to define the helix.
- The interplanar distance between the ring planes of the nucleic bases of 3.4 Å appears to be the geometric optimum not only for biomolecules such as B-DNA but also for artificial molecules such as compound **5.1** or hydrophobic guanine quadruplexes.[3]
- It is, in general, quite difficult to determine how the overall chirality of a biopolymer is determined by the chiral centres of the individual constituent molecules. B-DNA is a right-handed helix,[3a] compound **5.1** is a left-handed one, although the same set of chiral centres determines the conformation and constitution of the ribose ring.

6.2 Key Conclusions

- *Polyoxoanions form 1D coordination polymers with silver(I)-theobromine complexes. The methyl substituents on two of the N-atoms of the purine ring do not allow a build-up of higher dimensional coordinative frameworks. The coordination polymers are connected mainly by hydrogen bonds and stacking interactions typical for heteroaromatic constituents of nucleic acids.*
- *Organoamine solvents can compete with purines for positions in the silver(I) coordination sphere and replace them in the crystal structures.*
- *The protonated purine bases are arranged parallel to the faces of polyoxotungstates in the respective crystal structures to maximize Coulombic stabilization.*
- *Covalent hybrid of guanosine and Strandberg type anions exhibit gelator properties similar to other guanosine derivatives. The crystal structure of the respective compound is reminiscent of B-DNA.*

6.3 Notes and References

(1) The numbering in Figure 6.1 does not correspond to the numbering of the chapters dedictated to the types of compounds.

(2) The composition of the obtained crystalline mixtures was determined by the diffractometric cell parameters and partly by the crystal structure solution. The obtained crystals of new sodium paratungstate phases were of rather poor diffractometric quality and lie thematically outside the scope of this thesis. Hence a thorough discussion of these reaction mixtures is omitted.

(3) a) Voet, D.; Voet, J. G. In *Biochemistry*; 4 ed.; John Wiley & Sons, Inc.: United States of America, 2011, p 1145; b) González-Rodríguez, D.; van Dongen, J.; Lutz, M.; Spek, A.; Schenning, A.; Meijer, E. *Nature Chem.* **2009**, *1*, 151.

Erklärung

Ich versichere, dass ich die von mir vorgelegte Dissertation selbstständig angefertigt, die benutzten Quellen und Hilfsmittel vollständig angegeben und die Stellen der Arbeit – einschließlich Tabellen, Karten, Abbildungen, die anderen Werken im Wortlaut oder dem Sinn nach entnommen sind, in jedem Einzelfall als Entlehnung kenntlich gemacht habe; dass diese Dissertation noch keiner anderen Fakultät oder Universität zur Prüfung vorgelegen hat; dass sie – abgesehen von unten angegebenen Teilpublikationen noch nicht veröffentlicht worden ist sowie, dass ich eine Veröffentlichung vor Abschluss des Promotionsverfahrens nicht vornehmen werde. Die Bestimmungen der Promotionsordnung sind mir bekannt. Die von mir vorgelegte Dissertation ist von Prof. Dr. Gerd Meyer betreut worden.

Zur Wahrung der Priorität sind folgende Teile dieser Arbeit bereits publiziert:

Kulikov, V.; Meyer, G. *Cryst. Growth Des.* **2013**, *13*, 2916.

Lebenslauf

Vladislav Kulikov
Paulstr. 29
50354 Bonn
Tel.: +49163/2516335

Email: vladislav_kulikov@gmx.de

Persönliche Daten:

Geburtsdatum:	31.08.1983
Geburtsort:	Taschkent (Usbekistan)
Familienstand:	ledig
Staatsangehörigkeit:	deutsch/ usbekisch
Einreise in die BRD:	12.07.1999

Studium und Forschungsarbeit

10.2004-07.2008	Universität zu Köln; Diplom Chemie; Spezialisierung in Biochemie; Diplomarbeit im Fachbereich organische Chemie, extern an der Universität Berkeley (Kalifornien, USA) Gesamtnote: sehr gut
09.2010-08.2011	Wissenschaftlicher Mitarbeiter an der Universität zu Bonn. Forschungsschwerpunkt: „Neue Ruthenium-Alkylidin-Komplexe mit potentiellen Anwendungen als Alkinmetathese-Katalysatoren“
11.2011-heute	Wissenschaftlicher Mitarbeiter an der Universität zu Köln. Forschungsschwerpunkt: „Hybridmaterialien aus Silber(I)-Purin Komplexen, protonierten Purinen und Polyoxometallaten“

Publikationen:

- V. Kulikov und G. Meyer, *Cryst. Growth Des.* **2013**, *13*, 2916-2927.
- V. Kulikov und G. Meyer, *Acta Cryst. E* **2013**, *69*, i13.
- V. Kulikov und G. Meyer, *Acta Cryst. E* **2013**, *69*, o1027.

Methodenkenntnisse:

- Lösung und Verfeinerung der Kristallstrukturen
- Ausführliche Kenntnisse auf dem Gebiet der anorganischen, metallorganischen und organischen Synthese und Katalyse
- Analytik (Pulverdiffraktometrie, NMR, IR, GC-MS, HPLC, DNA-Gel-Elektrophorese)
- Alle gängigen Computerprograme für organisch- und anorganisch-chemische Analytik und Recherche sowie Anwendungssoftware (MS Office, Origin usw.)

Auslandserfahrung:

01.-04.2013	Glasgow, Großbritannien (Forschungsarbeit an der Synthese und Charakterisierung der Hybridmaterialien)
01.-02.2010	Brüssel, Belgien (Projekt zur Erhöhung der Profitabilität der DHL-Landesgesellschaft)
01.-06.2008	Berkeley, Kalifornien, USA (Diplomarbeit)

Außeruniversitäre Berufserfahrung:

03.2009 – 08.2010	Tätigkeit als Consultant bei Deutsche Post DHL Inhouse Consulting GmbH
08.2008-01.2009	Praktika bei Siemens Management Consulting und The Boston Consulting Group

Lehrerfahrung:

11.2011-heute	Organisation der praktischen Übungen in der allgemeinen und anorganischen Chemie für alle Biologiestudenten an der Universität zu Köln im 2. Semester.
09.2010-heute	Betreuung der Praktika der Chemiestudenten an den Universitäten Bonn und Köln.
01.2007-12.2007	Tutortätigkeit an der Universität zu Köln in den Fächern Chemie und Mathematik

Stipendien:

10.2004-07.2008	Studienstiftung des deutschen Volkes (Förderung für Studierende)
11.2012-heute	Studienstiftung des deutschen Volkes (Förderung für Doktoranden)

Weiteres Engagement:

08.2002	Praktikum im Forschungszentrum Jülich
WS 2002/03, SS 2004	Teilnahme am Projekt „Schüler an der Universität zu Köln“
07.2003	Teilnahme an der Internationalen Chemieolympiade in Athen (Silbermedaille)

Schulausbildung:

09.1990-06.1999	Allgemeinbildende Schule Nr. 145 zu Taschkent (Usbekistan)
08.1999-06.2004	Albert-Schweitzer-Gymnasium in Hürth Abitur mit der Gesamtnote 1,2

Sprachen:

Deutsch, Englisch, Russisch

Köln, den 13.08.2013